



Jimma University

School of Graduate Studies

Jimma Institute of Technology

Faculty of Electrical and Computer Engineering

**Comparative Performance Assessment of Different Rectangular
Microstrip Patch Antenna Array Configurations at 28GHz for 5G
Wireless Applications**

**A Thesis Submitted to Jimma Institute of Technology, School of
Graduate Studies in Partial Fulfillment of the Requirements for
Masters Degree in Communication Engineering**

**By:
Mulugeta Tegegn Gemed**

**June 16, 2020
Jimma, Ethiopia**



Jimma University
School of Graduate Studies
Jimma Institute of Technology
Faculty of Electrical and Computer Engineering

**Comparative Performance Assessment of Different Rectangular
Microstrip Patch Antenna Array Configurations at 28GHz for 5G
Wireless Applications**


By:
Mulugeta Tegegn Gemed

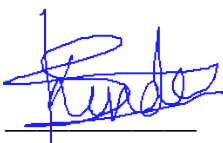
Advisor: Dr. Kinde Anlay

June 16, 2020
Jimma, Ethiopia

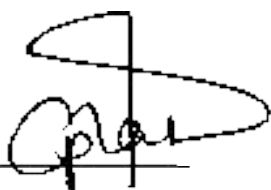
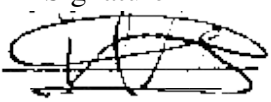
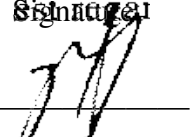
Declaration

I hereby declare that this thesis entitled "**Comparative Performance Assessment of Different Rectangular Microstrip Patch Antenna Array Configurations at 28GHz for 5G Wireless Applications**" is based on the results found by myself and materials of work found by other researcher mentioned by references. The contents of this thesis have not been submitted to any other Institute or University for the award of any degree.

Mulugeta Tegegn Gameda :  6/17/2020
Signature Date

Approved by advisors:
Kinde Anlay (PhD., Assistant Prof.)  17/06/2020
Signature Date

Approved by Faculty of Electrical and Computer Engineering Research Examination Members.

1. Ephrem Tesfale (PhD)  June 15/2020
Name Signature Date
2. Dr. Mulugeta Atlabachew (Ass. professor)  11/06/2020
Name Signature Date
3. Getachew Alemu  17/06/2020
Name Signature Date

Abstract

Advancements in wireless communication systems needs a low cost, minimal weight, and low-profile antenna arrays that are capable of providing high performance over a wide frequency band. With this regard, the patch antenna arrays are preferred to overcome some of the challenging requirements of the 5G mm-wave communication systems. However, the bandwidth of microstrip patch antenna (MSPA) is narrow; its directivity, gain, and radiation efficiency are low. In addition, integrating a large number of patch antenna in the form of an array leads to increased mutual coupling between the radiating elements that distorts the field pattern, reduces radiation efficiency, and directivity of the antenna.

Attempting to improve the performance of rectangular MSPA in terms of the directivity, radiation efficiency, and bandwidth; various design techniques have been reported in the scientific literature. These are: cutting a resonant slot inside the patch, deflected ground plane, modifying the physical geometry of the patch, by using changing array elements and substrate thickness. However, their design considerations were to achieve good performance only in terms of one or two performance metrics. Also, the main focus of the studies was only for single element and linear rectangular MSPA arrays, and less study has been carried out to explore planar array configuration at 28GHz using large number of array elements. Therefore, in this study the design and comparative performance assessment of different size of linear and planar rectangular MSPA array configurations have been proposed and simulated using CST antenna simulator. Besides, in order to boost some of the performance metrics; inset-feed and quarter-wavelength impedance matching techniques, and tuning the parameters of the antenna have been used.

The simulation results show that directivity of the proposed single element, 2x1, 4x1, 2x2, 4x4, and 8x8 rectangular MSPA arrays are 7.41dBi, 9.451dBi, 11.2dBi, 11.12dBi, 15.80dBi, 19.31dBi; the return losses are -20.24dB, -19.88dB, -27.42dB, -32.688dB, -33.15dB, -17.75dB. Moreover, the radiation efficiency is more than 94.95% for 1D MSPA arrays and 79% for 2D MSPA arrays. From simulated antenna structures it has been observed that, tuning the dimension of width of the patch, microstrip feeder line, ground plane, and inset gap has direct effect on the input impedance, bandwidth, directivity, and radiation efficiency of the antenna. The overall extensive comparative study of different antenna array structures using simulation shows that there is no single best design in terms of all the performance parameters of the antenna. Hence, there is a design trade-off that should be considered depending on the requirements of a particular application.

Keywords: Fifth-Generation (5G), Microstrip Patch Antenna, 28GHz, Millimeter-Wave.

Acknowledgment

First, I would like to express my most gratitude to the Almighty God for his everlasting help in all my life, and for all his kind support to write this research documents. Secondly, I would like to express my deepest gratitude to my advisor Kinde Anlay (PhD., Assistant Prof.) for his unlimited support through guidance and the provision of relevant information during advising time to carry out this research. I gratefully acknowledge my lovely brother Wondimu Tegegne (PhD., Associate prof.) for his support and encouragement throughout my academic career. Finally, I would like to thank everybody who was important to the successful realization of the thesis, as well as expressing my apology that I could not mention personally one by one.

Table of Contents

Declaration	i
Abstract	ii
Acknowledgment	iii
Table of contents	vi
List of Figures	ix
List of Tables	x
List of Acronyms	x
1 Introduction	1
1.1 Background of the Study	1
1.2 Statement of the Problem	3
1.3 Objectives of the Study	4
1.3.1 General Objective	4
1.3.2 Specific Objectives	4
1.4 Research Questions	4
1.5 Significance of the Study	5
1.6 Scope of the Study	6
1.7 Organization of the Thesis	6
2 Literature Review	7
2.1 Introduction	7
2.2 Review of Rectangular Microstrip Patch Antenna	7
2.2.1 Review of Single Element Rectangular Microstrip Patch Antenna	7
2.2.2 Review of Rectangular Microstrip Patch Antenna Array	10
2.3 Conceptual Frame Work of the Study	14
2.4 Rectangular Microstrip Patch Antenna	15
2.4.1 Microstrip Feeding Techniques	17
3 Design parameters of Rectangular Microstrip Patch Antenna	18
3.1 Introduction	18
3.2 Initial Design Parameters of Rectangular MSPA	18
3.3 Design parameters and Governing Equations of Rectangular Microstrip Patch Antenna	19
3.3.1 Height of the Substrate	19
3.3.2 Width of the Patch	20

3.3.3	Effective Dielectric Constant	20
3.3.4	Effective Length of the Patch	20
3.3.5	Length Extension of the Patch	21
3.3.6	Actual Length of the Patch	21
3.3.7	Ground Plane Dimension	21
3.3.8	Location of the Feed point	22
3.3.9	Impedance Matching	22
3.3.10	Width and Length of the Microstrip Feeder Line	23
3.3.11	Inset Dimension	24
3.3.12	Width and Length of the Feed Point	24
3.4	Transmission line Model of Rectangular MSPA	25
3.5	Performance Metrics of the Antenna	28
3.5.1	Return Loss and Voltage Standing Wave Ratio	28
3.5.2	Radiation Pattern	28
3.5.3	Directivity	29
3.5.4	Gain	29
3.5.5	Bandwidth	29
4	Design of Rectangular Microstrip Patch Antenna	30
4.1	Introduction	30
4.2	Design Procedures of Single Rectangular MSPA	30
4.3	Design of Single Inset-Fed Rectangular MSPA	31
4.4	Design Procedure of Linear Rectangular MSPA Array	35
4.5	Design of Linear Rectangular MSPA Array	36
4.5.1	2x1 Inset-feed Rectangular MSPA Array	36
4.5.2	4x1 Inset-feed Rectangular MSPA Array	39
4.6	Design Procedure of Planar Rectangular MSPA Array	42
4.7	Design of Planar Inset-feed Rectangular MSPA Array	43
4.7.1	2x2 Inset-feed Rectangular MSPA Array	43
4.7.2	4x4 Inset-feed Rectangular MSPA Array	47
4.7.3	8x8 Inset-feed Rectangular MSPA Array	51
5	Simulation Results and Discussion	54
5.1	Introduction	54
5.2	Simulation Results and Discussion of 1D MSPA Array	54
5.2.1	Single Inset-feed Rectangular MSPA	54
5.2.2	2x1 Inset-feed Rectangular MSPA Array	57
5.2.3	4x1 Inset-feed Rectangular MSPA Array	58

5.3	Simulation Result and Discussion of 2D MSPA Arrays	60
5.3.1	2x2 Inset-feed Rectangular MSPA Array	60
5.3.2	4x4 Inset-feed Rectangular MSPA Array	62
5.3.3	8x8 Inset-feed Rectangular MSPA Array	64
6	Conclusions and Recommendations	67
6.1	Conclusions	67
6.2	Recommendations	68
	References	69
	Appendix-One	73
	Appendix-Two	76

List of Figures

2.1	Rectangular Microstrip Patch Antenna.	15
2.2	Voltage, Current, and Impedance Distribution of Patch Antenna.	16
2.3	Side view showing the electric fields [16].	16
2.4	Patch Antenna with Microstrip Feed-Line [11].	17
2.5	Corporate Feed of MSPA Array.	17
3.1	Length Extension Due to Fringing Effects [31].	21
3.2	Quarter-wave length impedance Transformer Network.	23
3.3	Transmission line model of Rectangular MSPA.	25
3.4	Rectangular MSPA and its Equivalent Circuit in Transmission Line Model.	26
3.5	Recessed Microstrip-Line Feed [11].	27
3.6	Radiation Pattern of the Directional Antenna.	29
4.1	Design Procedure of Single Inset-Feed Rectangular MSPA.	30
4.2	Proposed Single Inset-Feed Rectangular MSPA.	34
4.3	Design Procedures of Linear MSPA Array.	36
4.4	Physical Structure of the Proposed 2x1 Inset-feed Rectangular MSPA Array.	36
4.5	Physical Structure of 1:2 Power Divider.	38
4.6	Physical Structure of the Proposed 4x1 Inset-feed Rectangular MSPA Array.	40
4.7	Physical Structure of 1:4 Power Divider in 4x1 Linear Array.	41
4.8	Design Procedure of Planar inset-feed rectangular MSPA Array.	43
4.9	Physical Structure of the Proposed 2x2 Inset-feed Rectangular MSPA Array.	43
4.10	Structure of Quarter-Wavelength Impedance Transformer.	45
4.11	Physical Structure of the Proposed 4x4 Inset-feed Rectangular MSPA Array.	47
4.12	Physical Structure of the Proposed 8x8 Inset-feed Rectangular MSPA Array.	51
5.1	Return loss versus frequency plot for the single element rectangular MSPA.	55
5.2	3D radiation pattern for the single element rectangular MSPA.	55
5.3	2D radiation pattern for the single element rectangular MSPA.	56
5.4	Return loss versus frequency plot for the 2x1 rectangular MSPA array.	57
5.5	3D radiation pattern for the 2x1 rectangular MSPA array.	57
5.6	2D radiation pattern for the 2x1 rectangular MSPA array.	58
5.7	Return loss versus frequency plot for the 4x1 rectangular MSPA array.	59
5.8	3D radiation pattern for the 4x1 rectangular MSPA array.	59
5.9	2D radiation pattern for the 4x1 rectangular MSPA array.	60

5.10	Return loss versus frequency plot for the 2x2 rectangular MSPA array. . . .	61
5.11	3D radiation pattern for the 2x2 rectangular MSPA array.	61
5.12	2D radiation pattern for the 2x2 rectangular MSPA array.	62
5.13	Return loss versus frequency plot for the 4x4 rectangular MSPA array. . . .	63
5.14	3D radiation pattern for the 4x4 rectangular MSPA array.	63
5.15	2D radiation pattern for the 4x4 rectangular MSPA array.	64
5.16	Return loss versus frequency plot for the 8x8 rectangular MSPA array. . . .	64
5.17	3D radiation pattern for the 8x8 rectangular MSPA array.	65
5.18	2D radiation pattern for the 8x8 rectangular MSPA array.	65

List of Tables

4.1	Calculated Physical Dimensions of Single Inset-feed Rectangular MSPA. . .	35
4.2	Calculated Physical Dimensions of 2x1 Inset-Feed Rectangular MSPA Array. . .	39
4.3	Calculated Physical Dimensions of 4x1 Inset-Feed Rectangular MSPA array. . .	42
4.4	Calculated Physical Dimensions of 2x2 Inset-Feed Rectangular MSPA Array. . .	46
4.5	Calculated Physical Dimensions of 4x4 Inset-Feed Rectangular MSPA Array. . .	50
4.6	Calculated Physical Dimensions of 8x8 Inset-Feed MSPA Array.	53
5.1	Performance comparison of the reported and proposed single element MSPA. . .	56
5.2	Performances comparison of the existing and proposed 2x1 MSPA array. . .	58
5.3	Performance comparison of the existing and proposed 4x1 MSPA array. . .	60
5.4	Final simulation results of the existing and proposed 2x2 MSPA array. . . .	62
5.5	Simulation results of all studied inset-feed rectangular MSPA array.	66

List of Acronyms

AF	Array Factor
3D	Three Dimensional
4G	Fourth-generation
5G	Fifth-generation
BW	Bandwidth
CMOS	Complementary metal-oxide semiconductor
CST	Computer Simulation Technology
DIR	Directivity
FO	Frequency of operation
FR-4	Flame Retardant, fiber glass epoxy
GHz	Giga-hertz
LOS	Line of sight
MHz	Mega-hertz
MIMO	Multiple input multiple out put
mm	Millimeter
MSPA	Microstrip patch antenna
MW	Microwave
PCB	Printed circuit board
PL	Length of the patch
PW	Width of the Patch
RF	Radio Frequency
ROG	Rogers
RL	Return loss
SH	Substrate height
SLL	Side lobe level
VSWR	Voltage Standing Wave Ratio

Chapter 1

Introduction

1.1 Background of the Study

Over the past few decades, the continuous development of new generations of wireless communication technology brought a significantly impact on the daily lives of human being. Therefore, nowadays more and more users have gotten their devices connected to the networks to access; high-speed data access, high-quality video streaming, intelligent hearth care, and intelligent transportation which are causing a constant increase in data traffic and device connections, and also causing the need for enormous capacity in the upcoming years. However, the allowable frequency ranges of the existing wireless network generations are too congested. Consequently, this cannot address the current rapid growth in wireless data traffic. To address the rapid growth of wireless data traffic and to control network traffic in the near future, the use of currently unused spectra is, therefore, being highly encouraged and therefore the next network generation is on emerging stage which is said to be fifth-generation wireless network [1][2][3].

Wireless communication networks in the fifth-generations (5G) are expected to have; improved data rate, low latency, high capacity, high throughput, and spectral efficiency. To realize these expectation, there are five basic enabling technologies that are expected to appear in 5G wireless communication systems; these are millimeter-wave (mm-wave), small cell, massive MIMO, beam-forming, and cognitive radio networks. From this pillar, mm-wave communications systems is much interested in research community and standardization company, and referred to as 5G mm-wave communication systems [4][5].

The emerging 5G wireless communication systems are expected to highly enhance communication capacity by exploiting enormous unlicensed bandwidth beyond the normal licensed wireless microwave band. Specifically, in the mm-wave band. It is also expected to be ready to provide and support very high rates the maximum amount as 100 times of 4G capacity which results in a replacement challenge on network requirements as well as in the antenna designs to satisfy the expected data rate and capacity. The working frequency for the 5G wireless communication systems continues to be being debated but 6GHz, 10GHz, 15GHz, 28GHz, and 38GHz bands are among the expected one. However, the federal communication commission approved the allocation of huge bandwidths at 28GHz, 37GHz, and 39GHz [6][7][8].

Antennas at 28GHz for 5G wireless communication systems are expected to be broadband to produce high data rate and also, they must have a high gain to mitigate the effect of increased path loss due to high operating frequency. In addition, antenna with high gain is required to mitigate obstructed radio environment where, among others, human bodies are likely blockers of the mm-wave interface. In this regard, the microstrip patch antennas are quite and represent a lucid choice for wireless devices due to their low fabrication cost, light weight and volume, and a low-profile configuration as compared to the other bulky sorts of antennas. However, the thickness of the dielectric substrate deteriorates the antenna bandwidth and radiation efficiency, by increasing surface wave and spurious feed radiation along with the feeding line. Consequently, undesired cross-polarized radiation is led by feed radiation effects [9][10][11].

Furthermore, the MSPA suffers from losses such as conductor, dielectric, and radiation which results in narrowing the bandwidth and lowering the gain. This poses a design challenge for the MSPA designer to meet the broadband requirements. However, the use of the thick substrate, a low dielectric substrate, multi-resonator stack configurations impedance matching, slot antenna geometry, and cutting a resonant slot inside the patch are recently reported methods to increase the radiation efficiency and the directivity of the patch antenna. In addition, to enhance a narrow bandwidth of MSPA, many broadband patch antennas are designed. Some of these designs include the patch with substrate integrated wave guide, multi-layer, and multi-patch designs, by incorporating multiple slots on the patch, by using a deflected ground plane dimension, by increasing dimension of the patch width, and using series feeding techniques [12][13][14][15].

In generally, the rectangular MSPA arrays have been utilized in a wide range of applications from communication systems to satellite and bio-medical applications. However, we cannot utilize the previously used low frequency design of rectangular MSPA directly for 5G mm-wave communication systems. Because the system requirements of the 5G mm-wave communication systems is different from the previous wireless communication systems. Therefore, rectangular MSPA requires extensive comparative analysis to fulfill all the requirements of 5G mm-wave communication systems. To address this requirement, in this study the comparative performance assessments of single element, 2x1, 4x1, 2x2, 4x4, and 8x8 rectangular MSPA array configuration at 28GHz for mm-wave applications have been presented.

1.2 Statement of the Problem

The first challenge to 5G systems is the high operating frequency, i.e., mm-wave bands, to avoid the already very crowded current 3 - 4G spectrum while benefit the availability of a wide portion of unused bandwidths in mm-wave bands. However, mm-waves have very different propagation conditions, atmospheric absorption, and hardware constraints compared to centimeter-waves. Therefore, to overcome the propagation effects of high frequency communication systems; the smaller antennas arranged as an array are highly required. With this regard, patch antenna arrays have been preferred for 5G wireless applications due to their extremely low profiles.

However, the patch antenna suffers losses such as conductor, dielectric, relatively high feed line and junction losses, and radiation. Which are causing patch antenna to have low; bandwidth, radiation efficiency, and gain. The performance of patch antenna is highly dependent on the selected substrate material type and thickness. The thickness of the dielectric substrate deteriorates bandwidth and radiation efficiency of the antenna, by increasing surface wave and spurious feed radiation along with the feeding line. Similarly, selected dielectric constant, dimension of patch width, number and configuration of considered array elements determines the radiation efficiency and bandwidth of rectangular MSPA.

In many applications it is necessary to design rectangular MSPA with very high directive and gain characteristics to extend the performance of the antenna. Therefore, the integration of a large number of rectangular MSPA in the array allows the feasibility of building large arrays with super directivity properties. However, it increases the effect of mutual coupling and thereby decreases radiation efficiency and directivity of the antenna. Furthermore, the impedance mismatch at the feed point, edge of the patch, and feeding structure of the patch antenna arrays will increase the return losses and voltage standing wave in the transmission line of the antenna. Consequently, it results in decreased radiation efficiency and increased extraneous radiation from feeds and junction.

Generally, to increase the performance of rectangular MSPA for 5G mm-wave application, several designs have been reported in scientific literature. However, the main focus of the studies was only for single element and linear rectangular MSPA array to achieve better performance only in terms of one or two performance metrics. Besides, less study has been carried out to explore planar array configuration of rectangular MSPA array at 28GHz using large number of array elements.

1.3 Objectives of the Study

1.3.1 General Objective

The general objective of this thesis is, to assess comparative performance of different rectangular microstrip patch antenna array configuration at 28GHz for mm-wave applications.

1.3.2 Specific Objectives

The specific objectives of this research are:

- To increase the directivity and beam gain of rectangular microstrip patch antenna array at 28GHz for millimeter-wave application.
- To increase the radiation efficiency and bandwidth of rectangular microstrip patch antenna array at 28GHz for millimeter-wave application.
- To minimize power losses due to the return losses and VSWR of rectangular microstrip patch antenna array at 28GHz.
- To minimize the side-lobe level and the impedance mismatch within an array environment of 28GHz rectangular microstrip patch antenna array.

1.4 Research Questions

In order to attain the above objectives, the study has attempted to answer the following research questions:

- How does the feeding structure part and patch edge impedance mismatch affect the radiation efficiency, beam directivity and gain, and bandwidth of rectangular MSPA at 28GHz resonant frequency?
- How does the variation of array elements and physical dimension of patch antenna affect the directivity, bandwidth, and radiation efficiency of rectangular MSPA at 28GHz operating frequency?
- How does the magnitude of the return losses and VSWR affect the input power and radiation efficiency of rectangular MSPA at 28GHz operating frequency?
- How does the side-lobe level and the impedance mismatch in feeding structure affect beam directivity, bandwidth and radiation efficiency of rectangular MSPA array at 28GHz operating frequency?

1.5 Significance of the Study

In the fifth-generation of wireless communication systems, using mm-wave frequency band along with compact antenna arrays are the major pillar technologies that are expected to satisfy the needs of high network capacity, improved data rate, and enhanced spectral efficiency. However, in the mm-wave frequency band, effective communications generally require the transmitter and the corresponding receiver to be located in the line-of-sight range. Under such circumstances, the surrounding buildings and trees may impose a significant influence on the performance of mm-wave cellular networks, especially for mobile device users. Therefore, the best way to overcome this problem is by designing a high-performance low profile antenna array.

The 5G wireless communication systems are expected to operate in extremely high-frequency bands. However, in this frequency band, the communication signals are easily blocked by the obstacle and thereby the path losses are increased. So, in order to mitigate this problem, antenna array with high gain is highly required. Accordingly, in this paper, different numbers of rectangular MSPA elements have been studied to increase beam directivity and gain of the antenna. Also, inset-feed and quarter-wavelength impedance matching have been simultaneously used to minimize the impedance mismatch at different parts of the array. Consequently, the radiation efficiency of the antenna is increased. Likewise, the return losses and VSWR are also minimized.

In this study, the important design parameters which can determine the overall performance of all the studied antennas have been tuned by analyzing the design parameter performance trade-off. As a result, the narrow bandwidth of rectangular MSPA is improved and high magnitude of mutual coupling is minimized. Therefore, the proposed inset-feed rectangular MSPA can be used for 5G mm-wave applications and can provide a high data rate for the large users. Besides, since the magnitude of the side lobe level of studied antenna is low, the noise level that could occur at the receiver side is highly minimized and leads to good system efficiency. Another contribution of this thesis is, the paper can be used as a base to conduct further studies and a reference for other researchers especially for those interested in the area of rectangular MSPA array design for 5G mm-wave communication systems. Hence, the proposed design provides a high contribution in all aspects.

1.6 Scope of the Study

One of the promising technologies in the 5G cellular communication systems is the utilization of mm-wave frequency band by integrating a very compact antenna in the 5G base stations and mobile devices. However, mm-wave signals are highly susceptible to blocking and have high propagation loss. Nowadays, researchers are interested in designing a high-performance MSPA array. To implement the rectangular MSPA array for 5G mm-wave application practically, basic modifications are needed to meet the requirements. With this regard, the main concept that is addressed in this paper is elaborated as follows:

The first concept that has been addressed in this paper is the design methodology and modeling of single element, 2x1, 4x1, 2x2, 4x4, and 8x8 inset-feed rectangular MSPA array at 28GHz for 5G mm-wave applications. In addition, by tuning the design parameters and simulating repeatedly, each of the designed inset-feed rectangular MSPA array performance has been analyzed and also, the simulation results has been compared with design reported in scientific literature in terms of return losses, beam directivity and gain, and radiation efficiency. Generally, in this thesis work, all of the studied antennas are successfully simulated using CST-MW studio software. However, to validate whether achieved simulation results are attainable in real world implementation, their hardware is not manufactured and tested in the antenna laboratory.

1.7 Organization of the Thesis

The thesis is organized under six chapters. The first chapter consists background of the study, statement of the problem, objectives of the study, research questions, significance of the study, scope of the study and organization of the study. The second chapter discusses reviews of proposed and simulated designs of single element and array of rectangular MSPA, conceptual frame work of the study, and basics of rectangular MSPA. The third chapter of the study presents the theoretical explanation of the design parameters and governing equations of rectangular MSPA. The fourth chapter discusses the design procedure and design calculations of single element, linear and planar inset-feed rectangular MSPA array. The fifth chapter is all about the simulation results and discussions of the studied rectangular MSPA array. Finally, the sixth chapter of the study is the conclusion and recommendation of future works.

Chapter 2

Literature Review

2.1 Introduction

In this chapter, the reviews of proposed and simulated designs of rectangular MSPA have been presented. Specifically, the overall chapter is organized as follows. In the first section, the detailed review of the single element rectangular MSPA is presented. In the second section, the detailed review of rectangular MSPA array has been presented. In section three, the conceptual framework of the study is discussed. Finally, theoretical explanation of rectangular MSPA and the feeding techniques of patch antenna is presented.

2.2 Review of Rectangular Microstrip Patch Antenna

2.2.1 Review of Single Element Rectangular Microstrip Patch Antenna

The improvement in wireless communication systems requires the development of low cost, minimal weight, low profile antennas that are capable of maintaining high performance over a wide spectrum of frequency. To meet the requirement, the technological trend has focused much effort to enhance the performance of rectangular MSPA array for the 5G wireless communication systems [12][34][36]. In the following reviews, the proposed single rectangular MSPA for the 5G wireless communication system reported in the scientific literature has been discussed.

Attempting to enhance the performance of rectangular MSPA, a compact inset-feed rectangular MSPA at 28GHz for 5G wireless application has been proposed in [19]. The patch was designed using high-frequency laminated RT5880 substrate. From the simulation, it was found that the antenna is resonating at 28.06GHz with a return losses of -17.4dB, the bandwidth of 1.1GHz, gain of 6.72dBi, directivity of 6.83dBi, and VSWR of 1.2785. The simulation result indicate that, wide bandwidth and low VSWR were achieved. However, the finding may have been more applicable if it had the return losses minimization and improving the directivity.

Similarly, in [10] the design of low profile MSPA at 28GHz frequency has been proposed for 5G mobile phone applications. The patch was designed using the FR-4 substrate with a dielectric constant of 4.4 and a thickness of 0.4mm. Also, the overall dimension of

the antenna was 5.5mm x 4.5mm x 0.4mm. The microstrip feeder line as a lumped port was used to excite the antenna having an input characteristic impedance of 50Ω . The simulated results show that, the antenna is resonating at 28GHz with a return loss of -31.3275dB, a gain of 2.875dB, and VSWR of 1.1155. The achieved result reveals that, the proposed MSPA has a minimum return losses and VSWR. However, performance enhancement in terms of beam gain is not studied. Hence, high path loss encountered due to increased resonant frequency cannot be mitigated by low gain.

In order to simplify the analysis and performance prediction, the shape of the patch is generally square, rectangular, circular, triangular, and elliptical. From this, the most popular shapes are the rectangular, square, and circular patch [11][13][14]. However, for some applications the shape of the patch can be modified to enhance the performance of MSPA in terms of one or more performance metrics. In related to both normal and modified geometry of the patch antenna, the design and analysis of mm-wave MSPA for 5G application has been proposed in [18].

The patch was designed using laminated RT5880 substrates and to match the impedance mismatch between the feeder and the edge of the patch, inset-feeding techniques were used. Before modifying the geometer, from the simulation it was found that the antenna is resonating at 27.48GHz with a return loss of -23.67dB, bandwidth of 1.15GHz, a gain of 6.7dB, directivity of 7.39dBi, radiation efficiency of 81.2%, and total radiation efficiency of 87.1%. However, after the geometer is modified the antenna was resonating at 28GHz with a return loss of -31.16dB, bandwidth of 1.009GHz, directivity of 7.64dB, side lobe level of -18.3dB and VSWR of 1.05.

The above result reveals that, a significant outcome has been achieved in terms of bandwidth and directivity. In addition, by comparing simulation results of both modified and normal geometry, the modified antenna has low return losses, high directivity, and narrow bandwidth. Because of an additional geometer, incompatibility issues will occur and which needs further design consideration. Besides, return loss minimization and improving the directivity, and bandwidth is not always evident to have better performance. Therefore, the study would have been more useful if it had antenna design parameters optimization techniques for further performance enhancement.

In [7] a 28 GHz rectangular MSPA for 5G application has been studied. In the paper, a Roger RT5880 substrate with a dielectric constant of 2.2 and a loss tangent of 0.0009 has been used to design the patch. The physical dimension of the antenna was 6.285mm x 7.235mm x 0.5mm. From the simulation, it was found that the antenna is resonating at 27.954GHz with a return loss of -13.48dB, the bandwidth of 847MHz, a gain of 6.63dB, the directivity of 8.37dBi, the radiation efficiency of 70.18%, SLL of -15.3dB, and VSWR of 1.5376. The key implication drawn from this result is that, good performance has been

achieved in terms of bandwidth, SLL, and directivity. However, the paper fails to take important antenna design parameter optimization into account to enhance the performance of the antenna. As a result, the achieved VSWR is large and the radiation efficiency is low.

In [3] design of MSPA at 28GHz for 5G application has been proposed. The patch was designed using the Rogers RT5880 substrate with a dielectric constant of 2.2, loss tangent of 0.0009 and a thickness of 0.254mm. The overall dimension of the antenna was 14.71mm x 7.9mm x 0.254mm. Moreover, to excite the antenna having an input characteristic impedance of 50Ω , the quarter-wavelength microstrip feeder line was considered as a lumped port to the edge of the patch. From the simulation, it was found that the antenna is resonating at 27.91GHz with a return loss of -12.59dB, bandwidth of 582MHz, a gain of 6.69dB, and VSWR of 1.77. Even though the design was pointing to enhance the bandwidth, the achieved VSWR is large which shows that a large input voltage is standing in the transmission line which leads to low radiation efficiency.

In previous studies, it has been displayed that a decrease in the size of an antenna led to a direct reduction in its gain and bandwidth [18]. In order to extend the use of MSPA for 5G application, the MSPA suffers losses such as conductor, dielectric, and radiation. Which result in narrow bandwidth and low gain. To mitigate this limitation, many broadband patch antennas have been proposed for the bandwidth enhancement. Some of the designs include patch with substrate integrated wave guide, multi-layer and multi-patch designs, different shape with multi slotted patch, co-planar parasitic patches, and stacked patches, or novel shapes patches such as the U and H - shaped patches [13][15][21].

Accordingly, in [21] design of U-slotted rectangular MSPA at 28GHz has been proposed for 5G applications. The antenna was designed using Roger RO4350 substrate with a thickness of 1.57mm, dielectric constant 3.66 and loss tangent of 0.004. Moreover, coaxial-probe feeding method has been used to excite the antenna. The simulated result shows that the antenna is resonating at 28.06GHz with a return loss of -20dB, a gain of 4.06dBi, the directivity of 4.15dBi, and VSWR value of 1.02. Even though the proposed design plays a vital role to enhance bandwidth and minimize the magnitude of VSWR, this approach failed to consider minimization of the impedance mismatch at the feed point targeted to have a minimum return losses. In addition to this, since 5G devices are expected to have a very compact size, the selected substrate thickness causes size incompatibility.

Further more, for the future 5G wireless communication systems the design of MSPA at 28GHz and 50GHz has been proposed in [20]. The proposed antenna was designed using Rogers RT5880 substrate with a dielectric constant of 2.2 and a miniaturized size of 4.4mm x 3.3mm. The dimensions of the antenna were 11mm x 8mm x 0.5mm. From the simulation, it was found that the antenna is resonating at 28.3GHz and 50.3GHz with a return loss of -21dB and -31dB respectively and the gain of 2.6dB. However, the design was

pointing to the need for minimization of MSPA return losses which failed to take important performance metrics enhancements into account.

The overall performance of the MSPA is determined by the selected substrate material type and thickness, the shape of the patch geometry and the dimension of the physical structure of the antenna. For instance, the thickness of the dielectric substrate deteriorates the antenna bandwidth and radiation efficiency, by increasing surface wave and spurious feed radiation along with the feeding line [12][14].

With this regard, the effect of dielectric constant and substrate height on radiation efficiency, beam directivity and gain, fringing field, and radiation pattern of mm-wave rectangular MSPA has been explicitly studied in [12] using polypropylene and alumina as substrate material. For the particular height of 1.5mm of polypropylene substrate, it was found that the radiation efficiency, directivity, and gain were 99.0257%, 8.688dB, and 8.604dB respectively. In the paper, it has been concluded that the polypropylene tape shows the highest radiation efficiency, directivity, and gain than the alumina substrate. The fringing field created by the patch antenna depends on the relative dielectric constant and height of the substrate. However, increasing SH leads to low radiation efficiency and directivity.

A novel design of compact 28GHz wide band printed antenna for 5G applications has been proposed in [40]. In the paper, the patch is designed using Rogers substrate material with dielectric constant of 2.2, thickness of 0.254mm, and tangent loss of 0.0009. The antenna is excited using coaxial feeding technique and X-shape slotted deflective ground surface is used in order to increase the bandwidth. The simulation result shows that, the return loss, bandwidth, gain, and radiation efficiency of the antenna are -20.03dB, 2.11GHz, 5.23dBi, and -0.8181dB respectively.

In [41] the design and simulation of a 28 GHz rectangular MSPA for 5G technology has been studied. The antenna is designed using Taconic substrate material with dielectric constant of 2.2, thickness of 0.12mm, and loss tangent of 0.0009. Using simulation, it was found that, the return loss of the antenna is -27.7dB, bandwidth is 463MHz, gain is 6.72dB and radiation efficiency is -1.199dB.

2.2.2 Review of Rectangular Microstrip Patch Antenna Array

From the above reviews, different study of rectangular MSPA structures using simulation show that there is no single best design in terms of all the performance metrics of the antenna. In attempting to improve the performance of rectangular MSPA by increasing the number of antenna elements, many studies have been reported for different applications. Therefore, in the following reviews, the design approach and achieved simulation result of the proposed rectangular MSPA array at 28GHz for 5G wireless communication system reported in the scientific literature have been discussed.

The design of a single element and 2x2 inset-feed rectangular MSPA array at 28GHz has been presented in [9]. The patch was designed using Rogers substrate with the dielectric constant of 2.9 and loss tangent of 0.0025. Besides, microstrip inset-feed and coaxial feeding techniques were used for matching the radiating patch to the 50 Ω microstrip feed line. Using the simulation, it was found that the proposed single patch antenna is resonating at 27.98GHz with a return loss, bandwidth, gain, directivity, radiation efficiency, total radiation efficiency, and VSWR of -20.533dB, 400MHz, 6.22dB, 7.966dBi, 65.6%, 64.98%, and 1.02294 respectively.

In addition, the coaxial feed based 2x2 inset-feed MSPA array which was made from four single MSPA is resonating at 27.904GHz with a return loss of -19.6611dB, the bandwidth of 400MHz, a gain of 8.393dBi, directivity of 10.13dBi, radiation efficiency of 67.096%, total radiation efficiency of 64.476%, and VSWR of 1.232. From the result, it has been observed that for both designs good performance were obtained in the aspect of bandwidth, directivity, and VSWR. However, within the feeding networks of the antenna, the impedance matching is poor which results in a large magnitude of the return loss. Therefore, the simulated results was limited in radiation efficiency and return loss.

Further more, in order to improve the performance of rectangular MSPA in terms of radiation efficiency and directivity, increasing the number of an array element and changing feeding techniques has been widely used. Accordingly, in [36] the design and simulation of directive high gain microstrip array antenna for 5G cellular communication has been studied. In the paper, single element, 2x1, 4x1, and 8x1 patch antenna array have been included and the patch were designed using Rogers RT5880 substrate with a dielectric constant 2.2, loss tangent of 0.0009 and thickness of 0.254mm.

From the simulation, it was found that single element, 2x1, 4x1, and 8x1 arrays are resonating at 28GHz with a return loss of -59.3692dB, -16.65dB, -37.579dB, and -50.99dB respectively. Similarly; the directivity of 8.41dBi, 12.44dBi, 16.45dBi, and 20.94dBi respectively; the gain is about 8.5dBi, 12.42dBi, 16.48dBi, and 21.04dBi respectively. The bandwidth of a single element and 8x1 array were 430MHz and 520MHz respectively. The key implication of achieved results is the significant outcome has been obtained in terms of the directivity, return loss, and beam gain. However, the proposed design was limited because, the physical structure of the proposed antenna may not be compatible due to phase shifter structure at feeding networks. In addition, the SLL of the linear array is large which leads to increased interference at the receiver side.

In [13] design and analysis of 28GHz rectangular MSPA array has been studied including single element, 2x1, and 4x1 array. The antenna was designed using FR-4 substrate type with a dielectric constant of 4.35, loss tangent of 0.005, and a thickness of 0.1mm. From the simulation, it was found that a single element, 2x1, and 4x1 arrays are resonating at 28GHz

with a return loss of -15.3527dB, -14.7dB, -21.44757dB, and the directivity of 6.921dBi, 9.853dBi, 11.99dBi respectively. Similarly, the VSWR were 1.7871, 1.624, 1.6502 and the radiation efficiency is about 87.77%, 92.7%, 83.95% respectively. The total radiation efficiency of the designed antenna was 80.77%, 87.43%, and 78.9% respectively. Even though the result is within the acceptable ranges, the study fails to take precise impedance matching between the feed point and edge of the patch, the radiation efficiency enhancement, and mutual coupling minimization. In addition, the height of the substrate is varied with array elements. Generally, design parameter optimization to improve overall performance needs further studies.

Similarly, the design and analysis of 28GHz mm-wave antenna array for 5G communication systems has been studied in [15]. In the paper, design of a single element, 2x1, and 4x1 patch antenna array have been included. The patch was designed using Rogers RT5880 substrate with a dielectric constant of 2.2 and a thickness of 0.254mm. The overall dimension of the single patch was 14.71mm x 7.9mm x 0.254mm. A quarter-wavelength microstrip transmission line as a lumped port was used to excite the antenna having an input characteristic impedance of 50 Ω .

Using the simulation it was found that, the resonant frequency of single patch, 2x1, and 4x1 antenna array was 27.87GHz, 27.91GHz, and 27.59GHz respectively. Besides, the bandwidth was 582MHz, 516.6MHz, and 519MHz respectively. The gain of 2x1 and 4x1 arrays were 10.07dB and 13.55dB respectively. Due to the lack of accurate design parameters, the resonant frequency of the antenna is not exactly at 28GHz. Also, the achieved performance was limited in terms of directivity and bandwidth.

The performance comparison of rectangular and circular Patch antenna array has been presented in [22]. In the paper, single element, 2x1, and 4x1 array of both shapes are designed and simulated. From the simulation, it was found that in both shapes gain and directivity are increasing as the number of elements is increased. However, planar array has better suppression for side lobe levels than the circular patch antenna array.

An extensive study of linear array synthesis has been presented in [27]. It was found that, the side lobe level and null placement in the desired direction are major issues in antenna array radiation pattern. A linear array has high directivity and it can form the narrowest main lobe in a given direction, but it does not perform efficiently in all azimuth directions. Therefore, one of the main constraints of linear array is inability to scan the beam in more than one dimension [28]. In the next sections, reviews of the proposed phased array antenna for the future 5G wireless communications have been discussed.

In [23] design of a phased array antenna with sub-array configurations was proposed to achieve 3D beam coverage. In the proposed design three planar phased sub-array configurations were used to switch the beam pattern to their distinct regions using chassis surface

wave excitation. The whole phased array switches the main beam between sub-arrays in the ϕ direction and scans the beam in the θ direction with variable phase shifts. The 3D spherical coverage is achieved by merging the beam patterns of sub-arrays with 2GHz 10dB impedance bandwidth at 28GHz. In the proposed design it was found that all the elements between sub-arrays have lower mutual coupling, high steering ranges, and moderate efficiency. However, the achieved in terms of directivity, beam gain, and stability is low.

Phased array antenna with switchable three-dimensional scanning for 5G mobile terminals was proposed in [24]. The proposed antenna contains three similar sub-arrays of patch antennas arranged along the edge of the mobile terminal and each sub-array consists of eight rectangular MSPA and element with beam scanning capability of ± 90 degree in the θ plane. It was found that the proposed design has achieved a 1GHz bandwidth in the frequency range from 21 to 22 GHz and it has a good beam-scanning range of -90 degree to $+90$ degree with a gain of more than 12.5dBi.

In [25] design of a 28GHz phased array antenna for future 5G mobile-phone applications has been proposed. The proposed antenna was designed on a low-cost substrate (FR-4) to operate at 28GHz and ten elements of slot-loop antenna elements have been used to form a uniform linear array on the top region of the cellular handset PCB. Besides, to validate the proposed design, a prototype has been made. The simulated and measured results found that the antenna has the S_{11} response less than -10dB in the frequency range of 27 to 29GHz. The radiation and total efficiency of the antenna arrays were higher than -0.5dB (90%) for the scanning range between 0 to 50 degrees, while the gains are higher than 13dB. They employed a new air-filled slot-loop structure as the radiator good performance has been achieved in terms of gain and radiation efficiency.

The design of an 8x8 planar phased array antenna with high efficiency and insensitivity Properties for 5G mobile base station has been presented in [26]. The proposed antenna was designed on a low-cost substrate to operate at 21-23.5GHz and 64 elements of slot-loop antenna elements as eight linear arrays (1x8) have been arranged to build planar 8x8 phased array antenna. The simulated results show that the proposed phased array antenna has high efficiency, acceptable gains and good beam steering characteristics at different scanning angles. However, due to the edge element of the array, the gain and radiation pattern of the antenna is highly fluctuating, and the steering range of the antenna is minimum.

A 28GHz printed antenna for 5G communication with improved gain has been proposed in [42]. The patch is designed using FR-4 substrate material with thickness of 1.6mm. To excite the proposed antenna, microstrip quarter-wavelength impedance transformer is used. From the simulation result, it has been observed that the return loss, bandwidth, and gain of the 2x2 antenna are -20dB, 0.95GHz, and 7.2dBi respectively.

Furthermore, in [43], design of a novel patch antenna array for 5G mm-wave appli-

cations has been proposed. In the paper, 1 x 4 linear and 2 x 2 planar multi-band array antennas are designed using Rogers substrate with dielectric constant of 2.2, thickness of 0.508mm, and tangent loss of 0.0013. The simulated results under six different frequencies of linear array indicate that return losses are less than -10dB and their radiation efficiency are in the range of 90%. It is concluded that linear setup has better gain than array of planar setup whereas bandwidth and return loss of planar array is better than linear array.

2.3 Conceptual Frame Work of the Study

All the papers reviewed above, the design considerations of the proposed single element and array of rectangular MSPA is to achieve good performance in one of the major performance metrics and to keep the remaining performance metrics in the acceptable ranges. With this regards, to design rectangular MSPA characterized by wide bandwidth various designs were proposed and simulated. These include; using slotted patch, modifying the physical geometer of the patch, increasing the physical structures of the antenna, and by using different feeding techniques as reported in [7][18][19][21].

Similarly, based on designs reported in [3][9][13][15][21], in order to minimize the impedance mismatch at the edge of the patch and feeding network structures, they have used quarter wavelength microstrip feed-line as inset-feed and lumped element to the edge of the patch. In addition, the width of the microstrip feeder-line has been selected randomly without analyzing the performance trade-off between the design parameters.

Furthermore, to design rectangular MSPA array characterized with high directivity, narrow beams, and low side lobe levels, many studies have been carried out. These includes: by increasing the physical dimension of the patch width and ground plane, and mainly by increasing the number of array elements. However, the main focus of the studies was only to design and simulate linear rectangular MSPA array. Therefore, further studies is required to design and simulate planar configuration of rectangular MSPA array.

In all of the proposed designs of rectangular MSPA arrays, the substrate height is varied with the array element to reduce the design challenges of the designer. Even though changing the substrate height with array elements provides good performance for specific performance metrics, it gives low or unacceptable performance for remaining parameters. Therefore, system stability and manufacturing complexity issues will occur which results difficulty in implementation for some of the designs.

Generally, from above the proposed design of rectangular MSPA, one can easily infer that the studies did not explore the performance comparison of different linear and planar rectangular MSPA array configuration at 28GHz using inset-feed and quarter-wavelength impedance matching techniques, and tuning the parameters of the antenna.

Therefore, to increase the performance of the rectangular MSPA for mm-wave communication systems, in this study the design and comparative performance assessment of different size of linear and planar rectangular MSPA array configurations at 28GHz have been studied.

2.4 Rectangular Microstrip Patch Antenna

A microstrip patch antenna is a single layer design which contains mainly four parts. These are: patch, ground plane, substrate and feeding part. A microstrip antenna consists of a radiating patch on one side of a dielectric substrate material which has a ground plane on another side as shown in Figure 2.1. The basic antenna element is a strip conductor of length PL and width PW on a dielectric substrate. The thickness of the patch being t with a substrate height of SH supported by a ground plane. The strip conductor is made from conducting material such as copper, silver or gold.

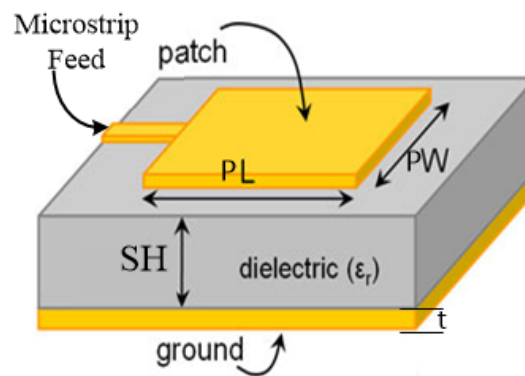


Figure 2.1: Rectangular Microstrip Patch Antenna.

The radiating patch can have any shape but to simplify the analysis and performance prediction, the shape of the patch is generally square, rectangular, circular, triangular, and elliptical or some other common shape. From these, the rectangular MSPA is the widely used of all the types of microstrip antennas that are present. Generally, the patch in the antenna is simple and very versatile in terms of resonant frequency, polarization, pattern, and impedance. Moreover, patch antennas can be mounted on the surface of high-performance aircraft, spacecraft, rockets, satellites, missiles, cars, and even hand-held mobile telephones. Therefore, the MSPA plays a vital role in the fastest-growing wireless communications industry [11][14][15].

Figure 2.2 given below shows that, voltage, current, and impedance distribution of patch antenna. As it can be depicted from figure, for particular design when the rectangular patch antenna is excited, the ratio of E to H-field is proportional to the impedance of the feed location. At the center of the patch the impedance is minimum and at the edge of the

patch the impedance is maximum which is around 300Ω . At the end of the patch current is zero and the voltage is maximum. Also, at the center of the patch the voltage is minimum and the current is maximum [11][16][30].

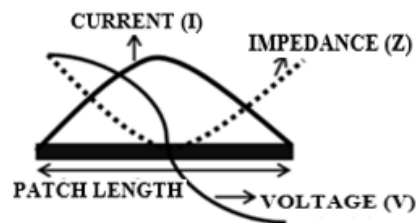


Figure 2.2: Voltage, Current, and Impedance Distribution of Patch Antenna.

The radiation of the rectangular patch antenna occurs from the fringing fields between the edge of the patch conductor and the ground plane. Therefore, fringing E-fields between the edges of the rectangular patch and the ground plane is add up in phase due to voltage distribution and produce the radiation. The produced fringing field around the edges of the rectangular patch is the extended parts of the electric field which does not abruptly end at the edge of the patch. Hence, with respect to the ground plane, the fields at the edges of the patch can be resolved into tangential and normal components as indicated in Figure 2.3.

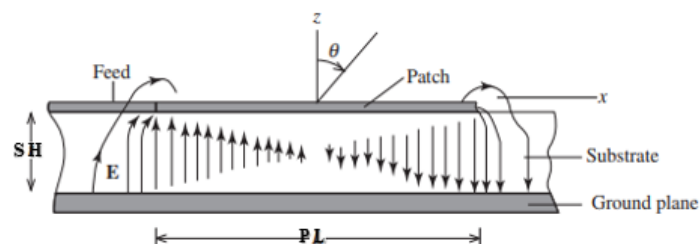


Figure 2.3: Side view showing the electric fields [16].

The normal components of the electric field at the two edges along the width are in opposite directions and out of phase, and they cancel each other in the broadside direction. Because, the patch is assumed to be $\lambda_{SM}/2$ long. Where λ_{SM} is the wavelength in the dielectric substrate material. Therefore, in phase tangential components fields are combined to give maximum radiated field normal to the surface of the patch. In general, the overall performance of the MSPA is determined by selected substrate material type, the dimension of the physical structure and the feeding techniques of the antenna. Moreover, the rectangular MSPA is used not only as single elements also they are very popular and suitable in the antenna array [11][16][38].

2.4.1 Microstrip Feeding Techniques

The patch antenna feeding methods including coaxial feed, aperture coupling, and proximity coupling. Among the methods, the microstrip feed-line is preferred as an efficient feeding scheme because of its simple fabrication, easy connection to the dielectric substrate and impedance matching property. In microstrip feeding techniques, the antenna excitation is provided using the microstrip-line. The microstrip feed line is a conducting strip, usually of a much smaller width compared to the patch. The advantages of microstrip feed line are easy to fabricate, to model, and simple to match by controlling the feed position. However, the disadvantage is as the substrate thickness increases the surface waves and spurious feed radiation is also increases, which limits the bandwidth between 2-5% for practical designs. Another drawback is the radiation from the feed line leads to an increase in the cross-polarization level [11][12].

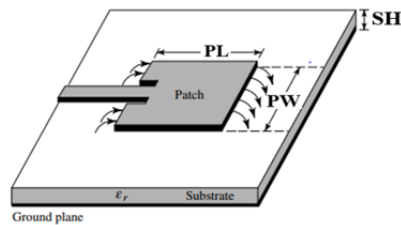


Figure 2.4: Patch Antenna with Microstrip Feed-Line [11].

Moreover, the microstrip-line feeding techniques can be extended to feed parallel array of rectangular MSPA. Microstrip corporate (Parallel) feeding array technique are general and versatile microstrip feeding techniques for MSPA array. The corporate-feed network is used to provide power splits of 2^n (i.e. $n=2, 4, 8, 16, 32$, etc.). This is accomplished by using tapered lines as shown in Figure 2.5 to match edge of the patch to a 50Ω feeder line.

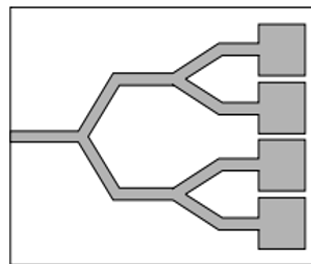


Figure 2.5: Corporate Feed of MSPA Array.

In the corporate-feeding techniques, amplitude and phase of each element are more controllable than the element in the series feed. Therefore, the phase of each element can be controlled using phase shifters while the amplitude can be adjusted using either amplifiers or attenuators which is a major advantage over other array implementations [11][16].

Chapter 3

Design parameters of Rectangular Microstrip Patch Antenna

3.1 Introduction

This chapter presents, the design parameters and governing equation of rectangular MSPA, transmission line model of rectangular microstrip patch antenna have been presented. Finally, performance metrics used to analyze the characteristics of the antenna is presented.

3.2 Initial Design Parameters of Rectangular MSPA

The very primary steps to begin the designing of the rectangular MSPA are choosing the operating frequency, substrate type, and substrate thickness. The frequency of operation is the frequency at which the antenna can receive or transmit the signals. It can be calculated when the height of the patch is known or can be selected before the design.

Similarly, a dielectric substrate is a substrate that does not conduct direct current and therefore used as an insulator. The dielectric constant (ϵ_r) is defined as the ratio of the permittivity of a substance to the permittivity of free space. The dielectric constants of the substrate are normally in the range of $2.2 \leq \epsilon_r \leq 12$, which enhances the fringing fields that account for radiation [12][14][30][36]. The parameters used to determine the electrical characteristic of the antenna is substrate type and thickness, and permittivity.

- **Substrate Thickness Effects:** The substrate thickness (SH) affects dispersion. A thicker substrate causes more dispersion. From a simple consideration, this seems to follow from the fact that the in-homogeneity of the transmission line is increased with more dielectric. A more rigorous approach is to compare the substrate thickness to the wavelength in the material. As the ratio of substrate thickness to wavelength in the material is reduced, the dispersion is also reduced.
- **Substrate Dielectric Constant Effects:** The substrate dielectric constant also affects dispersion and eye quality. The lower the dielectric constant which is closer to air is the homogeneous case i.e., no dispersion. In general, lower dielectric constant is used

to achieve higher bandwidth, better efficiency and low power loss. However, it causes the surface waves to propagate and spurious coupling.

Generally, in order to give support and protection for the patch element, the dielectric substrate has to be strong enough and able to endure high temperatures during the soldering process. Hence, the selection of dielectric substrate material with their thickness and dielectric constant need accuracy.

3.3 Design parameters and Governing Equations of Rectangular Microstrip Patch Antenna

The performance characteristics of rectangular patch antenna is mainly defined by the shape of the patch, the dimension of the physical structure, and the material properties from which it is made. After initial design parameters are chosen, the following design parameters is calculated with great attention. These includes; height of the substrate, length and width of the patch and feeder-line, effective length of the patch, the length extension of the patch, actual length of the patch, location of the feed point, and dimensions of ground plate. Therefore, all of these design parameters are discussed as follows.

3.3.1 Height of the Substrate

The height of the rectangular MSPA is associated with the substrate height or thickness. The patch antenna stops resonating with a very thick substrate. Therefore, it is usually in the range of $0.003 \lambda_0 \leq SH \leq 0.05 \lambda_0$. The limitation on the height of the substrate for a given material and F_0 is governed by [11][30][36]:

$$SH \leq 0.06 \frac{C}{2\pi F_0 \sqrt{\epsilon_r}} \quad (3.1)$$

The substrate height can be selected before calculating F_0 of the antenna or F_0 can be used to find the height or both can be selected before the design but it must meet the condition given at equation 3.1. If the thickness of the substrate of the MSPA is very small, there is a reflection of waves at the edge of the patch that is generated in the dielectric substrate. As a result, a very small amount of energy is radiated [11][16]. The height of the substrate (SH) is calculated using equation [11][34]:

$$SH = \frac{0.3C}{2\pi F_0 \sqrt{\epsilon_r}} \quad (3.2)$$

Where, C , F_0 , ϵ_r denotes speed of light, operating frequency, and dielectric constant.

3.3.2 Width of the Patch

The width of the patch has less effect on the resonant frequency and radiation pattern. But, it greatly affects the radiation efficiency and cross-polarization characteristics of the antenna. The width of the patch determines the range of antenna bandwidth. The radiation efficiency of patch antenna increase as the width increases up to half wavelength. The width of the patch antenna is calculated using [7][12][14][30][34]:

$$PW = \frac{C}{2F_0 \sqrt{\frac{\epsilon_r + 1}{2}}} \quad (3.3)$$

Where, PW denote the width of the patch, C is the speed of light, F_0 is operating frequency, and ϵ_r is a dielectric constant.

3.3.3 Effective Dielectric Constant

The effective dielectric constant is unique to a fixed dielectric transmission line system and provides a useful link between various wavelengths impedance and velocities. The effective dielectric constant is kept slightly less than the dielectric constant of the substrate so that the fields not entirely get confined to the substrate but also fringe and spread in the air. Therefore, the range of the effective dielectric constant is between $1 < \epsilon_{reff} < \epsilon_r$. After PW and SH is known the effective dielectric constant can be obtained using [11][12][16][18]:

$$\epsilon_{reff} = \left(\frac{\epsilon_r + 1}{2} \right) + \left(\frac{\epsilon_r - 1}{2} \right) \left(1 + 12 \left(\frac{SH}{PW} \right) \right)^{-0.5} \quad (3.4)$$

Where, ϵ_{reff} is effective dielectric constant, ϵ_r is a relative dielectric constant of the substrate, PW is the width of the patch, and SH is the height of the substrate.

3.3.4 Effective Length of the Patch

The effective length of the patch is the sum of the actual length and twice of extended length or it can be calculated using equation 3.5. Also, effective length of the patch is used to calculate the original length of the patch and mathematically given by [11][12][30][32]:

$$PL_{eff} = \frac{C}{2F_0 \sqrt{\epsilon_{reff}}} \quad (3.5)$$

Where, PL_{eff} is the effective length of the patch, C is the speed of light, ϵ_{reff} is effective dielectric constant, and F_0 is operating frequency.

3.3.5 Length Extension of the Patch

In the rectangular patch antenna, due to fringing field effects electrically the patch of the antenna looks greater than its physical dimensions. Therefore, the dimensions of the patch along its length is extended on each end by a distance of ΔPL as indicated in Figure 3.1.

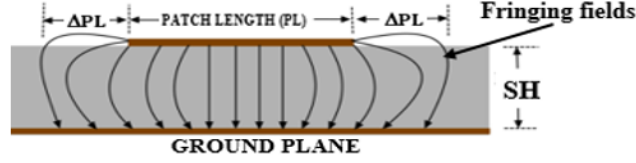


Figure 3.1: Length Extension Due to Fringing Effects [31].

The length extension is a function of the effective dielectric constant and a function ratio of the width-to-height, and calculated using the equation given below [12][14][16][20][32].

$$\Delta PL = (0.412SH) \frac{(\epsilon_{\text{reff}} + 0.3) \left(\left(\frac{PW}{SH} \right) + 0.264 \right)}{(\epsilon_{\text{reff}} - 0.258) \left(\left(\frac{PW}{SH} \right) + 0.8 \right)} \quad (3.6)$$

Where, ΔPL is the patch length extension, SH and PW , is the height of the substrate and width of the patch, and ϵ_{reff} is the effective dielectric constant of the substrate.

3.3.6 Actual Length of the Patch

In patch antenna design, the actual length of the patch is a critical parameter. Because it inherent narrow bandwidth of the patch and controls the resonant frequency. For a rectangular patch antenna the length of the patch is usually between $0.3333\lambda_0 < PL < 0.5\lambda_0$ [30]. Where, λ_0 is the free-space wavelength. The radiating fields are not confined to the patch but a small fraction of the radiating fields lie outside the physical dimension of the patch. Therefore, the actual length of the patch is the difference between the effective length and twice of patch length extension which computed using [11][12][14][18][36]:

$$PL = PL_{\text{eff}} - 2\Delta PL \quad (3.7)$$

Where, PL_{eff} is the effective length and ΔPL is the patch length extension.

3.3.7 Ground Plane Dimension

In practice, the fields are not only confined to the patch i.e. a fraction of the fields lies outside the physical dimensions of the patch because the dimensions are finite. Since some of the waves travel in the substrate and some in the air, effective permittivity is introduced

to account for the fringing field along all the edges of the patch and the wave propagation in the patch. The length and width of the substrate is more than the length and width of the patch. Therefore, the overall dimension of the substrate is designed to completely encapsulated the patch and the feed line. It means the ground plane dimension has to be large enough to support fringing fields. The ground plane dimension is calculated using the equation given below [7][12][14][18][36].

$$GL = PL + 6SH \quad (3.8)$$

$$GW = PW + 6SH \quad (3.9)$$

Where, GL, GW, PL, and PW are denotes length and width of the ground plane and the patch respectively.

3.3.8 Location of the Feed point

In order to match the impedance mismatch between edge of the patch and the feeder, the location of feed point to the rectangular patch antenna is located in X-Y coordinates as X_f and Y_f respectively. The feed point locations is calculated by [11][14]:

$$X_f = \frac{PL}{2\sqrt{\epsilon_{\text{reff}}}} \quad (3.10)$$

$$Y_f = \frac{PW}{2} \quad (3.11)$$

Where, X_f and Y_f are X-Y coordinates, PW and PL are the width and length of a patch.

3.3.9 Impedance Matching

As the electromagnetic wave travels to different parts of the antenna, they encounter different impedance at each interface. Therefore, whenever there is an impedance mismatch at any of the interfaces it causes some of the electromagnetic waves to reflect back to the source. Good matching enhances the performance of the antenna, thereby increasing the bandwidth of the antenna and reduces the signal loss due to reflection. Hence, the efficient coupling matching network is used which attempts to match the characteristics impedance of the two elements over the desired frequency range [11][12][16]. Theoretically, at the edge of the patch the impedance is around 300Ω . However, it can be matched to $Z_0 = 50\Omega$ transmission lines using different matching networks. The quarter-wavelength impedance transformer which is shown in figure below is commonly used to match the impedance between the transmission line and the edge of the patch.

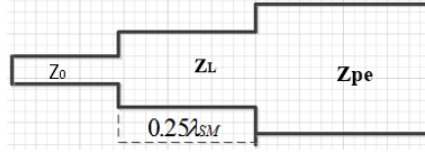


Figure 3.2: Quarter-wave length impedance Transformer Network.

Generally, the quarter-wavelength impedance transformer can be designed, first by calculating the impedance at the edge of the patch (Z_{pe}) and load impedance (Z_L), using the mathematical equation given below [12][16][35].

$$Z_L = \sqrt{Z_0 * Z_{pe}} \quad (3.12)$$

$$Z_{pe} = 90 \left(\frac{\epsilon_r^2}{\epsilon_r - 1} \right) \left(\frac{PL}{PW} \right)^2 \quad (3.13)$$

Where, Z_0 , Z_L , and Z_{pe} denotes characteristic, load, patch edge impedance respectively.

3.3.10 Width and Length of the Microstrip Feeder Line

A microstrip feeder line is positioned between the source and the antenna. The interface occurs between the antenna and the feed line along the width of the feeder line. Therefore, the impedance varies with the width rather than its length. Because with a given width of the feed line the impedance is almost independent of the variation in the length.

A. Length of the Microstrip Feeder Line $L_{(MFL1)}$

The length of the microstrip feeder line is calculated using equation given below [12].

$$L_{(MFL1)} = \frac{\lambda_{SM}}{4} = \frac{\lambda_0}{4\sqrt{\epsilon_r}} \quad (3.14)$$

but, free-space wave length (λ_0) is calculated by using :

$$\lambda_0 = \frac{C}{F_0} \quad (3.15)$$

Where, C is the speed of light, F_0 is the frequency of operation, λ_0 is the free-space wavelength, λ_{SM} is the wavelength in the substrate, and ϵ_r is a dielectric constant of the substrate.

B. Width of the Microstrip Feeder Line $W_{(MFL1)}$

The width of the microstrip feeder line is obtained by [7][12]:

$$W_{(MFL1)} = \frac{5.98SH \left(\frac{1}{\exp\left(\frac{Z_0\sqrt{\epsilon_r+1.41}}{87}\right)} \right) - t}{0.8} \quad (3.16)$$

Where, SH is substrate height, t is patch thickness, Z_0 is characteristic input impedance, and ε_r is relative dielectric constant.

3.3.11 Inset Dimension

A. Inset Length (Y_0)

At the edge of the patch, the input impedance is high. However, impedance falls rapidly if the inset position is moved from the edge of the patch towards the center. In order to provide impedance matching with a 50Ω connector, the inset feed depth (Y_0) is used. The inset length is calculated using [11][14][35]:

$$Y_0 = \left(\frac{PL}{\pi} \right) \cos^{-1} \sqrt{\left(\frac{Z_0}{Z_L} \right)} \quad (3.17)$$

Where, PL, Z_0 , and Z_L are denotes length of the patch, characteristic, load impedance respectively.

B. Inset Gap (G_p)

The resonant frequency of the patch antenna depends on the notch gap. The expression which relates inset-gap and the resonant frequency (F_0) is given by [36]:

$$G_p = \frac{4.65 * 10^{-12} * C}{F_0(\text{inGHZ})\sqrt{2 * \varepsilon_{\text{reff}}}} \quad (3.18)$$

Where, C is speed of light, and $\varepsilon_{\text{reff}}$ is effective dielectric constant.

3.3.12 Width and Length of the Feed Point

A. Width of feed point: Is calculated by using the equation given by [16][37]:

$$W_{(\text{FP})} = \frac{2SH}{\pi} \left[([B - 1] - \ln[2B - 1]) + \left(\frac{\varepsilon_r - 1}{\varepsilon_r} \left[\ln[B - 1] + 0.39 - \frac{0.6}{\varepsilon_r} \right] \right) \right] \quad (3.19)$$

Where, SH is substrate height, ε_r is dielectric constant, and B is constant. However, B and $Z_{(MFL1)}$ are calculated before calculating the width of the feed point. Therefore, $Z_{(MFL1)}$ is calculated by using equation 3.32 and B is calculated by [16]:

$$B = \frac{60\pi^2}{Z_{MFL1} \sqrt{\varepsilon_r}} \quad (3.20)$$

B. Length of the feed point: is calculated by using the equation given by:

$$L_{(\text{FP})} = \frac{\lambda_{\text{eff}}}{4} \quad (3.21)$$

But, effective wave length is given by:

$$\lambda_{\text{eff}} = \frac{\lambda_0}{\sqrt{\epsilon_{\text{reff}}}} \quad (3.22)$$

Where, λ_0 is free-space wavelength, λ_{eff} is effective wavelength, and ϵ_{reff} is effective dielectric constant of the substrate.

3.4 Transmission line Model of Rectangular MSPA

In the transmission line model, the patch antenna is represented by two radiating slots of width PW and height SH separated by a transmission line of length PL as shown in Figure 3.3. The patch antenna is considered as non-homogeneous of two dielectrics (i.e., the substrate and air). Therefore, most of the electric field lines reside in some parts in the air and the rest in the substrate which leads to the transmission model does not support the transverse electric magnetic mode of transmission, as phase velocities would be different in the substrate and the air [11][14].

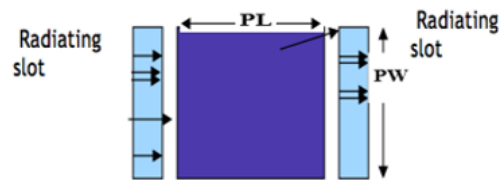
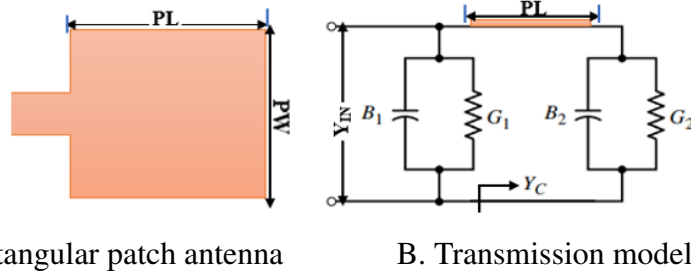


Figure 3.3: Transmission line model of Rectangular MSPA.

The transmission line model is easy to use and it gives good physical insight. Furthermore, due to its accuracy and numerical efficiency, transmission line model is used to predict the input characteristic of the patch. However, all types of configurations cannot be analyzed using transmission line model. Because, it does not take care of variation of field in the orthogonal direction to the direction of propagation and does not predict the input characteristic much beyond a fundamental resonance. The rectangular MSPA can be expressed as an equivalent electrical circuit. The equivalent circuit represents the whole antenna in the form of two radiating slots modeled using parallel RC circuits and the patch connecting these RC circuits is in the form of a transmission line whose characteristics are computed similarly as a normal microstrip transmission line. Therefore, in transmission line mode each radiating slot is represented by a parallel equivalent admittance (Y) with conductance

(G) and susceptance (B).



A. Rectangular patch antenna

B. Transmission model equivalent circuit

Figure 3.4: Rectangular MSPA and its Equivalent Circuit in Transmission Line Model.

Considering an infinitely wide and uniform slot, equivalent admittance of slot one is:

$$Y_1 = G_1 + jB_1 \quad (3.23)$$

Also, for a slot of finite width, conductance G and susceptance B is given by:

$$G_1 = \frac{PW}{120\lambda_0} \left[1 - \frac{1}{24} (K_0 SH)^2 \right], \frac{SH}{\lambda_0} < \frac{1}{10} \quad (3.24)$$

$$B_1 = \frac{PW}{120\lambda_0} \left[1 - 0.636 \ln(K_0 SH) \right], \frac{SH}{\lambda_0} < \frac{1}{10} \quad (3.25)$$

Where K_0 is the constant, SH is height of the substrate, λ_0 is free-space wavelength, PW is width of patch, B_1 and G_1 are susceptance and conductance of slot one respectively.

The total admittance produced at one radiating slot is determined by transforming the admittance at the other radiating slot using the transformation equations of the transmission line. Ideally, the two slots are separated by $\lambda_{SM}/2$. But, because of fringing effects the length of the patch is electrically longer than the actual length. Hence, the actual separation of the two slots is slightly less than $\lambda_{SM}/2$. But, if the length is properly chosen in the range of $0.48 \lambda_{SM} < PL < 0.49 \lambda_{SM}$, the transformed admittance of slot two can be written as:

$$Y_2^{\sim} = G_2^{\sim} + jB_2^{\sim} = G_1 - jB_1 \quad (3.26)$$

$$G_2^{\sim} = G_1 \quad (3.27)$$

$$B_2^{\sim} = B_1 \quad (3.28)$$

At the feeding network, perfect impedance matching is necessary to transfer maximum power from the port to the feed line which is connected to it. Hence, the input impedance plays an important role to determine the amount of power delivered to the feed line. The

total input admittance and the resonant input impedance is real and it is given by:

$$Y_{in} = Y_1 + Y_2 \approx 2G_1 \quad (3.29)$$

$$Z_{in} = \frac{1}{Y_{in}} = R_{in} = \frac{1}{2G_1} \quad (3.30)$$

The resonant input resistance can be decreased by increasing the width of the patch. This is acceptable as long as the ratio of PW/PL does not exceed two. Because the aperture efficiency of a single patch begins decreasing PW/PL increases beyond two. Therefore, when slot one is considered as a reference slot, the resonant input resistance is calculated using the equation 3.30. However, equation 3.30 does not consider the mutual effects between the slots. So, by considering the mutual effects between the slots, the resonant input resistance is calculated by using equation given below [11].

$$Z_{in} = \left[\frac{1}{G_1 \pm G_{12}} \right] \quad (3.31)$$

In the above equation, the plus sign in the denominator is used for modes with odd (anti-symmetric) resonant voltage distribution beneath the patch and between the slots while the minus sign is used for modes with even (symmetric) resonant voltage distribution. In order to change the resonant input resistance an inset feed, recessed a distance Y_0 from slot one is also used as shown in Figure 3.5. This technique can be used effectively to match the patch antenna using a microstrip-line feed whose characteristic impedance is given by [11]:

$$Z_{(MFL1)} = \frac{120\pi\sqrt{\epsilon_{reff}}}{\frac{W_{(MFL1)}}{SH} + 1.393 + 0.667\ln\left(\frac{W_{(MFL1)}}{SH} + 1.44\right)}, \frac{W_{(MFL1)}}{SH} > 1 \quad (3.32)$$

Where, $W_{(MFL1)}$ is the width of the feeder, SH is the height of the substrate, and ϵ_{reff} is effective dielectric constant.

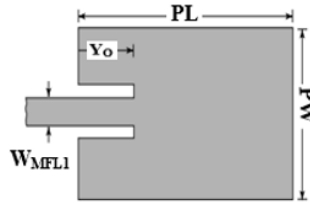


Figure 3.5: Recessed Microstrip-Line Feed [11].

The mutual conductance is defined in terms of the far-zone fields as:

$$G_{12} = \frac{1}{|V_0|^2} \text{Re} \int \int_S \mathbf{E}_1 \times \mathbf{H}_2^* \cdot d\mathbf{s} \quad (3.33)$$

Where, E_1 is electric field radiated by slot one, H_2^* is magnetic field radiated by slot two, V_0 is voltage across the slot, and the integration is performed over a sphere of large radius.

3.5 Performance Metrics of the Antenna

To describe the performance of the antenna, definition of the various parameter is necessary. Some of the parameters are interrelated and not all of them need be specified for a complete description of the antenna performance. Under this section, the parameters that are used to analyze the performance of the patch antenna is presented.

3.5.1 Return Loss and Voltage Standing Wave Ratio

Return loss (RL) is defined as the loss of signal power due to the reflection at a discontinuity in a transmission line. The discontinuity can arise from a mismatch between the feed line and the port or with a device inserted in the line. Similarly, VSWR is a measure of the efficiency of RF power transmission through a transmission line. For the ideal transmission line, VSWR is one with the entire amount of input power getting transferred without any reflection and in practical cases, any value less than two is also considered to be satisfactory. The return loss is expressed in dB and given by [11][13][16].

$$\text{RL(dB)} = -20\log |\Gamma| \quad (3.34)$$

But the reflection coefficient Γ can be expressed as:

$$|\Gamma| = \frac{V_0^-}{V_0^+} = \frac{Z_L - Z_0}{Z_L + Z_0} \quad (3.35)$$

Where, v_0^+ is the incident wave, v_0^- is the reflected wave and Z_L , Z_0 are the load and characteristic impedance.

3.5.2 Radiation Pattern

The radiation pattern is a graphical representation of the antenna radiation properties, as a function of the angular position and radial distance from the antenna. Radiation properties include power flux density, radiation intensity, field strength, directivity, and phase or polarization. Radiation pattern is determined in the far-field region and is represented as a function of the directional coordinates. The radiation pattern is consists of the main lobe, side lobes and back lobe, and which are indicated in figure below [11][13][16].

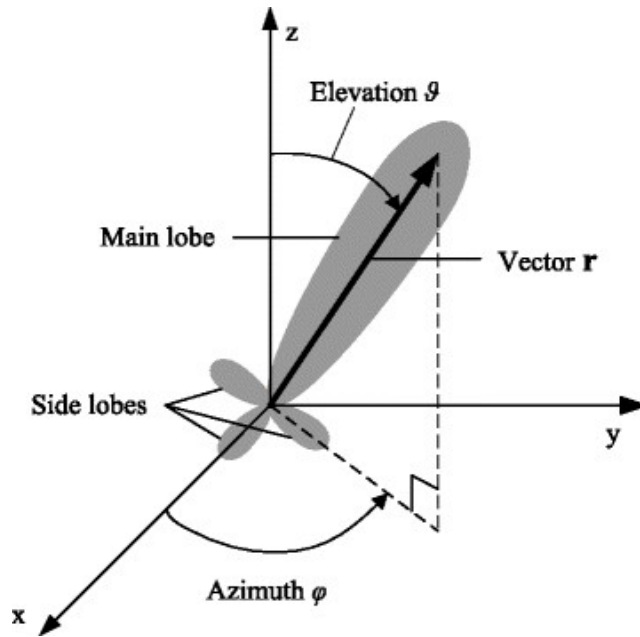


Figure 3.6: Radiation Pattern of the Directional Antenna.

3.5.3 Directivity

The shape of the radiation beam depends on the directivity while the amount of power-packed in the beam is due to the gain of the antenna. The directivity is given by [11]:

$$\text{DIR} = \frac{4\lambda U}{P_{\text{rad}}} \quad (3.36)$$

Where, DIR is directivity, U is radiation intensity, and P_{rad} is total radiated power.

3.5.4 Gain

The Gain of the antenna is used to indicate the capability of the antenna to concentrate energy in a specified direction. The gain of the antenna can be calculated using [11]:

$$G = \eta * D \quad (3.37)$$

Where, η is radiation efficiency and D is the directivity of the antenna.

3.5.5 Bandwidth

The bandwidth of an antenna specifies the range of frequencies over which the antenna can transmit or receive the signal. A practical method of obtaining the bandwidth of the antenna is to use the -10dB frequencies in the plot of return loss [11].

Chapter 4

Design of Rectangular Microstrip Patch Antenna

4.1 Introduction

In this chapter, the design procedures and numerical calculation of six different rectangular MSPA array have been presented. The over all chapter is organized as follows; in the first section, design procedure and numerical calculation of single element rectangular MSPA is presented. The second section, design procedure and numerical calculation of linear rectangular MSPA arrays are discussed. Finally, in the third section, design procedure and numerical calculation of planar rectangular MSPA arrays have been presented.

4.2 Design Procedures of Single Rectangular MSPA

The overall goal of any antenna design is to achieve specific performance characteristics at a desired operating frequency. The very basic steps to begin the design of the rectangular MSPA are, selecting the operating frequency, a suitable substrate type, and substrate thickness. Moreover, after initial design parameters are chosen, dimensioning of all physical antenna structure will continue. This includes: calculation of width and length of the patch, width and length ground plane, width and length of microstrip feeder line, and the location point. Finally, after all physical dimensioning is done, modeling and simulating the structure of the antenna will be the next work. Generally, the design procedure of single inset-feed rectangular MSPA is shown in Figure below.

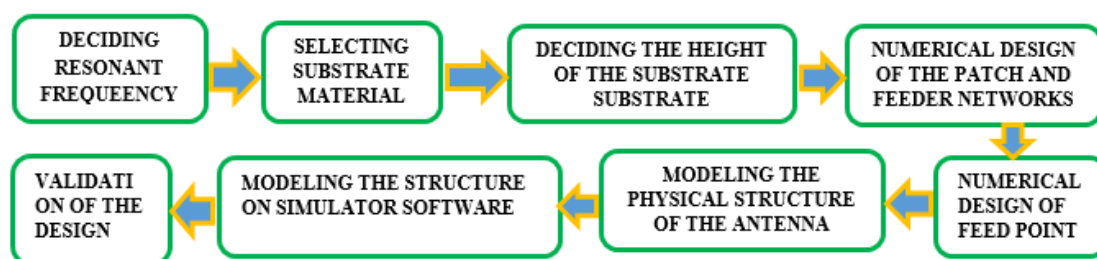


Figure 4.1: Design Procedure of Single Inset-Feed Rectangular MSPA.

4.3 Design of Single Inset-Feed Rectangular MSPA

The proposed single rectangular MSPA is designed using the FR-4 substrate with a dielectric constant (ϵ_r) of 4.4, a loss tangent of 0.0025, and radiating copper metal thickness of 0.035mm to operate at 28GHz frequency. After above initial design parameters are chosen, the remaining physical dimensions of single rectangular MSPA is calculated as follows.

1. Height of the substrate

The height of the substrate is calculated by substituting $C = 3 * 10^8 m/sec$, $\epsilon_r = 4.4$, and $F_0 = 28GHz$ in the equation 3.2 i.e.,

$$SH = \frac{0.3C}{2\pi F_0 \sqrt{\epsilon_r}} = \frac{0.3 * 3 * 10^8 m/sec}{2 * 3.14 * 28 * 10^9 / sec * \sqrt{4.4}} = 0.244mm$$

2. Width of the patch

Also, by substituting $C = 3 * 10^8 m/sec$, $\epsilon_r = 4.4$ and $F_0 = 28GHz$ in the equation 3.3, the width of the patch is calculated as:

$$PW = \frac{C}{2F_0 \sqrt{\frac{\epsilon_r + 1}{2}}} = \frac{3 * 10^8 m/sec}{2 * 28 * 10^9 / sec * \sqrt{\frac{5.4}{2}}} = 3.26025mm$$

3. Effective dielectric constant

After, the patch width and substrate height is obtained, effective dielectric constant is calculated by substituting $C = 3 * 10^8 m/sec$, $\epsilon_r = 4.4$, $PW = 3.26025mm$, $SH = 0.244mm$ and $F_0 = 28GHz$ in equation 3.4, then the effective dielectric constant is calculated as:

$$\epsilon_{reff} = \left(\frac{5.4}{2}\right) + \left(\frac{3.4}{2}\right) \left(1 + 12 \left(\frac{0.244mm}{3.2605mm}\right)\right)^{-0.5} = 3.93393$$

4. Effective length of the patch

Next, by substituting $C = 3 * 10^8 m/sec$, $\epsilon_{reff} = 3.93393$ and $F_0 = 28GHz$ in equation 3.5, the effective length of the patch is calculated as:

$$PL_{eff} = \frac{C}{2F_0 \sqrt{\epsilon_{reff}}} = 2.70097mm$$

5. Length extension of the patch

After effective dielectric constant is obtained the patch length extension is calculated by substituting $PW = 3.26025mm$, $SH = 0.244mm$ and $\epsilon_{reff} = 3.93393$ in equation 3.6.

$$\Delta PL = (0.412 * 0.244mm) \left[\frac{(3.93393 + 0.3)(13.3618 + 0.264)}{(3.93393 - 0.258)(13.3618 + 0.8)} \right] = 0.111397mm$$

6. Actual length of the patch

The actual length of the patch is calculated by substituting $PL_{eff} = 2.700971\text{mm}$ and $\Delta PL = 0.111397\text{mm}$ in equation 3.7 i.e.,

$$PL = PL_{eff} - 2\Delta PL = 2.47818\text{mm}$$

7. Ground plane dimensions

By substituting $PL = 2.47818\text{mm}$, $PW = 3.26025\text{mm}$, and $SH = 0.244\text{mm}$ in the equation 3.8 and 3.9, the length and width of the ground plane is calculated as follows:

$$GL = PL + 6SH = 3.942177\text{mm}, GW = PW + 6SH = 4.7245\text{mm}$$

8. Location of the Feed point

The location of feed point along the X and Y axis is obtained by substituting $PL = 2.47818\text{mm}$, $PW = 3.26025\text{mm}$ and $\varepsilon_{reff} = 3.93393$ in equation 3.10 and 3.11, X_f and Y_f are calculated as follows.

$$X_f = \frac{PL}{2\sqrt{\varepsilon_{reff}}} = \frac{2.47818\text{mm}}{2 * \sqrt{3.93393}} = 0.624726\text{mm}, Y_f = \frac{PW}{2} = \frac{3.26025\text{mm}}{2} = 1.630125\text{mm}$$

9. Impedance matching

To calculate Z_L , first Z_{pe} should be calculated by substituting $PW = 3.26025\text{mm}$, $PL = 2.47818\text{mm}$, and $\varepsilon_r = 4.4$ in equation 3.13, Z_{pe} is calculated as follows.

$$Z_{pe} = 90 \left(\frac{\varepsilon_r^2}{\varepsilon_r - 1} \right) \left(\frac{PL}{PW} \right)^2 = 90 \left(\frac{4.4^2}{3.4} \right) \left(\frac{2.47818\text{mm}}{3.26025\text{mm}} \right)^2 = 296.09549\Omega$$

After Z_{pe} is calculated Z_L calculated by substituting the value of Z_{pe} in equation 3.12, then the value of Z_L is:

$$Z_L = \sqrt{Z_0 * Z_{pe}} = \sqrt{50\Omega * 296.09549} = 121.67487\Omega$$

10. Width and length of the Microstrip feed-line

A. Length of the microstrip feeder line

To calculate the length of the microstrip feeder line first λ_0 is calculated by substituting $F_0 = 28\text{GHz}$ and $C = 3 * 10^8\text{m/sec}$ in equation 3.15. Therefore, λ_0 is calculated as:

$$\lambda_0 = \frac{C}{F_0} = \frac{3 * 10^8\text{m/sec}}{28 * 10^9\text{sec}} = 10.7143\text{mm}$$

Then, substituting $\lambda_0 = 10.7143\text{mm}$ and $\varepsilon_r = 4.4$ in equation 3.14, the dimension of $L_{(MFL1)}$

is calculated as:

$$L_{(MFL1)} = \frac{\lambda_0}{4\sqrt{\varepsilon_r}} = \frac{10.7143mm}{4 * \sqrt{4.4}} = \frac{10.7143mm}{8.390471mm} = 1.27696mm$$

B. Width of Microstrip Feeder Line

Assuming the characteristic impedance of the microstrip feeder line as 50Ω . Then, the width of the microstrip feeder line can be calculated by using equation 3.16. However, the impedance of the microstrip feeder line is highly dependent on the width of the patch. Therefore, it is better to find the impedance of the microstrip feeder line corresponding to the calculated width of the patch. Then after, calculating the width of the microstrip feeder line by assuming calculated impedance as the characteristic impedance of the feeder line (i.e, $Z_{(MFL1)} = Z_0$). Hence, by substituting $\varepsilon_r = 4.4$, SH = 0.244mm, PW = 3.26025mm and $\varepsilon_{reff} = 3.93393$ in equation 3.32 then, $Z_{(MFL1)}$ is calculated as:

$$Z_{(MFL1)} = \frac{120 * 3.14 * \sqrt{3.93393}}{13.3618 + 1.393 + 0.667 * \ln(14.801)} = 45.1515\Omega$$

Next, by substituting SH = 0.244mm, $Z_{(MFL1)} = 45.1515\Omega$, $\varepsilon_r = 4.4$ and t = 0.035mm in equation 3.16, Width of the microstrip feeder line is calculated as:

$$W_{(MFL1)} = \frac{5.98 * 0.244mm * \left(\frac{1}{\exp\left(\frac{108.83291}{87}\right)} \right) - 0.035mm}{0.8} = 0.4783mm$$

11. Inset Dimension

A. Inset Length (Y_0)

By substituting PL = 2.47818mm, $Z_0 = 50\Omega$ and $Z_L = 121.67487\Omega$ in equation 3.17, the length of inset feed is calculated as:

$$Y_0 = \left(\frac{PL}{\pi} \right) \cos^{-1} \sqrt{\left(\frac{Z_0}{Z_L} \right)} = \left(\frac{2.47818mm}{3.14} \right) \cos^{-1} \sqrt{\left(\frac{50}{121.6748} \right)} = 0.905498mm$$

B. Inset Gap (G_p)

Similarly, by substituting the value of C = $3 * 10^8 m/sec$, $\varepsilon_{reff} = 3.93393$ and $F_0 = 28GHz$ in equation 3.18, the inset gap is calculated as:

$$G_P = \frac{4.65 * 10^{-12} * C}{F_0(inGHz) \sqrt{2 * \varepsilon_{reff}}} = \frac{4.65 * 10^{-12} * 3 * 10^8 m/sec}{28 \sqrt{2 * 3.93393}} = 0.0177612mm$$

12. Width and length of the feed point

A. Width of the feed point

Width of feed point can be calculated by using the equation 3.19 and given below.

$$W_{(FP)} = \frac{2SH}{\pi} \left[((B - 1) - \ln(2B - 1)) + \left(\frac{\epsilon_r - 1}{\epsilon_r} \left[\ln(B - 1) + 0.39 - \frac{0.6}{\epsilon_r} \right] \right) \right]$$

But, B is calculated using equation 3.20 which is:

$$B = \frac{60\pi^2}{Z_{(MFL1)}\sqrt{\epsilon_r}} = \frac{60(3.14)^2}{45.1515\sqrt{4.4}} = \frac{591.576}{45.1515 * 2.0976} = \frac{591.576}{914.709} = 6.2462$$

Then, by substituting the value of B in equation 3.19, $W_{(FP)}$ is calculated as follows:

$$W_{(FP)} = \frac{0.488mm}{\pi} \left[((5.2462) - \ln(11.49)) + \left(\frac{3.4}{4.4} \left[\ln(5.2462) + 0.39 - \frac{0.6}{4.4} \right] \right) \right]$$

$$W_{(FP)} = 0.665376mm$$

B. Length of the feed point:

By substituting $\lambda_o = 10.7143mm$ and $\epsilon_{reff} = 3.93393$ in equation 3.22 then, λ_{eff} is calculated as:

$$\lambda_{eff} = \frac{\lambda_o}{\sqrt{\epsilon_{reff}}} = \frac{10.7143mm}{1.98341} = 5.40196mm$$

Next, by substituting the values of λ_{eff} in equation 3.21, the dimension of L_{FP} is;

$$L_{(FP)} = \frac{\lambda_{eff}}{4} = \frac{5.40196mm}{4} = 1.35049mm$$

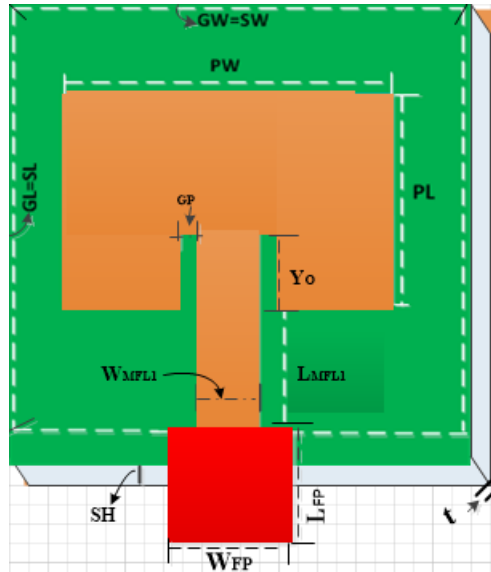


Figure 4.2: Proposed Single Inset-Feed Rectangular MSPA.

The design parameters of single inset-feed rectangular MSPA is explicitly calculated in above section and the final value of the calculation has been tabulated in Table 4.1. In general, the above designed single element rectangular MSPA is used as building block to design all other rectangular MSPA array.

Table 4.1: Calculated Physical Dimensions of Single Inset-feed Rectangular MSPA.

No	Constant Parameter	Symbols	Values
1	Resonant frequency	F_0	28GHz
2	Dielectric constant	ϵ_r	4.4
3	Input characteristic impedance	Z_0	50 Ω
4	Thickness of metal patch	t	0.035mm
No	Design Parameter	Symbols	Values
1	Width of the patch	PW	3.26025 mm
2	Effective dielectric constant	ϵ_{reff}	3.93393
3	Effective length of the patch	PL_{eff}	2.70097mm
4	Length extension of the patch	ΔPL	0.111397mm
5	Actual length of the patch	PL	2.47818mm
6	Width of the ground plane	GW	4.7245mm
7	Length of the ground plane	GL	3.942177mm
8	Length of inset feed	Y_0	0.905498mm
9	Inset gap	G_p	0.017761mm
10	Location of the feed point along the x-axis	X_f	0.624726mm
11	Location of the feed point along the y-axis	Y_f	1.630125mm
12	Length of the microstrip feeder line	$L_{(MFL1)}$	1.2769mm
13	Width of the microstrip feeder line	$W_{(MFL1)}$	0.4783mm
14	Length of the feed point	$L_{(FP)}$	1.35049mm
15	Width of the feed point	$W_{(FP)}$	0.665376mm
16	Substrate height	SH	0.244mm

4.4 Design Procedure of Linear Rectangular MSPA Array

Most compact rectangular MSPA design shows decreased antenna gain owing to the antenna size reduction. To overcome the limitation and enhance the performance of the antenna, several designs with various feeding techniques, patch shapes and impedance matching were proposed. However, the design parameters of rectangular MSPA for 5G wireless communication systems needs high accuracy. Because since their operating frequency is within extremely high-frequency band, the size of antenna elements is very small and therefore, a small deviation of the design parameter leads to large performance variation. In this study, the procedure that has been used in order to design all studied linear rectangular MSPA is indicated below.

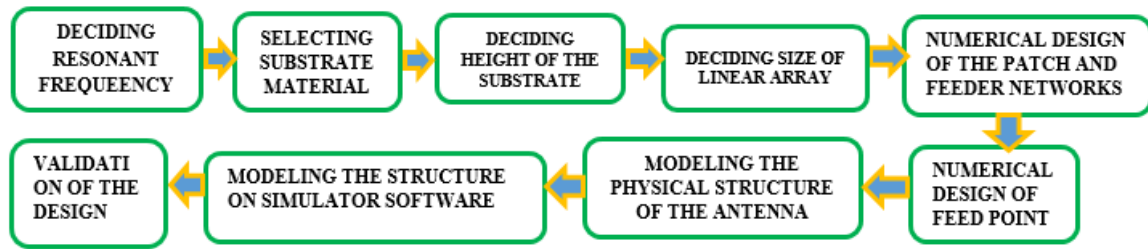


Figure 4.3: Design Procedures of Linear MSPA Array.

4.5 Design of Linear Rectangular MSPA Array

4.5.1 2x1 Inset-feed Rectangular MSPA Array

This section introduces the design of linear 2x1 inset-feed rectangular MSPA array to improve the performance of single inset-feed rectangular MSPA. Because by using single antenna, high performance cannot be obtained for all major performance metrics. A linear 2x1 inset-feed rectangular MSPA array can be designed by connecting one pair of single element inset-feed rectangular MSPA using 1:2 corporate power divider. In this particular structure, a microstrip transmission line of 1:2 power divider is used to feed the two and hence the line widths are adjusted accordingly to optimize the performance trade-offs. The physical structure of 2x1 inset-feed rectangular MSPA array is indicated in Figure 4.4.

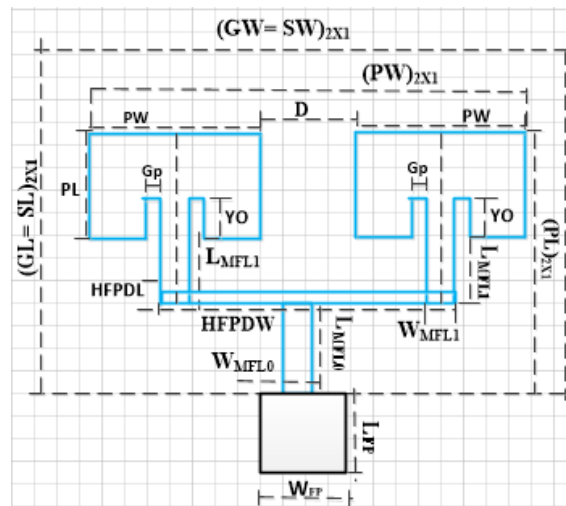


Figure 4.4: Physical Structure of the Proposed 2x1 Inset-feed Rectangular MSPA Array.

The antenna is designed using FR-4 substrate material with a dielectric constant of $\epsilon_r = 4.4$, a dielectric loss tangent of 0.0025. The substrate height, length of the patch, and width of the patch are 0.244mm, 2.47818mm, and 3.26025mm respectively. Moreover, in order to match the impedance to 50Ω width of microstrip feeder line should be designed properly.

Because the impedance is highly varies with the width the feeder and almost constant with the length of the feeder. Therefore, in this paper a microstrip feeder line with a width of 0.4783mm and quarter-wavelength is used to match the impedance to 50Ω characteristic impedance. However, the remaining design parameters are calculated by using the above parameters as initial parameters. After numerical calculation, important design parameters of the antenna will be tuned during the simulation to find better performance in terms of directivity, beam gain, bandwidth, and radiation efficiency.

1. The separation distance between the elements

The mutual coupling between the array elements decreases the radiation efficiency of the antenna by increasing the side lobe level. Therefore, to minimize mutual coupling, the separation distance has to be greater than half of the free-space wavelength ($D \geq 0.5\lambda_0$). Also, to avoid grating lobe separation distance (D) should be less than the free-space wavelength ($D \leq \lambda_0$) i.e. the selection should be between $\lambda_0 \geq D \geq 0.5\lambda_0$. In this design separation distance of $0.504\lambda_0$ has been selected.

$D = 0.504\lambda_0$, By substituting $\lambda_0 = 10.7143\text{mm}$, D is calculated as:

$$D = 0.504 * 10.7143\text{mm} = 5.4000072\text{mm} \simeq 5.4\text{mm}$$

2. Length and width of horizontal feed of 1:2 power divider (HFPDW and HFPDL)

A. Width of horizontal feed of 1:2 power divider (HFPDW)

$$\text{HFPDW} = D + 2(0.5\text{PW}) + W_{(MFL1)}$$

By substituting $\text{PW} = 3.26025\text{mm}$, $D = 5.4\text{mm}$ and $W_{(MFL1)} = 0.4783\text{mm}$ then, HFPDW is calculated as:

$$\text{HFPDW} = 5.4\text{mm} + 3.26025\text{mm} + 0.4783\text{mm}$$

$$\text{HFPDW} = 5.4\text{mm} + 3.73855\text{mm} = 9.13855\text{mm}$$

B. Length of horizontal feed of 1:2 power divider (HFPDL)

With the initial design parameter of $F_0 = 28\text{GHz}$, $\text{SH} = 0.244\text{mm}$, $\epsilon_r = 4.4$ and $Z_0 = 50\Omega$ the width of the microstrip feeder line is 0.4783mm. But, the HFPDL is a microstrip transmission line with 100Ω . Therefore, HFPDL is half of the width of the 50Ω microstrip feeder line. $\text{HFPDL} = 0.5W_{(MFL1)}$ but, the dimension of $W_{(MFL1)}$ is 0.4783mm then, HFPDL is:

$$\text{HFPDL} = 0.5W_{(MFL1)} = 0.5 * 0.4783\text{mm} = 0.23915\text{mm}$$

3. Length and width of last feed of power divider arm ($L_{(MFL1)}$ and $W_{(MFL1)}$)

By substituting $\lambda_0 = 10.7143\text{mm}$ and $\epsilon_r = 4.4$, then the dimension of $L_{(MFL1)}$ is calculated as follows.

$$L_{(MFL1)} = \frac{\lambda_0}{4\sqrt{\epsilon_r}} = \frac{10.7143\text{mm}}{4 * \sqrt{4.4}} = \frac{10.7143\text{mm}}{8.390471\text{mm}} = 1.27696\text{mm}$$

B. $W_{(MFL1)} = W_{(MFL0)}$ But, the dimension of $W_{(MFL0)}$ is 0.4783mm

$$W_{(MFL1)} = 0.4783\text{mm}$$

4. Length and Width of connected 2x1 MSPA ($PL_{(2X1)}$ and $PW_{(2X1)}$)

A. Length of connected 2x1 MSPA ($PL_{(2X1)}$)

$PL_{(2X1)} = PL + L_{(MFL0)} + L_{(MFL1)}$. But, $L_{(MFL0)} = L_{(MFL1)}$. Therefore, the equation is simplified to:

$$PL_{(2X1)} = PL + 2L_{(MFL1)}$$

By substituting $PL = 2.47818\text{mm}$ and $L_{(MFL1)} = 1.27696\text{mm}$, $PL_{(2X1)}$ is calculated as:

$$PL_{(2X1)} = 2.47818\text{mm} + 2 * 1.27696\text{mm} = 5.032097\text{mm}$$

B. Width of connected 2x1 MSPA ($PW_{(2X1)}$)

$$PW_{(2X1)} = D + 2PW$$

By substituting $PW = 3.26025\text{mm}$ and $D = 5.4\text{mm}$, then $PW_{(2X1)}$ is calculated as:

$$PW_{(2X1)} = 5.4\text{mm} + 2 * 3.26025\text{mm} = 11.9205\text{mm}$$

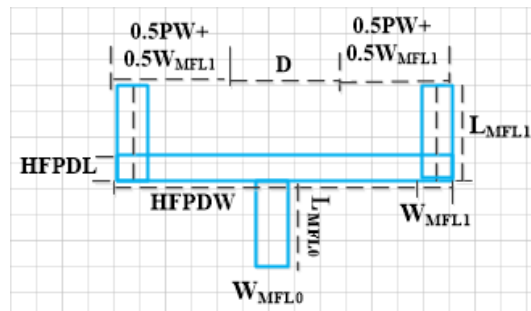


Figure 4.5: Physical Structure of 1:2 Power Divider.

5. Length and width of the ground plane ($GL_{(2X1)}$ and $GW_{(2X1)}$)

A. Length of the ground plane ($GL_{(2X1)}$)

$$GL_{(2X1)} = PW_{(2X1)} + 6(SH)$$

By substituting $PL_{(2X1)} = 5.032097\text{mm}$ and $SH = 0.244\text{mm}$, $GL_{(2X1)}$ is calculated as:

$$GL_{(2X1)} = 5.032097\text{mm} + 6(0.244\text{mm}) = 6.496097\text{mm}$$

B. Width of ground plane $GW_{(2X1)}$

$$GW_{(2X1)} = PW_{(2X1)} + 6(SH)$$

By substituting $PW_{(2X1)} = 11.9205\text{mm}$ and $SH = 0.244\text{mm}$, $GW_{(2X1)}$ is calculated as:

$$GW_{(2X1)} = 11.9205\text{mm} + 6(0.244\text{mm}) = 13.3845\text{mm}$$

6. Length and width of last feed of the power divider ($LFL_{(2x1)}$ and $LFW_{(2x1)}$)

A. Length of last feed of the power divider ($LFL_{(2x1)}$)

But, the dimension of λ_{SM} is 5.107842mm , then $LFL_{(2X1)}$ is calculated as:

$$LFL_{(2X1)} = \frac{5.107842\text{mm}}{4} = 1.27696\text{mm}$$

B. Width of last feed of the power divider ($LFW_{(2x1)}$) $LFW_{(2X1)} = W_{(MFL0)}$ But, the dimension of $W_{(MFL0)}$ is 0.4783mm . Therefore, $LFW_{(2X1)}$ is equal to 0.4783mm .

The detail numerical calculation of 2x1 MSPA array design parameters in above section is tabulated in table below.

Table 4.2: Calculated Physical Dimensions of 2x1 Inset-Feed Rectangular MSPA Array.

No	Constant Parameter	Symbols	Values
1	Resonant frequency	F_0	28GHz
2	Substrate height	SH	0.244mm
3	Dielectric constant	ϵ_r	4.4
4	Input characteristic impedance	Z_0	50 Ω
5	Thickness of metal patch	t	0.035mm
No	Design Parameters	Symbols	Values
1	Width of the patch	PW	3.26025mm
2	Length of the patch	PL	2.47818mm
3	Width of the ground plane	$GW_{(2X1)}$	13.3845 mm
4	Length of the ground plane	$GL_{(2X1)}$	6.496097mm
5	Length of inset feed	Y_0	0.905498mm
6	Inset gap	G_p	0.017761mm
7	Length of the microstrip feeder line	$L_{(MFL1)}$	1.27696mm
8	Width of the microstrip feeder line	$W_{(MFL1)}$	0.4783mm
9	Length of Horizontal feed power divider	HFPDL	0.23915mm
10	Width of Horizontal feed power divider	HFPDW	9.13855mm
11	Length of the feed point	$L_{(FP)}$	1.35049 mm
12	Width of the feed point	$W_{(FP)}$	0.665376mm
13	Length of last microstrip feeder line	$LF L_{(2X1)}$	1.27696mm
14	Width of last microstrip feeder line	$LF W_{(2X1)}$	0.4783mm
15	Distance between the patch	D	5.4 mm

4.5.2 4x1 Inset-feed Rectangular MSPA Array

A linear 4x1 inset-feed rectangular MSPA array is proposed to increase the performance of 2x1 inset-feed rectangular MSPA array. In order to design 4x1 inset-feed rectangular MSPA array, two pairs of a single inset-feed rectangular MSPA or one pair of 2x1 inset-feed rectangular MSPA array is required. Therefore, linear 4x1 inset-feed rectangular MSPA array can be designed by connecting one pair of 2x1 inset-feed rectangular MSPA array to the second 1:2 power divider. Specifically, in 4x1 inset-feed rectangular MSPA arrays design, single 2x1 inset-feed rectangular MSPA array is considered as one radiating point with two-element and connected to one arm of 1:4 power divider (second 1:2 power divider) as indicated in below figure. Hence, by connecting two 2x1 rectangular MSPA array and using its calculated design parameters, the remaining design parameters for 4x1 inset-feed rectangular MSPA array are obtained.

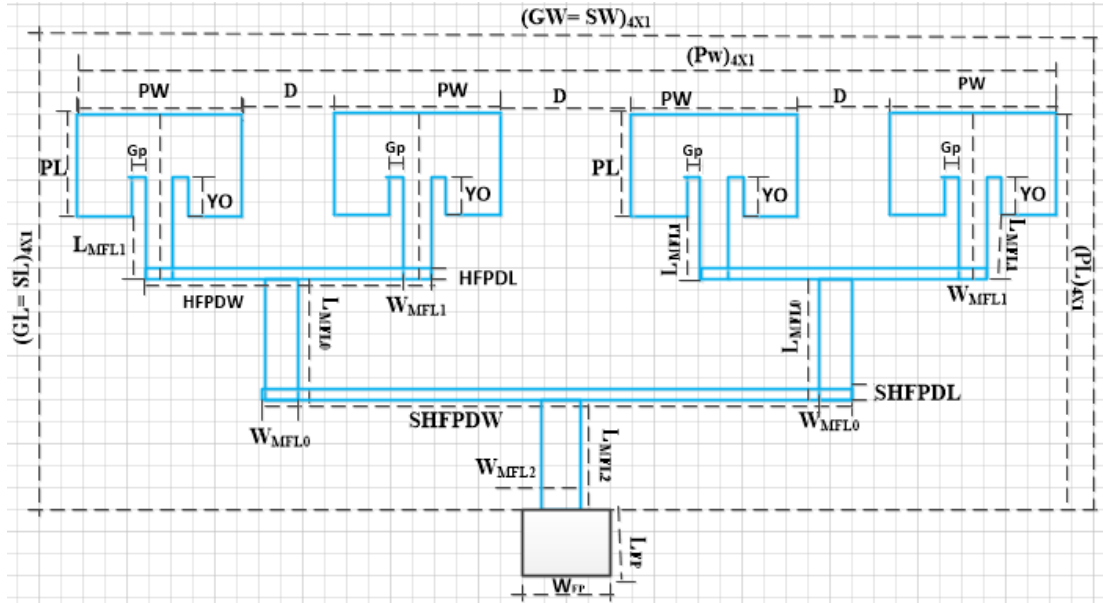


Figure 4.6: Physical Structure of the Proposed 4x1 Inset-feed Rectangular MSPA Array.

1. Length and width Horizontal feed of the second power divider (SHFPDW and SHFPDL)

A. Width of Horizontal feed of the second power divider (SHFPDW)

$$SHFPDW = 2D + 2PW + W_{(MFL0)}$$

By substituting $D = 5.4\text{mm}$, $PW = 3.26025\text{mm}$ and $W_{(MFL0)} = 0.4783\text{mm}$, then SHFPDW is calculated as:

$$SHFPDW = 2 * 5.4\text{mm} + 2 * 3.26025\text{mm} + 0.4783\text{mm} = 17.7988\text{mm}$$

B. Length of Horizontal feed of the second power divider (SHFPDL)

$$SHFPDL = 0.5(W_{(MFL0)})$$

But, the dimension of $W_{(MFL0)}$ is 0.4783mm , then SHFPDL is:

$$SHFPDL = 0.5 * 0.4783\text{mm} = 0.23915\text{mm}$$

2. Length and Width of connected 4x1 MSPA array ($PL_{(4X1)}$ and $PW_{(4X1)}$)

A. Length of connected 4x1 MSPA array ($PL_{(4X1)}$)

$$PL_{(4X1)} = PL_{(2X1)} + L_{(MFL2)} \text{ or } PL_{(4X1)} \text{ can be calculated by using:}$$

$PL_{(4X1)} = PL + L_{(MFL0)} + L_{(MFL1)} + L_{(MFL2)}$. But, $L_{(MFL0)} = L_{(MFL1)} = L_{(MFL2)}$ then it is simplified to:

$$(PL_{(4X1)} = PL + 3 * L_{(MFL1)})$$

By substituting $PL = 2.47818\text{mm}$ and $L_{(MFL1)} = 1.27696\text{mm}$, $PL_{(4X1)}$ is calculated as:

$$PL_{(4X1)} = 2.47818\text{mm} + 3 * 1.27696\text{mm} = 6.309057\text{mm}$$

B. Width of connected 4x1 MSPA array ($PW_{(4X1)}$)

$$PW_{(4X1)} = 4 * PW + 3D$$

By substituting $PW = 3.26025\text{mm}$ and $D = 5.4\text{mm}$, then $PW_{(4X1)}$ is calculated as:

$$PW_{(4X1)} = 4 * 3.26025mm + 3 * 5.4mm = 29.241mm$$

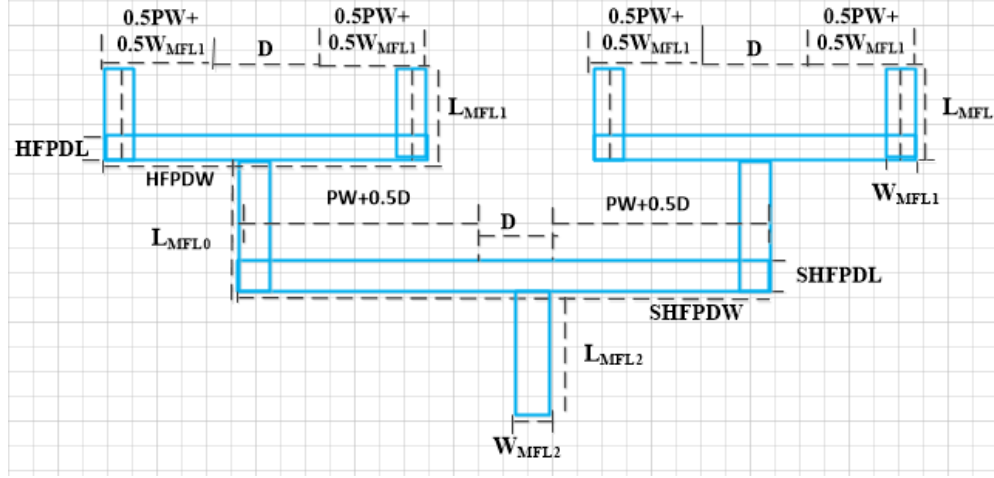


Figure 4.7: Physical Structure of 1:4 Power Divider in 4x1 Linear Array.

3. Length and Width of ground plane ($GL_{(4X1)}$ and $GW_{(4X1)}$)

A. Length of ground plane ($GL_{(4X1)}$)

$$GL_{(4X1)} = PL_{(4X1)} + 6(SH)$$

By substituting $PL_{(4X1)} = 6.309057mm$ and $SH = 0.244mm$, $GL_{(4X1)}$ is calculated as:

$$GL_{(4X1)} = 6.309057mm + 6(0.244mm) = 7.773057mm$$

B. Width of ground plane ($GW_{(4X1)}$)

$$GW_{(4X1)} = PW_{(4X1)} + 6(SH)$$

By substituting $PW_{(4X1)} = 29.54mm$ and $SH = 0.244mm$ then, $GW_{(4X1)}$ is calculated as:

$$GW_{(4X1)} = 29.241mm + 6(0.244mm) = 30.705mm$$

4. Length and width of last feed of the second power divider ($SL_{(MFL0)}$ and $SW_{(MFL0)}$)

A. Length of last feed of the second power divider ($SL_{(MFL0)}$)

$$SL_{(MFL0)} = LFL_{(4X1)} = L_{(MFL1)} = \frac{\lambda_{SM}}{4}$$

But, the dimension of λ_{SM} is $5.107842mm$ then, the dimension of $SL_{(MFL0)}$ is calculated as:

$$SL_{(MFL0)} = 5.107842mm/4 = 1.27696mm$$

B. Width of last feed of the second power divider ($SW_{(MFL0)}$)

$$SW_{(MFL0)} = LFW_{(4X1)} = 0.4783mm$$

Generally, the numerically designed parameters of 4x1 inset-feed rectangular MSPA array has been explicitly presented in above section and summarized in table below.

Table 4.3: Calculated Physical Dimensions of 4x1 Inset-Feed Rectangular MSPA array.

No	Constant Parameter	Symbols	Values
1	Resonant frequency	F_0	28GHz
2	Substrate height	SH	0.244mm
3	Dielectric constant	ϵ_r	4.4
4	Input characteristic impedance	Z_0	50 Ω
5	Thickness of metal patch	t	0.035mm
No	Design Parameters	Symbol	Values
1	Width of the patch	PW	3.26025mm
2	Length of the patch	PL	2.47818mm
3	Width of the ground plane	$GW_{(4x1)}$	30.705mm
4	Length of the ground plane	$GL_{(4x1)}$	7.773057mm
5	Length of inset feed	Y_0	0.905498mm
6	Inset gap	G_p	0.017761mm
7	Length of the microstrip feeder line	$L_{(MFL1)}$	1.27696mm
8	Width of the microstrip feeder line	$W_{(MFL1)}$	0.4783mm
9	Horizontal feed length of the first power divider	HFLFPD	0.23915mm
10	Horizontal feed width of the first power divider	HFWFPD	9.13855mm
11	Horizontal feed length of the second power divider	HFLSPD	0.23915mm
12	Horizontal feed width of the second power divider	HFWSPD	17.7988mm
13	Length of last microstrip feeder line	$LFL_{(4x1)}$	1.27696mm
14	Width of last microstrip feeder line	$WFL_{(4x1)}$	0.4783mm
15	Length of the feed point	$L_{(FP)}$	1.35049 mm
16	Width of the feed point	$W_{(FP)}$	0.665376mm
17	Distance between the patch	D	5.4 mm
18	Length of second microstrip power divider	$SL_{(MFL0)}$	1.27696mm
19	Width of second microstrip power divider	$SW_{(MFL0)}$	0.4783mm

4.6 Design Procedure of Planar Rectangular MSPA Array

Different size of linear inset-feed rectangular MSPA arrays have been used to scan either the elevation plane or azimuth plane. However, in many application high-performance antenna arrays with ability to scan both dimensional planes (i.e. the elevation and azimuth plane) is highly required. Therefore, the planar array antenna plays crucial role in such applications. With this regard, in order to design different size of planar inset-feed rectangular MSPA array, the following design procedure shown in Figure 4.8 is being used. As shown in above block diagram, after initial design parameters are selected, the next step is deciding number of array elements to be included in the arrays followed by dimensioning of feeding networks.

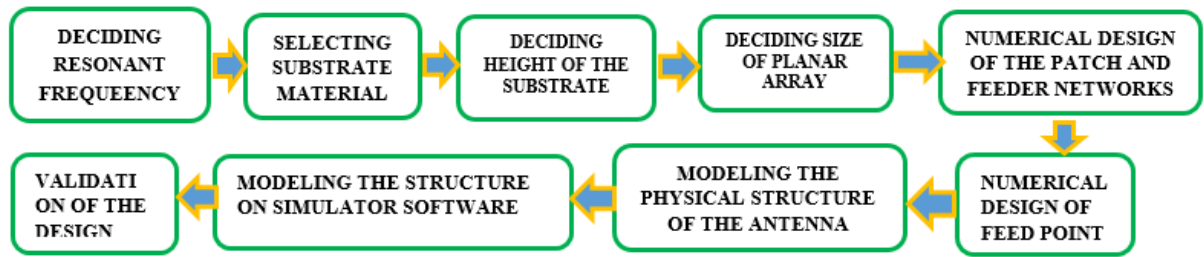


Figure 4.8: Design Procedure of Planar inset-feed rectangular MSPA Array.

4.7 Design of Planar Inset-feed Rectangular MSPA Array

4.7.1 2x2 Inset-feed Rectangular MSPA Array

The first planar array proposed in this study is 2x2 inset-feed rectangular MSPA array and needed to improve the performance of linear antenna. To design 2x2 inset-feed rectangular MSPA array, four single inset-feed rectangular MSPA elements are required. The elements are grouped into one pair of 2x1 linear inset-feed rectangular MSPA array. From Figure 4.9, it can be observed that planar 2x2 inset-feed rectangular MSPA array is designed by connecting a pair of 2x1 inset-feed rectangular MSPA linear array using 100Ω feeder line. In order to reduce the return loss of the antenna, a quarter wave impedance transformer is used. The quarter wave impedance transformer improves the matching quality of the radiating element and the feeder line. This is the unique feature introduced in this study and which is indicated in Figure 4.10.

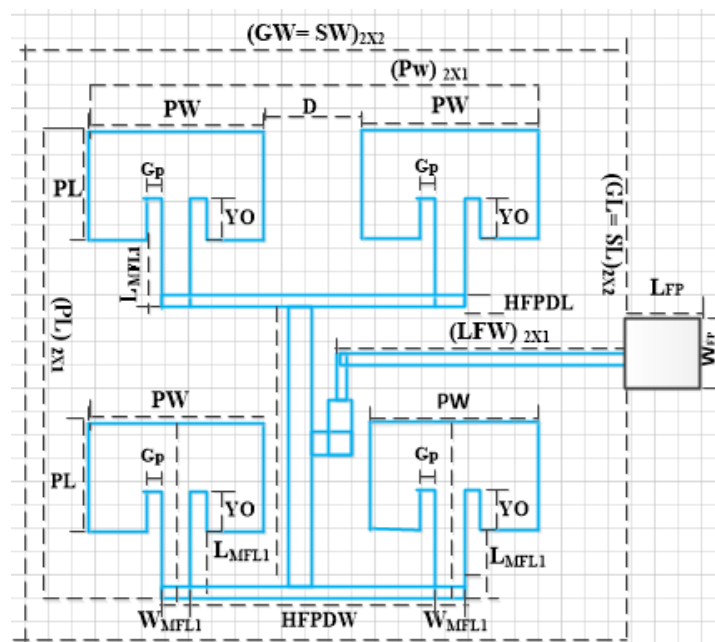


Figure 4.9: Physical Structure of the Proposed 2x2 Inset-feed Rectangular MSPA Array.

The design parameters of 2x1 linear antenna is used to design 2x2 inset-feed rectangular MSPA array and the remaining design parameters of 2x2 inset-feed rectangular MSPA array is calculated as shown below.

1. Length and width of Microstrip transmission line connecting upper and bottom 2x1 MSPA array (CTLW and CTLL)

A. Width of Microstrip transmission line connecting upper and bottom 2x1 MSPA array

$$CTLW = W_{(MFL1)}$$

But, the dimension of $W_{(MFL1)}$ is 0.4783mm, then the dimension of CTLW is:

$$CTLW = 0.4783\text{mm}$$

B. Length of Microstrip transmission line connecting upper and bottom 2x1 MSPA array (CTLL)

$$CTLL = D + PL + L_{(MFL1)}$$

By substituting $D = 5.4\text{mm}$, $PL = 2.47818\text{mm}$, and $L_{(MFL1)} = 1.27696\text{mm}$, then CTLL is calculated as:

$$CTLL = 5.4\text{mm} + 2.47818\text{mm} + 1.27696\text{mm} = 9.15778\text{mm}$$

2. First, second, third quarter transformation length and width

I. Length and width of first-quarter transform (FQTW and FQTL)

A. Width of first-quarter transform (FQTW)

$$FQTW = 0.5 * \frac{\lambda_{SM}}{4} = \frac{\lambda_{SM}}{8}$$

But, the dimension of λ_{SM} is 5.107842mm, then FQTW is calculated as:

$$FQTW = 5.107842\text{mm}/8 = 0.6384803\text{mm}$$

B. Length of first-quarter transform (FQTL)

$$FQTL = W_{(MFL1)}$$

But, the dimension of $W_{(MFL1)}$ is 0.4783mm then, FQTL is:

$$FQTL = 0.4783\text{mm}$$

II. Length and width of second-quarter transform (SQTW and SQTL)

A. Length of second-quarter transform (SQTL)

$$SQTL = 0.5 * \frac{\lambda_{SM}}{4} = \frac{\lambda_{SM}}{8}$$

But, the dimension of λ_{SM} is 5.107842mm, then SQTL is:

$$SQTL = 5.107842\text{mm}/8 = 0.6384803\text{mm}$$

B. Width of second-quarter transform (SQTW)

$$SQTW = W_{(MFL1)}$$

But, the dimension of $W_{(MFL1)}$ is 0.4783mm, then SQTW is:

$$SQTW = 0.4783\text{mm}$$

III. Length and width of third-quarter transform (TQTW and TQTL)

A. Length of third-quarter transform (TQTL)

$$TQTL = \frac{\lambda_{SM}}{4}$$

But, the dimension of λ_{SM} is 5.107842mm, then TQTL is:

$$TQTL = 5.107842\text{mm}/4 = 1.27686\text{mm}$$

B. Width of third-quarter transform (TQTW)

$$TQTW = 0.5 * W_{(MFL1)}$$

But, the dimension of $W_{(MFL1)}$ is 0.4783mm, then TQTW is:

$$TQTW = 0.23915\text{mm}$$

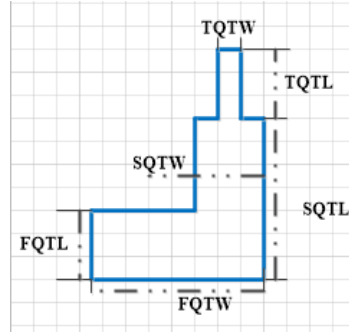


Figure 4.10: Structure of Quarter-Wavelength Impedance Transformer.

3. Length and Width of connected 2x2 MSPA array ($PL_{(2x2)}$ and $PW_{(2x2)}$)

A. Length of connected 2x2 MSPA array ($PL_{(2x2)}$)

$$PL_{(2x2)} = 2PL + D + 2 * L_{(MFL1)}$$

By substituting $PL = 2.47818\text{mm}$, $D = 5.4\text{mm}$, $L_{(MFL1)} = 1.27686\text{mm}$, $PL_{(2x2)}$ is calculated as:

$$PL_{(2x2)} = 2 * 2.47818\text{mm} + 5.4\text{mm} + 2 * 1.27686\text{mm} = 12.91356\text{mm}$$

B. Width of connected 2x2 MSPA array ($PW_{(2x2)}$)

$$PW_{(2x2)} = 2PW + D$$

By substituting $PW = 3.26025\text{mm}$ and $D = 5.4\text{mm}$, then $PW_{(2x2)}$ calculated as:

$$PW_{(2x2)} = 2 * 3.26025\text{mm} + 5.4\text{mm} = 11.9205\text{mm}$$

4. Length and Width of ground plane ($GL_{(2x2)}$ and $GW_{(2x2)}$)

A. Length of ground plane ($GL_{(2x2)}$)

$$GL_{(2x2)} = PL_{(2x2)} + 6(\text{SH})$$

By substituting $PL_{(2x2)} = 12.91356\text{mm}$ and $\text{SH} = 0.244\text{mm}$, $GL_{(2x2)}$ is calculated as:

$$GL_{(2x2)} = 12.91356\text{mm} + 6(0.244\text{mm}) = 14.37756\text{mm}$$

B. Width of the ground plane ($GW_{(2x2)}$)

$$GW_{(2x2)} = PW_{(2x2)} + 6(\text{SH})$$

By substituting $PW_{(2x2)} = 11.9205\text{mm}$ and $\text{SH} = 0.244\text{mm}$, $GW_{(2x2)}$ is calculated as:

$$GW_{(2x2)} = 11.9205\text{mm} + 6(0.244\text{mm}) = 13.3845\text{mm}$$

5. Length and width of last feed of 2x2 MSPA array ($LFL_{(2x2)}$ and $LFW_{(2x2)}$)

A. Width of last feed of 2x2 MSPA array ($LFW_{(2x2)}$)

$$LFW_{(2X2)} = 0.5*GW - (FQW - SQTW) - 0.25*SQTW - 0.5*CTLW$$

By substituting $GW_{(2X2)} = 13.3845\text{mm}$, $FQW = 0.63838\text{mm}$, $SQTW = 0.4783\text{mm}$, and $CTLW = 0.4783\text{mm}$, then $LFW_{(2X2)}$ is calculated as:

$$LFW_{(2X2)} = 6.69225\text{mm} - 0.16008\text{mm} - 0.11957\text{mm} - 0.23915\text{mm} = 6.173445\text{mm}$$

B. Length of last feed of 2x2 MSPA array ($LFL_{(2X2)}$)

$$LFL_{(2X2)} = 0.5*W_{(MFL1)} = 0.5 * 0.4783\text{mm} = 0.23915\text{mm}$$

6. Width and length of the feed point

Width of feed point for microstrip feeder line of 0.4783mm is calculated in chapter three. which is equal to 0.665376mm. Therefore, for microstrip feeder line width of 0.23915mm is half of 0.4783mm which is 0.332688mm. The impedance is less dependent on the length of the transmission line. Hence, length of the feed point is 1.35049mm.

The above physical dimension calculation of 2x2 inset-feed rectangular MSPA array is tabulated in Table 4.4.

Table 4.4: Calculated Physical Dimensions of 2x2 Inset-Feed Rectangular MSPA Array.

No	Design Parameters	Symbol	Values
1	Width of the patch	PW	3.26025mm
2	Length of the patch	PL	2.47818mm
3	Width of the ground plane	$GW_{(2X2)}$	13.3845mm
4	Length of the ground plane	$GL_{(2X2)}$	14.37756mm
5	Length of inset feed	Y_0	0.905498mm
6	Inset gap	G_p	0.017761mm
7	Length of the microstrip feeder line	$L_{(MFL1)}$	1.27696mm
8	Width of the microstrip feeder line	$W_{(MFL1)}$	0.4783mm
9	Horizontal feed length of power divider	HFLPD	0.23915mm
10	Horizontal feed width of power divider	HFWD	9.13855mm
11	First quarter transform width	FQW	0.63838mm
12	First-quarter transform Length	FQTL	0.4783mm
13	Second quarter transform width	SQTW	0.4783mm
14	Second quarter transform length	SQTL	0.63838mm
15	Third-quarter transform width	TQW	0.23915mm
16	Third-quarter transform length	TQTL	1.27696mm
17	Width of transmission line connecting two 2X1 MSPA	CTLW	0.4783mm
18	Length of transmission line connecting two 2X1 MSPA	CTLL	9.15778mm
19	Length of last microstrip feeder line	$LFL_{(2X2)}$	0.23915mm
20	Width of last microstrip feeder line	$LFW_{(2X2)}$	6.173445mm
21	Length of the feed point	$L_{(FP)}$	1.35049 mm
22	Width of the feed point	$W_{(FP)}$	0.332688mm
23	Distance between the patch	D	5.4 mm

4.7.2 4x4 Inset-feed Rectangular MSPA Array

Even-though 2x2 inset-feed rectangular MSPA array can improve the scanning capacity of linear MSPA arrays, the performance which will be obtained by 2x2 inset-feed rectangular MSPA array may not be large enough for different applications. Therefore, to enhance the performance of 2x2 inset-feed rectangular MSPA array in this section design of 4x4 inset-feed rectangular MSPA array is proposed. In order to design planar 4x4 inset-feed rectangular MSPA array, 16 single inset-feed rectangular MSPA elements are required as shown in Figure 4.11.

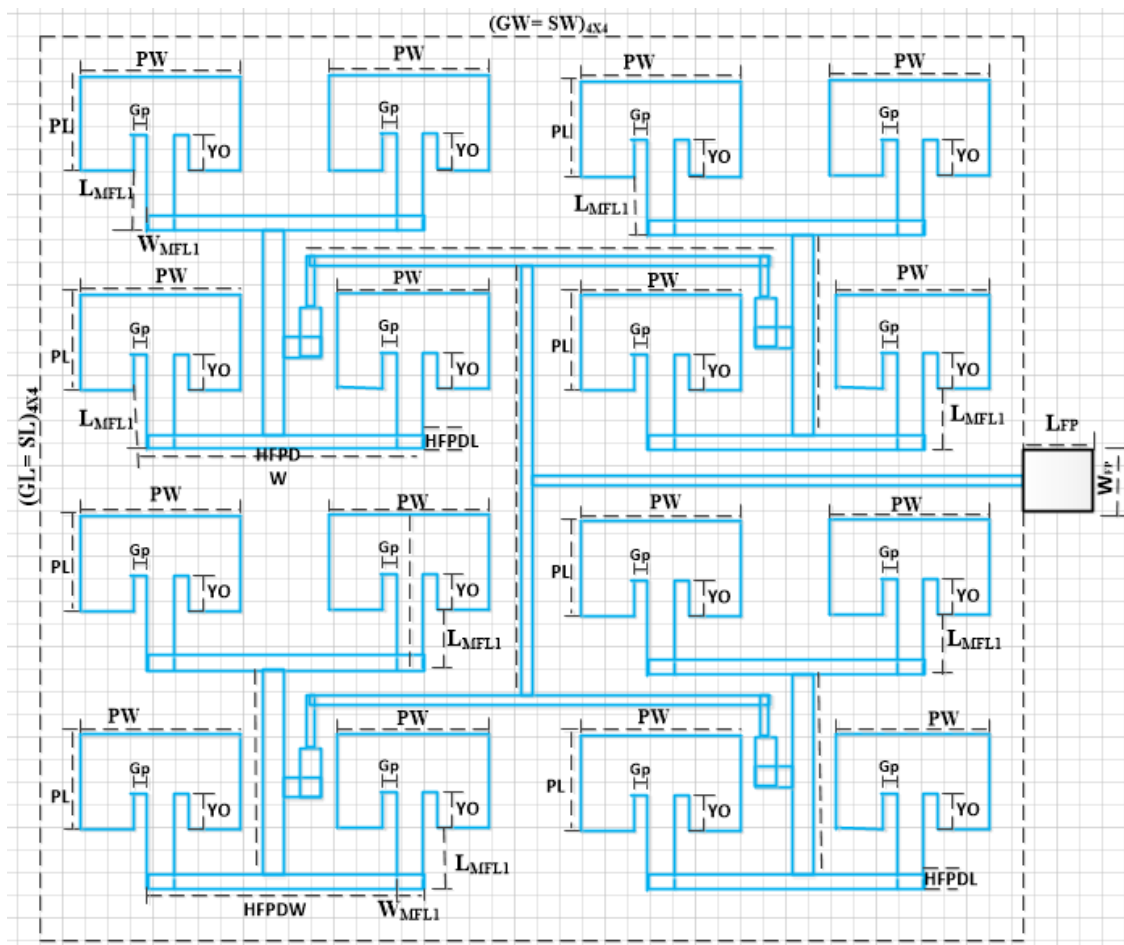


Figure 4.11: Physical Structure of the Proposed 4x4 Inset-feed Rectangular MSPA Array.

During the configuration, all sixteen elements are grouped into two to form two pairs of 2x2 planar configuration as indicated in Figure 4.9. Next, each group of 2x2 planar configurations is placed over each quadrant of the X-Y coordinate axis. So, designed parameters for 2x2 inset-feed rectangular MSPA array is directly used and remaining design parameters are calculated as follows.

1. Length and width of Microstrip transmission line connecting two 2x2 MSPA array (CTLW and CTLL)

A. The gap between the quarter transform and edge along the length of the patch

$0.5HFPDW_{(2x1)} = 0.5W_{(MFL1)} + FQTW + X(\text{gap}) + 0.5PW + 0.5W_{(MFL1)}$ which can be simplified to:

$$0.5HFPDW_{(2x1)} = W_{(MFL1)} + FQTW + X(\text{gap}) + 0.5PW$$

By substituting $W_{(MFL1)} = 0.4783\text{mm}$, $FQTW = 0.63838\text{mm}$, $PW = 3.26025\text{mm}$ and $0.5HFPDW_{(2x1)} = 0.5*9.13855\text{mm}$, then gap between quarter transform and left edge of the patch can be calculated as:

$$X(\text{gap}) = 0.5HFPDW_{(2x1)} - (W_{(MFL1)} + FQTW + 0.5PW)$$

$$X(\text{gap}) = 0.5*9.13855\text{mm} - (0.63838 + 0.4783 + 0.5*3.26025)\text{mm} = 1.82247\text{mm}$$

B. Width of Microstrip transmission line connecting two 2x2 MSPA (CTLW)

$$CTLW = 2PW + 2*X(\text{gap}) + 0.5SQTW + 4TQTW + D$$

By substituting $PW = 3.26025\text{mm}$, $SQTW = 0.4783\text{mm}$, and $TQTW = 0.23915\text{mm}$, then CTLW can be calculated as:

$$CTLW = 2*3.26025\text{mm} + 2*1.82247\text{mm} + 0.5*0.4783\text{mm} + 4*0.23915\text{mm} + 5.4\text{mm}$$

$$CTLW = 16.76119\text{mm}$$

C. Length of Microstrip transmission line connecting two 2x2 MSPA (CTLL)

$$CTLL = 0.5 * W_{(MFL1)}$$

By substituting $W_{(MFL1)} = 0.4783\text{mm}$, then CTLL can be calculated as:

$$CTLL = 0.5*0.4783\text{mm} = 0.23915\text{mm}$$

2. Length and width of Microstrip transmission line connecting two 2x4 MSPA array (CCTLW and CCTLL)

A. Length of Microstrip transmission line connecting two 2x4 MSPA array (CCTLL)

$$CCTLL = D + 2PL + 2L_{(MFL1)}$$

By substituting $D = 5.4\text{mm}$, $PL = 2.47818\text{mm}$ and $L_{(MFL1)} = 1.27696\text{mm}$, CCTLL is calculated as:

$$CCTLL = 5.4\text{mm} + 2*2.47818\text{mm} + 2*1.27696\text{mm} = 12.910271\text{mm}$$

B. Width of Microstrip transmission line connecting two 2x4 MSPA array (CCTLW)

$$CCTLW = 0.5W_{(MFL1)}$$

But the dimension of $W_{(MFL1)}$ is 0.4783mm then, CCTLW can be calculated as:

$$CCTLW = 0.5*0.4783\text{mm} = 0.23915\text{mm}$$

3. Length and width of connected 4x4 MSPA array

A. Width of connected 4x4 MSPA array

$$PW_{(4X4)} = 4PW + 3D$$

By substituting $PW = 3.2605\text{mm}$ and $D = 5.4\text{mm}$, then $PW_{(4X4)}$ is calculated as:

$$PW_{(4X4)} = 4*3.26025\text{mm} + 3*5.4\text{mm} = 29.241\text{mm}$$

B. Length of connected 4x4 MSPA array

$$PL_{(4X4)} = 4PL + 3D$$

By substituting $PL = 2.47818\text{mm}$ and $D = 5.4\text{mm}$, then $PL_{(4X4)}$ is calculated as:

$$PL_{(4X4)} = 4*2.47818\text{mm} + 3*5.4\text{mm} = 26.11271\text{mm}$$

4. Ground plane dimension ($GW_{(4x4)}$ and $GL_{(4x4)}$)

A. Ground plane width ($GW_{(4X4)}$)

$$GW_{(4X4)} = PW_{(4X4)} + 6(\text{SH})$$

By substituting $PW = 29.241\text{mm}$ and $\text{SH} = 0.244\text{mm}$, then $GW_{(4X4)}$ is calculated as:

$$GW_{(4X4)} = 29.241\text{mm} + 6*0.244\text{mm} = 30.705\text{mm}$$

B. Ground plane length ($GL_{(4X4)}$)

$$GL_{(4X4)} = PL_{(4X4)} + 6(\text{SH})$$

By substituting $PL = 26.1127\text{mm}$ and $\text{SH} = 0.244\text{mm}$, then $GL_{(4X4)}$ is calculated as:

$$GL_{(4X4)} = 26.11271\text{mm} + 6*0.244\text{mm} = 27.576708\text{mm}$$

5. Length and width of last feed of 4x4 MSPA array ($LFL_{(4x4)}$ and $LFW_{(4x4)}$)

A. Width of last feed of 4x4 MSPA array ($LFW_{(4X4)}$)

$$LFW_{(4X4)} = 0.5GW_{(4X4)} - 0.5\text{CCTLW}$$

By substituting $\text{CCTLW} = 0.23915\text{mm}$ and $GW_{(4x4)} = 30.705\text{mm}$, then $LFW_{(4x4)}$ is calculated as:

$$LFW_{(4X4)} = 0.5*30.705\text{mm} - 0.5*0.23915\text{mm} = 15.232925\text{mm}$$

B. Length of last feed of 4x4 MSPA array ($LFL_{(4X4)}$)

$$LFL_{(4X4)} = 0.5W_{(MFL1)}$$

But, the dimension of $W_{(MFL1)}$ is 0.4783mm , then the dimension of $LFL_{(4X4)}$ is:

$$LFL_{(4X4)} = 0.5*0.4783\text{mm} = 0.23915\text{mm}$$

The designed parameters of 4x4 rectangular MSPA array is summarized in Table 4.5.

Table 4.5: Calculated Physical Dimensions of 4x4 Inset-Feed Rectangular MSPA Array.

No.	Constant Parameter	Symbol	Values
1	Resonant frequency	F_0	28GHz
2	Substrate height	SH	0.244mm
3	Dielectric constant	ϵ_r	4.4
4	Input characteristic impedance	Z_0	50 Ω
5	Thickness of metal patch	t	0.035mm
No.	Design Parameters	Symbol	Values
1	Width of the patch	PW	3.26025mm
2	Length of the patch	PL	2.47818mm
3	Width of ground plane	$GW_{(4x4)}$	30.705mm
4	Length of ground plane	$GL_{(4x4)}$	27.57671mm
5	Length of inset feed	Y_0	0.905498mm
6	Inset gap	G_P	0.017761mm
7	Length of the microstrip feeder line	$L_{(MFL1)}$	1.27696mm
8	Width of the microstrip feeder line	$W_{(MFL1)}$	0.4783mm
9	Horizontal feed length of power divider	HFLPD	0.23915mm
10	Horizontal feed width of power divider	HFWD	9.13855mm
11	First quarter transform width	FQTW	0.63838mm
12	First-quarter transform Length	FQTL	0.4783mm
13	Second quarter transform width	SQTW	0.4783mm
14	Second quarter transform length	SQTL	0.63838mm
15	Third-quarter transform width	TQTW	0.23915mm
16	Third-quarter transform length	TQTL	1.27696mm
17	Width of microstrip line connecting two 2X1 MSPA	CTLW	0.4783mm
18	Length of microstrip line connecting two 2X1 MSPA	CTLL	9.15778mm
19	Width of microstrip line connecting two 2X2 MSPA	CTLW	16.76119mm
20	Width of microstrip line connecting two 2X2 MSPA	CTLW	0.23915mm
21	Width of microstrip line connecting two 2X4 MSPA	CCTLW	0.23915mm
22	Length of microstrip line connecting two 2X4 MSPA	CCTLL	12.91027mm
23	Length of last microstrip feeder line	$LFL_{(4x4)}$	15.2329mm
24	Width of last microstrip feeder line	$LFW_{(4x4)}$	0.23915mm
25	Length of the feed point	$L_{(FP)}$	1.35049 mm
26	Width of the feed point	$W_{(FP)}$	0.332688mm
27	Distance between the patch	D	5.4mm

4.7.3 8x8 Inset-feed Rectangular MSPA Array

Attempting to further performance improvement of planar inset-feed rectangular MSPA array, in this section numerical design approach of 8x8 inset-feed rectangular MSPA array has been proposed. Because, by using above proposed 4x4 MSPA array maximum performance may not be achieved. To design planar 8x8 inset-feed rectangular MSPA array, sixty-four (64) single inset-feed rectangular MSPA elements are required. These all elements are grouped into two pairs of 4x4 planar configuration and then, each of 4x4 planar configurations is placed over each quadrant of the X-Y coordinate axis. Therefore, the design parameter of 4x4 planar array is used to design an 8x8 inset-feed rectangular MSPA array even though the remaining design parameters are calculated as shown below.

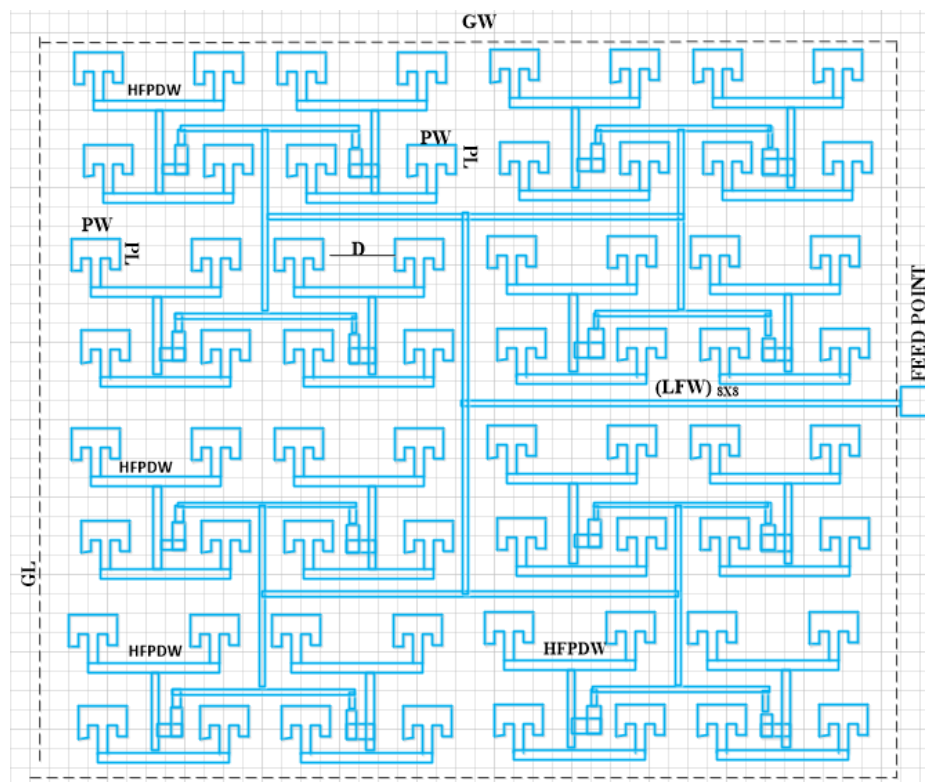


Figure 4.12: Physical Structure of the Proposed 8x8 Inset-feed Rectangular MSPA Array.

1. Length and width of Microstrip transmission line connecting two 4x4 MSPA array (F2FCTLW and F2FCTLL)

A. Width of Microstrip transmission line connecting two 4x4 MSPA array (F2FCTLW)

$$F2FCTLW = 2((0.5D - 0.25W_{(MFL1)}) + 2PW + D) = 29.0018\text{mm}$$

B. Length of Microstrip transmission line connecting two 4x4 MSPA (F2FCTLL)

$$F2FCTLL = 0.5W_{(MFL1)}$$

But, the dimension of $W_{(MFL1)}$ is 0.4783mm, then F2FCTLL is calculated as:

$$F2FCTLL = 0.5 * 0.4783\text{mm} = 0.23915\text{mm}$$

2. Length and width of Microstrip transmission line connecting two 4x8 MSPA array (F2ECTLW and F2ECTLL)

A. Length of Microstrip transmission line connecting two 4x8 MSPA array (F2ECTLL)

$$F2ECTLL = 2((0.5D - 0.25W_{(MFL1)})) + 4D + 4PL + 4L_{(MFL1)}$$

By substituting $W_{(MFL1)} = 0.4783\text{mm}$, $PL = 2.47818\text{mm}$, and $D = 5.4\text{mm}$, then F2ECTLL is calculated as:

$F2ECTLL = D - 0.5W_{(MFL0)} + 4D + 4PL + 4L_{(MFL1)}$ which can be simplified to:

$$F2ECTLL = 5D + 4PL + 4L_{(MFL1)} - 0.5W_{(MFL0)}$$

$$F2ECTLL = 5*5.4\text{mm} + 4*2.47818\text{mm} + 4*2.47818\text{mm} - 0.23915\text{mm} = 41.781158\text{mm}$$

B. Width of Microstrip transmission line connecting two 4x8 MSPA array (F2ECTLW)

$F2ECTLW = 0.5W_{(MFL1)}$ But, $W_{(MFL1)}$ is 0.4783mm , then F2ECTLW is:

$$F2ECTLW = 0.5*0.4783\text{mm} = 0.23915\text{mm}$$

3. Length and width of connected 8x8 MSPA array

A. Width of connected 8x8 MSPA array ($PW_{(8X8)}$)

$$PW_{(8X8)} = 8PW + 7D = 2PW_{(4X4)} + D$$

By substituting $PW_{(4X4)} = 29.241\text{mm}$ and $D = 5.4\text{mm}$, then $PW_{(8X8)}$ is calculated as:

$$PW_{(8X8)} = 2(29.241\text{mm}) + 5.4\text{mm} = 63.882\text{mm}$$

B. Length of connected 8x8 MSPA array ($PL_{(8X8)}$)

$$PL_{(8X8)} = 8PL + 7D + 8*L_{(MFL)} = 2PL_{(4x4)} + D$$

By substituting $PL_{(4X4)} = 26.11271\text{mm}$ and $D = 5.4\text{mm}$, then $PL_{(8X8)}$ is calculated as:

$$PL_{(8X8)} = 2(26.11271\text{mm}) + 5.4\text{mm} = 57.62542\text{mm}$$

4. Ground plane dimension of 8x8 MSPA ($GL_{(8X8)}$ and $GW_{(8X8)}$)

A. Ground plane width of 8x8 MSPA ($GW_{(8X8)}$)

$$GW_{(8X8)} = PW_{(8X8)} + 6(\text{SH})$$

By substituting $PW_{(8X8)} = 63.882\text{mm}$ and $\text{SH} = 0.244\text{mm}$, then $GW_{(8X8)}$ is calculated as:

$$GW_{(8X8)} = 63.882\text{mm} + 6*0.244\text{mm} = 65.346\text{mm}$$

B. Ground plane length of 8x8 MSPA ($GL_{(8X8)}$)

$$GL_{(8X8)} = PL_{(4X4)} + 6(\text{SH})$$

By substituting $PL_{(4X4)} = 57.625416\text{mm}$ and $\text{SH} = 0.244\text{mm}$, then $GL_{(8X8)}$ is calculated as:

$$GL_{(8X8)} = 57.625416\text{mm} + 6*0.244\text{mm} = 59.089416\text{mm}$$

5. Length and width of last feed of 4x4 MSPA array ($LFL_{(8X8)}$ and $LFW_{(8X8)}$)

A. Width of last feed of 4x4 MSPA array ($LFW_{(8X8)}$)

$$LFW_{(8X8)} = 0.5*(GW_{(8X8)} - 0.5*E2ECTLW) = 32.55343\text{mm}$$

B. Length of last feed of 4x4 MSPA array ($LFL_{(8X8)}$)

$$LFL_{(8X8)} = 0.5W_{(MFL1)} = 0.23915\text{mm}.$$

The design parameters of 8x8 inset-feed rectangular MSPA array are tabulated in Table 4.6.

Table 4.6: Calculated Physical Dimensions of 8x8 Inset-Feed MSPA Array.

No	Constant Parameter	Symbol	Values
1	Resonant frequency	F_0	28GHz
2	Substrate height	SH	0.244mm
3	Dielectric constant	ϵ_r	4.4
No	Design Parameters	Symbol	Values
1	Width of the patch	PW	3.26025 mm
2	Length of the patch	PL	2.47818mm
3	Width of the substrate	$SW_{(8x8)}$	65.346mm
4	Width of the ground plane	$GW_{(8x8)}$	65.346mm
5	Length of inset feed	Y_0	0.905498mm
6	Inset gap	G_P	0.017761mm
7	Length of the microstrip feeder line	L_{MFL1}	1.27696mm
8	Width of the microstrip feeder line	W_{MFL1}	0.4783 mm
9	Horizontal feed length of power divider	HFLPD	0.23915mm
10	Horizontal feed width of power divider	HFWPD	9.23855mm
11	First quarter transform width	FQTW	0.63838mm
12	First-quarter transform Length	FQTL	0.4783 mm
13	Second quarter transform width	SQTW	0.4783 mm
14	Second quarter transform length	SQTL	0.63838mm
15	Third-quarter transform width	TQTW	0.23915mm
16	Third-quarter transform length	TQTL	1.27696mm
17	Width of microstrip line connecting two 2X1 MSPA	CTLW	0.4783 mm
18	Length of microstrip line connecting two 2X1 MSPA	CTLL	9.15778mm
19	Width of microstrip line connecting two 2X2 MSPA	CTLW	16.96119mm
20	Width of microstrip line connecting two 2X2 MSPA	CTLW	0.23915mm
21	Width of microstrip line connecting two 2X4 MSPA	CTLW	0.23915mm
22	Length of microstrip line connecting two 2X4 MSPA	CTLL	13.01027mm
23	Distance between the patch	D	5.4 mm
24	Width of microstrip line connecting two 4X4 MSPA	F2FCTLW	29.0018mm
25	Length of microstrip line connecting two 4X4 MSPA	F2FCTLL	0.23915mm
26	Width of microstrip line connecting two 4X8 MSPA	F2ECTLW	0.23915mm
27	Length of microstrip line connecting two 4X8 MSPA	F2ECTLL	41.78116mm
28	Width of last microstrip feeder line	$LFW_{(8x8)}$	32.55343mm
29	Length of last microstrip feeder line	$LFL_{(8x8)}$	0.23915mm
30	Length of the feed point	$L_{(FP)}$	1.35049 mm
31	Width of the feed point	$W_{(FP)}$	0.332688mm

Chapter 5

Simulation Results and Discussion

5.1 Introduction

In this chapter, the simulation results and discussion of all the studied rectangular MSPA array configurations have been presented. The over all chapter is organized into two major sub-sections. The first sub-section presents, simulation results and discussion of one-dimensional inset-feed rectangular MSPA arrays. In the second sub-section, simulation results and discussion of two-dimensional inset-feed rectangular MSPA arrays have been presented. Besides, under each sub-section, the performance of the studied antenna is analyzed in terms of; return losses, bandwidth, beam directivity and gain, radiation efficiency, and side lobe level. Generally, to validate the performance of all the proposed antenna CST-MW studio antenna simulator software has been used.

5.2 Simulation Results and Discussion of 1D MSPA Array

In this section, the simulation result and discussion of single element, 2x1, and 4x1 inset feed rectangular MSPA array has been presented. For studied antenna initially calculated dimensions are summarized in the Table 4.1, Table 4.2, and Table 4.3 respectively. The tuned dimensions of the design parameters that have been used for the simulations are listed in the Table 1, Table 2, and Table 3 in the Appendix one respectively. Also, the physical structure of antenna for the tuned parameters are indicated in Figure 1, Figure 2, and Figure 3 in the Appendix-two respectively.

5.2.1 Single Inset-feed Rectangular MSPA

The return loss versus frequency plot of the proposed single inset-feed rectangular MSPA is indicated in Figure 5.1. From the plot, it can be observed that the return losses of the proposed antenna is less than -10dB between 27.71GHz and 28.282GHz. At the resonant frequency, the return loss is -20.2365dB and VSWR is 1.2156. As compared to design reported in [7][13][40], achieved return loss is minimum. This is because of, the impedance mismatch at feeder point and the edge of the patch has been minimized using inset-feed impedance matching techniques, width of quarter-wavelength impedance transformer, and

tuned antenna parameters. As a result, a large amount of input power is transmitted to the transmission line and small input power is returned as a return loss which leads to dip S_{11} plot at the resonant frequency. The -10dB bandwidth of the proposed antenna is 572MHz. Using the tuned width of the patch and ground plane dimension, wide bandwidth is achieved as compared to the design reported in [9][41]. However, achieved bandwidth is narrow as compared to design reported in [7][40].

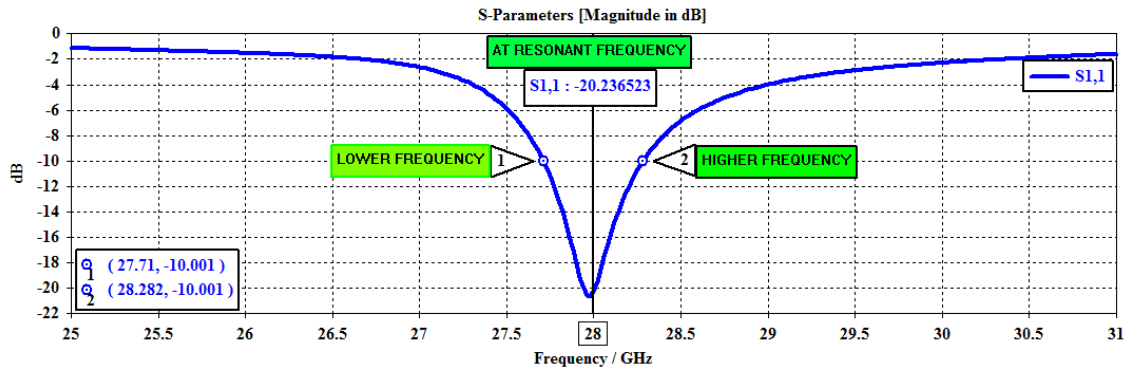


Figure 5.1: Return loss versus frequency plot for the single element rectangular MSPA.

Another parameter which is often used to characterize antenna is the radiation pattern. The 3D radiation pattern of the proposed single inset-feed MSPA is shown in Figure 5.2. As depicted in the figure, the directivity, gain, radiation efficiency, and total efficiency of the designed antenna are 7.404dBi, 7.18dBi, 94.95% and 94.27% respectively. Achieved efficiency is higher than simulation result reported in [7][9][13][41]. The radiation efficiency is significantly higher because of, in the design two impedance matching techniques have been simultaneously used. As a result, the impedance mismatch at the feeding network and the edge of the patch is highly minimized. In addition, the effect of the design parameter on radiation efficiency has been properly analyzed in order to find the dimension where good radiation efficiency is obtained.

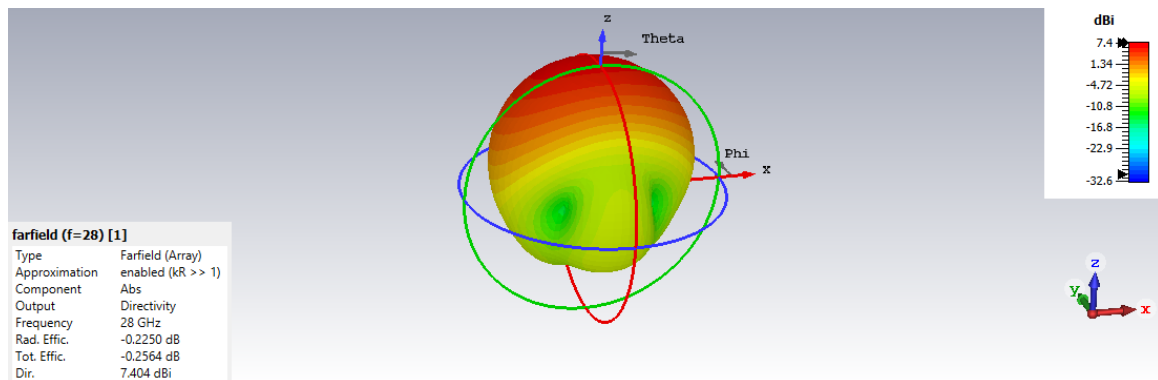


Figure 5.2: 3D radiation pattern for the single element rectangular MSPA.

From the simulated 2D radiation pattern shown in Figure 5.3, the side lobe level of the studied single inset-feed MSPA is -12.1dB. The key implication of this result is the proposed antenna radiates highly towards the desired direction and less in other directions. In addition, half-power beam width of the radiation pattern is occurred at 72.3 degree.

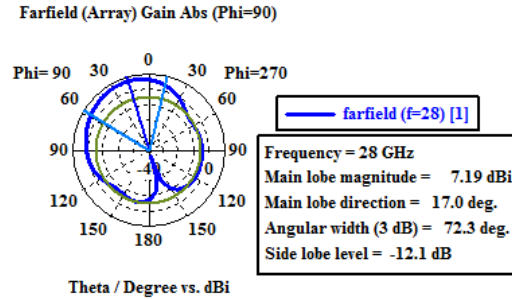


Figure 5.3: 2D radiation pattern for the single element rectangular MSPA.

Performance comparison of the proposed single inset-feed rectangular MSPA with reported designs in literature is shown in Table 5.1. In terms of the directivity and gain, the proposed design outperforms the designs reported in [7][13][18][19][40][41]. Similarly, in terms of the radiation efficiency and total radiation efficiency, the proposed design outperforms the designs reported in [7][9][13][18][40][41]. Lastly, in terms of the return losses the proposed design outperforms the designs reported in [7][13][19][40]. Therefore, it can be said that the proposed single element patch antenna gives highly competitive performance as compared to other single element patch antenna reported in scientific literature.

Table 5.1: Performance comparison of the reported and proposed single element MSPA.

Ref.	Subs. Type	F_O (GHz)	S_{11} (dB)	DIR (dBi)	GAIN (dBi)	VSWR	η_{tot} (%)	η_{rad} (%)	BW (MHz)
[7]	ROG	28	-13.480	6.2	4.48	1.5376	70.177	78.9	847
[9]	ROG	28	-20.534	7.966	6.219	1.0289	64.98	65.6	400
[13]	FR-4	28	-15.35	-	6.921	1.787	80.77	87.77	-
[18]	ROG	28	-23.67	7.39	-	-	80.77	87.1	1150
[19]	ROG	28	-17.4	-	6.72	1.279	-	-	-
[40]	ROG	28	-20.03	-	5.23	1.220	95.9	-	21100
[41]	Taco	28	-27.70	-	6.72	1.220	86.73	-	463
This work	FR-4	28	-20.24	7.404	7.18	1.216	94.27	94.95	572

Where, η_{rad} , η_{tot} , S_{11} , ROG, and TAC are denotes radiation efficiency, total radiation efficiency, return loss, Rogers, and Taconic respectively.

5.2.2 2x1 Inset-feed Rectangular MSPA Array

The simulated return loss of 2x1 inset-feed rectangular MSPA array is shown in Figure 5.4. From the plot, the return loss is less than -10dB between 27.755GHz and 28.33GHz. At 28GHz, it is -19.8859dB and also, the VSWR is 1.3436. Besides, the -10dB return loss bandwidth of the proposed 2x1 rectangular MSPA array is 575MHz, which is wider than that of the single patch antenna described in the above section. In general, as compared to designs reported in [13][36][42], achieved return loss is minimum. This is because of, both the inset-feed and quarter-wavelength impedance matching techniques has been used to minimize impedance mismatch at the edge of the patch and, also important dimensions of the antenna is tuned.

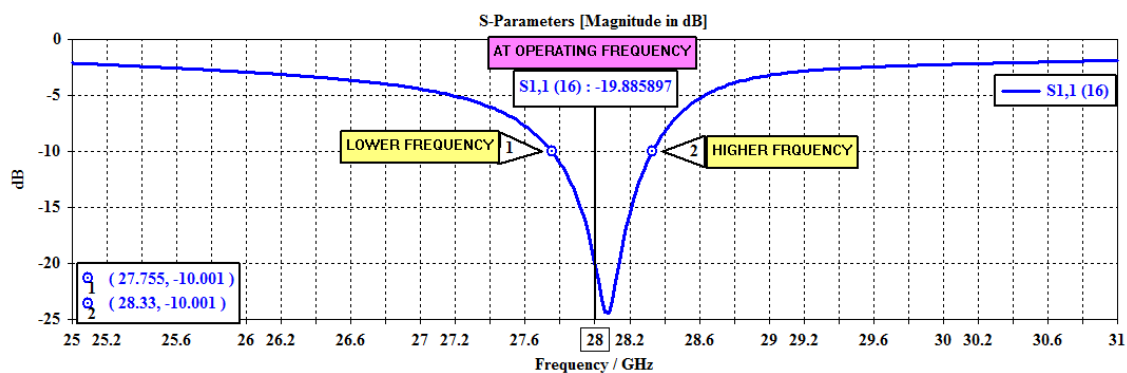


Figure 5.4: Return loss versus frequency plot for the 2x1 rectangular MSPA array.

The 3D radiation pattern of the studied 2x1 rectangular MSPA array is indicated in Figure 5.5. From the figure, the directivity and gain of the antenna are 9.451dBi and 9.299dBi respectively. Similarly, the radiation efficiency and total efficiency of the antennas are 96.56% and 92.53% respectively. The designed 2x1 MSPA array increases the directivity and gain of a single patch antenna by 2.047dBi and 2.119dBi respectively. Hence, the stuided 2x1 MSPA array shows superior performance than the single patch antenna.

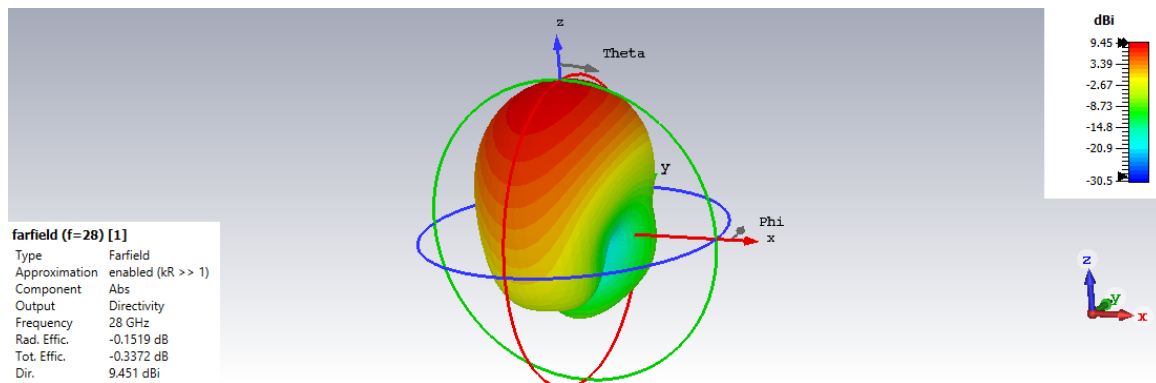


Figure 5.5: 3D radiation pattern for the 2x1 rectangular MSPA array.

Figure 5.6 shows the 2D radiation pattern of the proposed 2x1 inset-feed rectangular MSPA array. From the graph, the side lobe level is -16.8dB. Besides, half-power beam width of the radiation pattern is occurred at 78.9 degree.

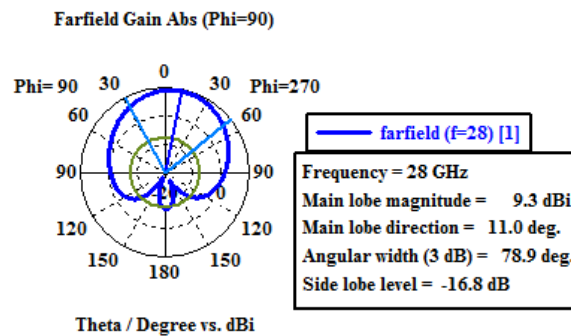


Figure 5.6: 2D radiation pattern for the 2x1 rectangular MSPA array.

The summarized comparative analysis of 2x1 antenna array designs reported in literature is shown in Table 5.2. The proposed design achieves better radiation efficiency than the design reported in [13][42]. In addition, in terms of the return losses the proposed design outperforms the designs in reported [13][36][42].

Table 5.2: Performances comparison of the existing and proposed 2x1 MSPA array.

Ref.	Subs. type	F_O (GHz)	S_{11} (dB)	DIR (dBi)	GAIN (dBi)	VSWR	η_{rad} (%)	η_{tot} (%)	BW (MHz)
[13]	FR-4	28	-14.70	9.853	-	1.624	92.7	87.77	-
[36]	ROG	28	-16.65	12	12.40	-	-	-	-
[42]	FR-4	28	-14.80	6.740	6.150	-	86.28	-	-
This work	FR-4	28	-19.89	9.451	9.299	1.344	96.56	92.53	575

Where, η_{rad} , η_{tot} , and S_{11} are denotes; radiation efficiency, total radiation efficiency, and magnitude of the return loss respectively.

5.2.3 4x1 Inset-feed Rectangular MSPA Array

The simulated S_{11} plot of 4x1 rectangular MSPA array is shown in Figure 5.7. From the plot, the return loss is less than -10dB between 27.131GHz and 28.525GHz. At 28GHz, it is -27.4218dB and also VSWR is 1.1059. The -10dB bandwidth of the antenna is 1.394GHz. Achieved bandwidth is wider than the bandwidth of single patch antenna and 2x1 MSPA array by 842MHz and 819MHz respectively. The bandwidth is significantly increased because of; successive branching of parallel feeding networks with equal path lengths to each element and tuned width of the patch has been used to minimized input impedance of the antenna which in turns to increase the radiation efficiency and bandwidth of the antenna.

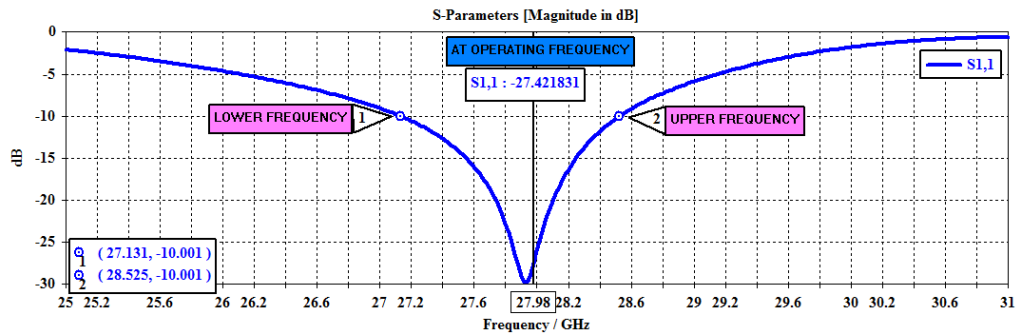


Figure 5.7: Return loss versus frequency plot for the 4x1 rectangular MSPA array.

The 3D radiation pattern of the proposed 4x1 MSPA array is shown in Figure 5.8. From the graph the beam gain, directivity, radiation efficiency and total radiation efficiency of the designed 4x1 MSPA array are; 11.06dBi, 11.2dBi, -0.1140dB (97.41%) and -0.3170dB (96.56%) respectively. In general, the proposed 4x1 inset-feed rectangular MSPA array increases the gain and directivity of single MSPA by 3.88dBi and 3.796dBi respectively. Similarly, the gain and directivity of 2x1 inset-feed MSPA array are maximized by 1.761dBi and 1.749dBi respectively.

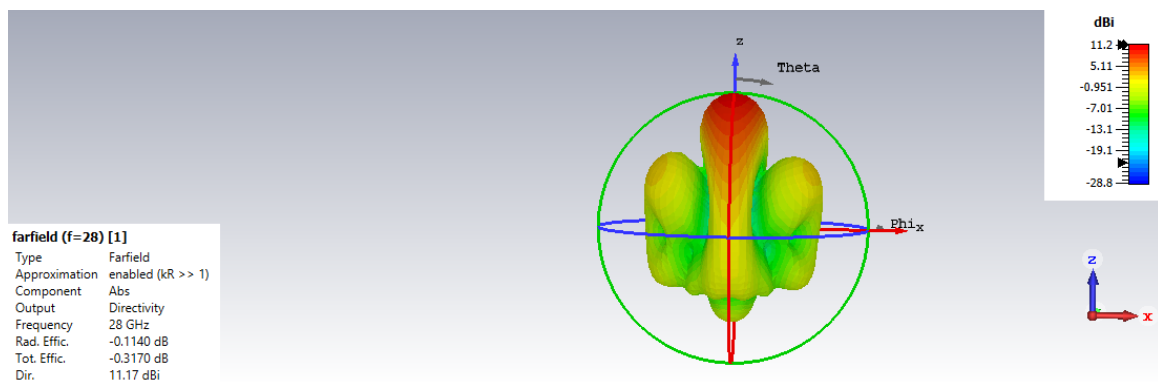


Figure 5.8: 3D radiation pattern for the 4x1 rectangular MSPA array.

The simulated 2D radiation pattern of the 4x1 inset-feed rectangular MSPA array model is given in Figure 5.9. The side lobe level of this antenna is -11.8dB and the half-power beam width of the radiation pattern is occurred at 72.3 degree.

The performance of the proposed 4x1 antenna array structure is compared with antenna of the same structured reported in literature. As shown in Table 5.3, in terms of the return loss and radiation efficiency the proposed design outperforms the design reported in [13][15].

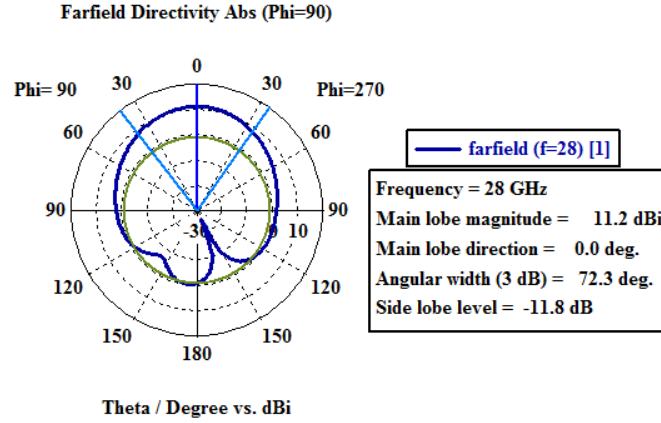


Figure 5.9: 2D radiation pattern for the 4x1 rectangular MSPA array.

Table 5.3: Performance comparison of the existing and proposed 4x1 MSPA array.

Ref.	Subs. type	F_O (GHz)	S_{11} (dB)	DIR (dBi)	GAIN (dBi)	VSWR	η_{rad} (%)	η_{tot} (%)	BW (GHz)
[13]	FR-4	28	-21.4476	11.99	-	1.6502	83.95	78.9	-
[15]	FR-4	28	-17.6	-	-	-	79.9	-	0.540
This work	FR-4	28	-27.4218	11.2	11.06	1.1059	97.41	96.56	1.394

Where, η_{rad} denotes radiation efficiency, η_{tot} denotes total radiation efficiency, S_{11} denotes return losses, and BW denotes bandwidth.

5.3 Simulation Result and Discussion of 2D MSPA Arrays

In this section, the simulation result and discussions of 2x2, 4x4, and 8x8 inset-feed rectangular MSPA array has been presented. For proposed antennas, initially calculated dimensions are tabulated in the Table 4.4, Table 4.5, and Table 4.6 respectively. The design parameters that are used for the simulations are listed in the Table 4, Table 5, and Table 6 in the Appendix-one respectively. Similarly, the physical structure antenna for the tuned parameters are indicated in Figure 4, Figure 5, and Figure 6 in the Appendix-two respectively.

5.3.1 2x2 Inset-feed Rectangular MSPA Array

Figure 5.10 shows S_{11} plot of the proposed 2x2 rectangular MSPA array. From the plot, between 27.823GHz and 28.149GHz the return loss is less than -10dB. At a resonant frequency, the return loss is -32.6876dB and VSWR is 1.04752. Therefore, the reason for the achieved minimum result is, due to good impedance matching made between the last

100Ω microstrip feeder line and center microstrip transmission of 50Ω line using a quarter-wavelength impedance transformer. Also, using inset-feed impedance matching techniques, the impedance mismatch between the arm of 1:2 power divider and the edge of the patch is matched to required values. Besides, the obtained -10dB bandwidth of the proposed 2x2 rectangular MSPA array is 326MHz.

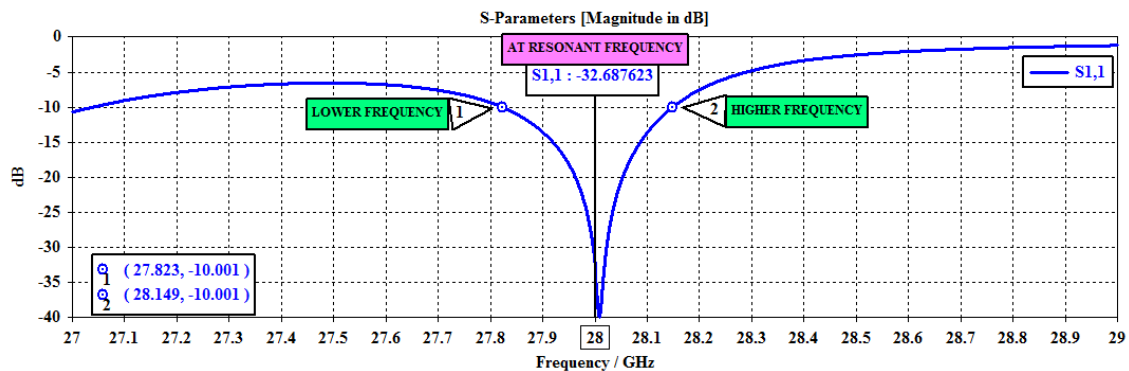


Figure 5.10: Return loss versus frequency plot for the 2x2 rectangular MSPA array.

The 3D radiation pattern of designed 2x2 inset-feed rectangular MSPA array is shown in Figure 5.11. From the figure, the achieved directivity, gain, radiation efficiency, total radiation efficiency of the proposed antenna are; 11.12dBi, 10.71dBi, -0.4143dB (90.9%), -0.4677dB (89.79%) respectively. Generally, in terms of radiation efficiency, the proposed design outperforms the design reported in [9][43]. The improvement is achieved because of, the impedance mismatch at the feed-point, at the edge of the patch, and microstrip feeder line have been minimized in addition to the inset-feed impedance matching techniques and tuning of design parameters, quarter-wavelength impedance transformer is introduced.

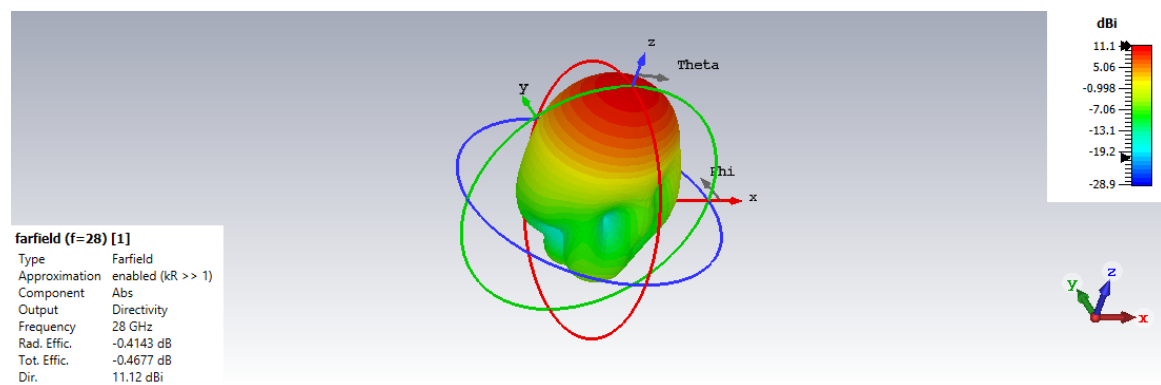


Figure 5.11: 3D radiation pattern for the 2x2 rectangular MSPA array.

The Simulated 2D radiation pattern of the designed 2x2 inset-feed rectangular MSPA array is shown in Figure 5.12. From the figure, mutual coupling between the elements of the array is -15dB which is acceptable and minimum. Performance comparison the proposed

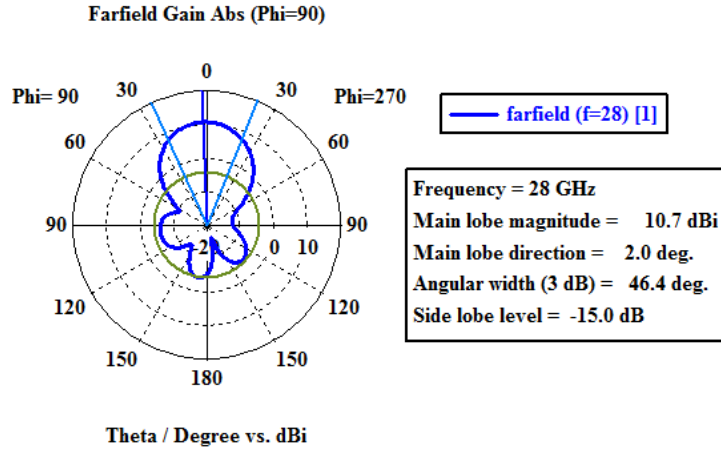


Figure 5.12: 2D radiation pattern for the 2x2 rectangular MSPA array.

antenna and previously reported design is given in Table 5.4. In terms of the return losses, the proposed design outperforms the designs reported in [9][42][43]. Similarly, in terms of beam directivity and gain the proposed design outperforms the designs reported in [9][42] but design reported in [43] out performs the proposed antenna. Lastly, in terms of the radiation efficiency, the proposed design outperforms the designs reported in [9][43].

Table 5.4: Final simulation results of the existing and proposed 2x2 MSPA array.

Ref.	Subs. type	F_O (GHz)	S_{11} (dB)	DIR (dBi)	GAIN (dBi)	VSWR	η_{rad} (%)	η_{tot} (%)	BW (MHz)
[9]	ROG	28	-19.66	10.13	8.393	1.232	82.85	-	400
[42]	FR-4	28	-20	6.866	7.2	-	-	-	950
[43]	ROG	28	-21.5	-	12.51	1.160	98.31	-	940
This work	FR-4	28	-32.69	11.12	10.71	1.0475	90.9	89.79	326

Where, η_{rad} denotes radiation efficiency, η_{tot} denotes total radiation efficiency, S_{11} denotes the magnitude of the return losses, and BW denotes bandwidth.

5.3.2 4x4 Inset-feed Rectangular MSPA Array

The S_{11} plot of the proposed 4x4 rectangular MSPA array is indicated in Figure 5.13. From the plot, between 27.819GHz and 28.151GHz the return loss is less than -10dB. At the resonant frequency, the return loss is -33.1499dB and VSWR is 1.04499. The -10dB bandwidth of the proposed antenna is 332MHz.

The bandwidth of 4x4 is wider than that of the 2x2 rectangular MSPA array by 6MHz. This because of the number of the array elements are increased to sixths and thereby overall radiation efficiency is high and results to significantly improved bandwidth.

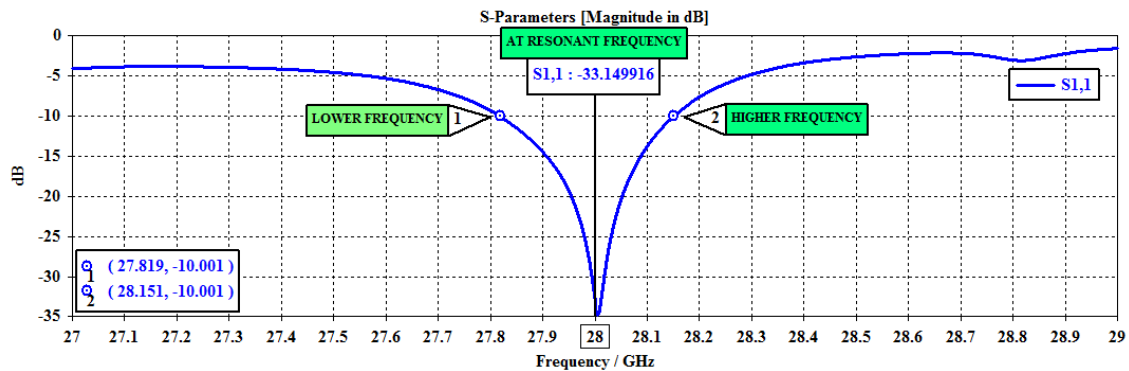


Figure 5.13: Return loss versus frequency plot for the 4x4 rectangular MSPA array.

The simulated 3D far-field radiation pattern of the studied antenna array is shown in Figure 5.14. From the figure, the radiation efficiency and total efficiency are -0.6277dB (86.543%) and -0.7019dB (85.08%) respectively. The directivity and gain of the the proposed 2x2 inset-feed MSPA array introduced in above section are 11.12dBi and 10.71dBi respectively. Whereas, the directivity and gain of the proposed 4x4 inset-feed MSPA array is increased to 15.8dBi and 15.17dBi respectively. The number of array elements are increased from 4 to 16 element which leads to the directivity and gain of 2x2 inset-feed MSPA array is improved by 4.68dBi and 4.46dBi respectively.

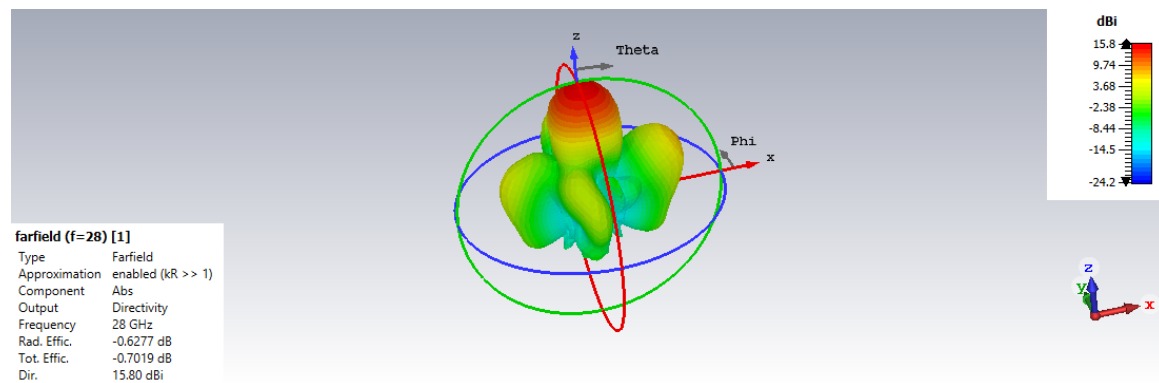


Figure 5.14: 3D radiation pattern for the 4x4 rectangular MSPA array.

The 2D radiation pattern of the designed 4x4 inset-feed rectangular MSPA array is shown in Figure 5.15. From Figure 5.12, the SLL of the proposed 2x2 inset-feed MSPA array is found to be -15dB. Whereas, the SLL of the proposed 4x4 inset-feed MSPA is -11.1dB as indicated in Figure 5.15. Even though the design parameters are properly tuned, the effect of mutual coupling is increased with array elements. Because minimum mutual coupling

from each of the quadrant planes is added together to increase the overall mutual coupling of the array. However, for both design minimum magnitude of SLL is achieved.

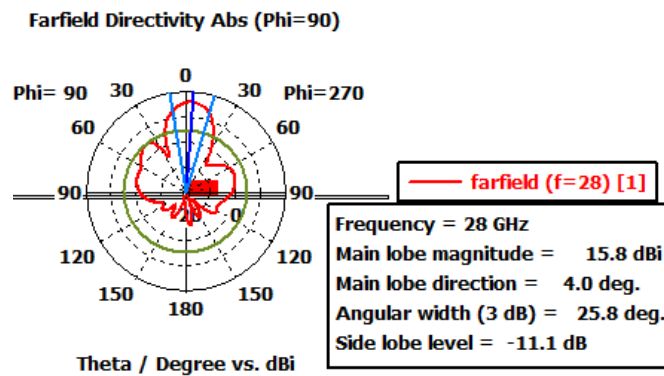


Figure 5.15: 2D radiation pattern for the 4x4 rectangular MSPA array.

5.3.3 8x8 Inset-feed Rectangular MSPA Array

Figure 5.16 shows the S_{11} plot of the designed 8x8 inset-feed rectangular MSPA array. From the plot, at the resonant frequency the return loss is -17.797dB and also, the VSWR of the proposed 8x8 rectangular MSPA array is 1.2977 which is acceptable and minimum. The -10dB return loss bandwidth of the proposed antenna is 368MHz. As compared to the proposed 2x2 and 4x4 rectangular MSPA array introduced in above section, bandwidth of the studied 8x8 rectangular MSPA array is wider by 42MHz and 36MHz respectively.

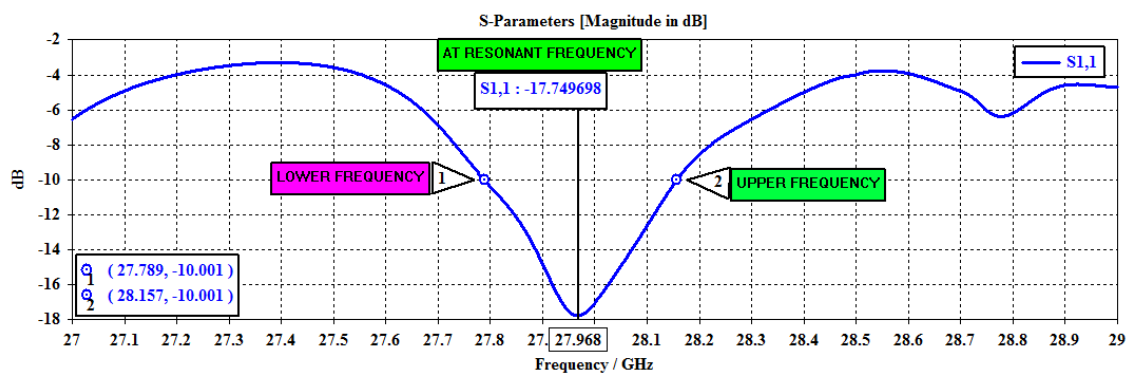


Figure 5.16: Return loss versus frequency plot for the 8x8 rectangular MSPA array.

The 3D radiation pattern of the designed 8x8 MSPA array is shown in Figure 5.17. From the figure, achieved radiation efficiency and total radiation efficiency of the antenna are -0.9836dB (79.733%) and -1.291dB (74.28%) respectively. The directivity and gain of the studied 2x2 inset-feed rectangular MSPA array were 11.12dBi and 10.71dBi respectively. Whereas, the directivity and gain of the proposed 8x8 MSPA array are 19.31dBi and 18.33dBi respectively.

From achieved results it can be seen that, the designed 8x8 inset-feed MSPA array improves the directivity and gain of the proposed 4x4 MSPA array by 3.51dBi and 3.16dBi. In addition, the directivity and gain of the proposed 2x2 MSPA array is improved by 8.19dBi and 7.62dBi respectively.

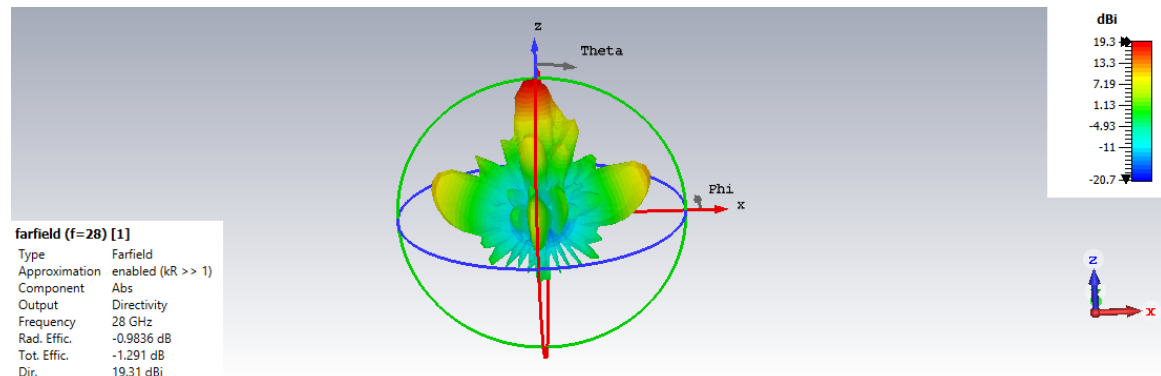


Figure 5.17: 3D radiation pattern for the 8x8 rectangular MSPA array.

Figure 5.18 shows the 2D radiation pattern of designed 8x8 inset-feed rectangular MSPA array. From the figure, the mutual coupling of 8x8 inset-feed rectangular MSPA array is -10dB. Whereas, the mutual coupling of 4x4 inset-feed rectangular MSPA is -11.1dB.

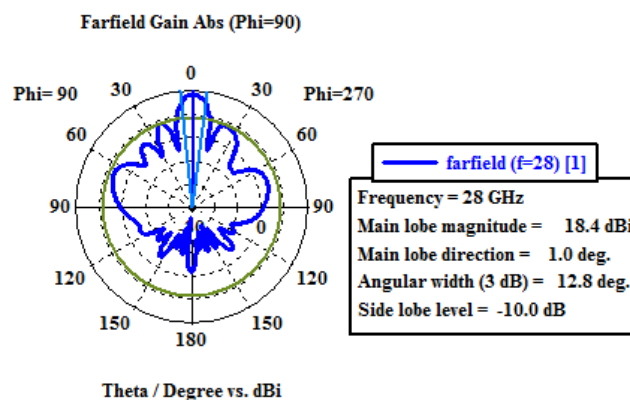


Figure 5.18: 2D radiation pattern for the 8x8 rectangular MSPA array.

In general, simulation results of all the studied inset-feed rectangular MSPA arrays are summarized in Table 5.5. The performance of the linear antenna array is improved as the number of radiating elements increases from one to four. However, it has been observed that the trend cannot be continued further. For instance, the performance of a linear 8x1 inset-feed rectangular MSPA array is significantly lower than that of 4x1 in terms of the magnitude the return loss and VSWR, and out of the acceptable range.

Besides, linear increment of the antenna array size reduces the compactness of the structure, which is not desired for many applications. Also, two dimensional antenna array structure achieves the lowest values of the return loss and VSWR, due to the introduction of

quarter wave impedance transformer in the matching network design. The planar structures have lower radiation efficiency as compared to the linear inset-feed rectangular MSPA array structures. This is because of the increased loss and mutual coupling between the elements in the planar inset-feed rectangular MSPA array structures. However, their directivity and gain are significantly higher than that of the linear structures. Overall, extensive study of different antenna array structures using simulation shows that there is no single best design in terms of all the performance parameters of the antenna. Hence, there is a design trade-off that should be considered depending on the requirements of a particular application.

Table 5.5: Simulation results of all studied inset-feed rectangular MSPA array.

Type	F_0 (GHz)	S_{11} (dB)	DIR (dBi)	GAIN (dBi)	VSWR	η_{rad} (%)	η_{tot} (%)	SLL (dB)	BW (MHz)
1x1	28	-20.2365	7.404	7.18	1.2156	94.95	94.27	-12.1	572
2x1	28	-19.8859	9.451	9.299	1.3436	96.56	92.53	-16.8	575
4x1	28	-27.4218	11.2	11.06	1.1059	97.41	96.56	11.8	1394
2x2	28	-32.6876	11.12	10.71	1.0475	90.9	89.79	-15	326
4x4	28	-33.1499	15.8	15.17	1.0449	86.54	85.08	-11.1	332
8x8	28	-17.797	19.31	18.33	1.2977	79.73	74.28	-10	368

Where, η_{rad} denotes radiation efficiency, η_{tot} denotes total radiation efficiency, S_{11} denotes return losses, and BW denotes bandwidth.

Chapter 6

Conclusions and Recommendations

6.1 Conclusions

In this paper, comparative performance assessment of single element, 2x1, 4x1, 2x2, 4x4, and 8x8 inset-feed rectangular MSPA arrays have been successfully studied at 28GHz for mm-wave applications. At the resonant frequency it has been found that, the return loss and bandwidth of the studied single element, 2x1, and 4x1 inset-feed rectangular MSPA arrays are -20.2365dB, -19.885dB, -27.4218dB and 572MHz, 575MHz, 1.394GHz; the beam directivity and radiation efficiency are 7.41dBi, 9.451dBi, 11.2dBi and 94.95%, 96.56%, 97.41% respectively. Besides, the return loss and bandwidth of the studied 2x2, 4x4, and 8x8 inset-feed rectangular MSPA arrays are -32.679dB, -33.1499dB, -17.748dB and 326MHz, 332MHz, 368MHz; the beam directivity and radiation efficiency are 11.12dBi, 15.8dBi, 19.31dBi and 90.9%, 86.543%, 79.73% respectively.

In the proposed design, the ground plane dimension and inter-element space have been reasonably chosen in such a way that the radiation from each array elements are constructively added together in the desired direction and destructively in other direction. As a result, the side-lobe level is minimum which in turns to the increased total radiation efficiency and directivity of the antenna. In addition, in both linear and planar array by tuning the width of the patch and using successive branching of the parallel feeding networks with equal path lengths to each of array elements are minimizes the input impedance mismatch of the feeding part. Consequently, the radiation efficiency and bandwidth of the antenna is significantly increased.

In this study, the inset-feed impedance matching techniques, quarter-wavelength impedance transformer method and tuning the parameters of the antenna have been used together. As a results, all the studied rectangular MSPA arrays configurations at 28GHz shows better performance in terms of; beam directivity and gain, bandwidth, and radiation efficiency. Besides, the return losses of the antenna is acceptable and minimum. As compared to antenna array designs reported in the scientific literature, the proposed antenna arrays show significantly improved performance. Generally, the overall extensive study of different antenna array structures using simulation shows that there is no single best design in terms of all the performance parameters of the antenna. Hence, there is a design trade-off that should be considered depending on the requirements of a particular application.

6.2 Recommendations

In this paper, inset-feed impedance matching, quarter-wavelength impedance transformer, and tuning the dimensions of the antenna have been simultaneously used to increase the performance of rectangular MSPA arrays at 28GHz for mm-wave application applications. For all studied antennas, acceptable simulation results have been achieved with suitable performance characteristics such as compact size, high beam directivity and gain, low return losses and VSWR, good radiation efficiency, and wide bandwidth. Therefore, in this paper, the proposed inset-feed rectangular MSPA arrays are good candidate antenna type for the 5G mm-wave applications. However, still further investigation is needed. These are:

- Analyzing the performance of inset-feed rectangular MSPA by incorporating slot on the patch and using different patch shapes apart from rectangular shape needs further studies.
- Analyzing the performance of the Co-planar array configuration to check the feasibility of the inset-feed rectangular MSPA array for 5G mm-wave base station by using 8x8 inset-feed rectangular MSPA arrays as a sub-array.
- Analyzing the performance of both multi-band linear and planar array configuration of inset-feed rectangular MSPA array or 5G mm-wave application is another interesting research area.

References

- [1] Dahlman, Mildh. G, Parkvall. S, Peisa. J, Sachs. J, Selen. Y, and Skold. J, “5G wireless access: Requirements and realization,” *IEEE Communication Magazine*, pp. 42-47, 2014.
- [2] Gu, X. “A multilayer organic package with 64 dual-polarized antennas for 28GHz 5G communication,” in *Proceedings of the IEEE International Microwave Symposium*, pp. 1899-1901, June, 2018.
- [3] Dheeraj Mungur and Shankar Duraikannan, “Microstrip Patch Antenna at 28GHz for 5G Applications,” *Journal of Science Technology Engineering and Management Advanced Research and Innovation*, Vol. 1, Issue 1, January, 2018.
- [4] Marcus. M. J. “5G and IMT for 2020 and beyond,” *IEEE Wireless Communication*, 2015.
- [5] E. Annalakshmi and D. Prabakaran, “A Patch Array Antenna for 5G Mobile Phone Applications,” *Asian Journal of Applied Science and Technology*, Vol. 1, Issue 3, pp. 48-51, April, 2017.
- [6] Zhang. J, Guizani. M, and Zhang. Y, “5G Millimeter-Wave Antenna Array: Design and Challenges,” *IEEE Wireless Communication*, pp. 106-112, 2017.
- [7] Omar Darboe, Dominic Bernard Onyango Konditi, and Franklin Manene, “A 28GHz Rectangular Microstrip Patch Antenna for 5G Applications,” *International Research Publication House, Journal of Engineering Research and Technology*, Vol. 12, No. 6, pp. 854-857, 2019.
- [8] B. G. Hakanoglu, O. Sen, and M. Turkmen, “A Square Microstrip Patch Antenna with Enhanced Return Loss through Defected Ground Plane.” *Second URSI AT-RASC*, June, 2018.
- [9] Safpbri. J, Muhammad. A, Shaifol. I, and Mohd. N, “28GHz Microstrip Patch Antennas for Future 5G,” *Malaysian Journal of Engineering and Science Research*, Vol. 2, No. 4, pp. 01-06, 2018.
- [10] N. L.Vamsi Priya. K, G. Sai Sravanthi, K. Narmada, K. Naga Kavya, G. Yedukondalu Swamy, and M. Durgarao, “A Microstrip Patch Antenna Design at 28GHz for 5G Mobile Phone Applications,” *International Journal of Electronics, Electrical and Computational System*, Vol. 7, Issue 3, March, 2018.

- [11] Constantine A. Balanis, "Antenna Theory Analysis and Design," Third Edition. Hoboken, New Jersey: John Wiley and Sons, Inc., 2005.
- [12] Md. Abubakar Siddik, Md. Mahabub Hossain, Md. Dulal Haque, and Md. Omar, "Design and Radiation Characterization of Rectangular Microstrip," American Journal of Engineering Research, Vol. 8, Issue 1, pp. 273-281, 2019.
- [13] Mohamed Bakry El Mashade and E. A. Hegazy, "Design and Analysis of 28GHz Rectangular Microstrip antenna," WSEAS Transactions on Communications, Vol. 17, pp. 2224-2864, 2018.
- [14] Kukunuri Suraj and M. Neelaveni Ammal, "Design and Development of Microstrip Patch Antenna at 2.4 GHz for Wireless Applications," Indian Journal of Science and Technology, Vol. 11(23), June, 2018.
- [15] Dheeraj Mungur and Shankar Duraikannan, "Design and Analysis of 28 GHz Millimeter-Wave Antenna Array for 5G Communication Systems," Peacock Scientific Publication, Journal of Science Technology Engineering and Management, Vol. 1, Issue 3, August, 2018.
- [16] Gary A. Thiele and Warren L. Stutzman, "Antenna Theory and Design," Third edition, John Wiley and Sons, Inc., 2013
- [17] Aqeel Hussain Naqvi and Sungjoon Lim, "Review of Recent Phased Arrays for Millimeter-Wave Wireless Communication", September, 2018.
- [18] Misbah Abdelsalam Misbah Omar, Abdalla Mohamed Elgnai Zayid, and Essam Hassan Abu Samra, "Design and Analysis of Millimeter Wave Microstrip Patch Antenna for 5G Applications," International Conference on Technical Sciences, pp.137-142, March, 2019.
- [19] Ravi Kumar Goyal and Uma Shankar Modani, "A Compact Microstrip Patch Antenna at 28 GHz for 5G Wireless applications," IEEE, Third International Conference and Workshops on Recent Advances and Innovations in Engineering, November, 2018.
- [20] T. Kiran, N. Mounisha, Ch.Mythily, and T.V.B.Phani Kumar, "Design of Microstrip Patch Antenna for 5G Applications," IOSR-Journal of Electronics and Communication Engineering, Vol. 13, pp. 14-17, February. 2018.
- [21] Neha Kothari and Sunil Sharma, "A 28GHz U-slot Microstrip Patch Antenna for 5G applications," International Journal of Electromagnetic Development and Research (IJEDR), Vol. 6, Issue 1, 2018.

- [22] Melad. M Olaimat, "Comparison Between Rectangular and Circular Patch Antennas Array," *International Journal of Computational Engineering Research*, Vol. 6, pp. 2250-3005, September, 2016.
- [23] Zhang. S, Chen. X, Strytsin. I, Pedersen. G, "A Planar Switchable 3D Coverage Phased Array Antenna and It's User Effects for 28GHz Mobile Terminal Applications," *IEEE Transactions on Antennas and Propagation*, pp. 6413-6421, 2017.
- [24] Ojaroudiparchin, Shen. M, Zhang. and S, Pedersen. G, "A Switchable 3D Coverage Phased Array Antenna Package for 5G Mobile Terminals," *IEEE Antennas and Wireless Propagation*, pp. 1747-1750, 2016.
- [25] Venu Adepu, "A 28GHz FR-4 Compatible Phased Array Antenna for 5G," *International Journal of Engineering Science and Advanced Technology*, Vol. 7, Issue 4, pp. 305-310, August, 2017.
- [26] Ojaroudiparchin, N., Shen, M., and Pedersen, G. F., "8x8 Planar Phased Array Antenna with High Efficiency and Insensitivity Properties for 5G Mobile Base Stations," *IEEE Tenth European Conference on Antennas and Propagation (EuCAP)*, 2016.
- [27] Jaspreet Kaur and Sonia Goyal, "A Comparative study on Linear Array Antenna Pattern Synthesis using Evolutionary Algorithms," *International Journal of Advanced Research in Computer Science*, Vol. 8, No. 5, pp. 1582-1587, June, 2017.
- [28] Rajesh Berra, Ragini Lanjewara, Durbadal Mandala, Rajib Kara, and Sakti Prasad Ghoshal. B, "Comparative Study of Circular and Hexagonal Antenna Array Synthesis using Improved Particle Swarm Optimization," *International Conference on Advanced Computing Technologies and Applications*, pp. 651-660, 2015.
- [29] Anouar Dalli, Lahbib Zenkouar, and Seddik Bri, "Comparison of Circular Sector and Rectangular Patch Antenna Arrays in C-band," *Journal of Electromagnetic Analysis and Applications*, Vol. 4, No. 11, October, 2012.
- [30] P. Kokila, T. Saranya, and S. Vanitha, "Analysis and Design of Rectangular Microstrip Patch," *Ever-science Publications, Journal of Network Communications and Emerging Technologies*, Vol. 6, Issue 4, April, 2016.
- [31] Anuj Mehta, "Microstrip Antenna," *International Journal of Scientific and Technology Research*, Vol. 4, Issue 3, March, 2015.
- [32] Vivekananda Lanka Subrahmanya, "Pattern Analysis of the rectangular Microstrip patch antenna," *University of Hogskolaniboras, Master's Thesis*, January, 2009.

- [33] N. H. Nor, M. H. Jamaluddin, M. R. Kamarudin, and M. Khalily, "Rectangular Dielectric Resonator Antenna Array for 28GHz application," Malaysia University of Technology, Progress on Electromagnetic Research C, Vol. 63, pp. 53-61, 2016.
- [34] S. Gnanamurugan, B. Narmadha, A. Shamina, and M. Sindhu, "Gain and Directivity Enhancement of Rectangular Microstrip Patch Antenna," Asian Journal of Applied Science and Technology, Vol. 1, Issue 2, pp.127-131, March, 2017.
- [35] Corey Bergsrud, Chase Freidig, Matthew Anderson, Matthew Clausing, Timothy Dito, and Sima Noghianian, "Inset-Feed and Edge-Feed Patch Antennas With Rectifying Circuit".
- [36] P. Jeyakumar, Prof. P. Chitraand, and Ms. G. Christina, "Design and Simulation of Directive High Gain Microstrip Array Antenna for 5G Cellular Communication," Asian Journal of Applied Science and Technology, Vol. 2, Issue 2, pp 301-313, June, 2018.
- [37] Steve winder, "Analog and Digital Filter Design," Elsevier Science, Second Edition, 2002.
- [38] Shannon Wanner, "Phased array system design," Retrospective Theses and Dissertations, 2008.
- [39] Andy Vesa, "The Radiation Pattern for Uniform Array Antennas," pp. 13-16, 2010.
- [40] Prachi, Vishal Gupta, and Sandip Vijay, "A Novel Design of Compact 28 GHz Printed Wide-band Antenna for 5G Applications", Blue Eyes Intelligence Engineering and Sciences Publication, Journal of Innovative Technology and Exploring Engineering, Vol. 9 Issue 3, January, 2020.
- [41] M Darsono and A R Wijaya, "Design and simulation of a rectangular patch microstrip antenna for the frequency of 28 GHz in 5G technology", International Conference on Innovation on Research, Conference Series 1469, 2020.
- [42] Dr. M. Kavitha, T. Dinesh Kumar, Dr. A. Gayathri, V. Koushick, "28GHZ Printed Antenna for 5G Communication with Improved Gain Using Array", International Journal of Scientific and Technology Research", Vol. 9, Issue. 03, March, 2020.
- [43] Lixia Chen, "Millimeter-Wave Wide Band Antenna Array for 5G Mobile Applications", University of Ottawa, Ottawa, Master's Thesis, 2019.

Appendix-One

Tuned design parameters of all Proposed MSPA array

Table 1. Tuned parameters of a single inset-feed rectangular MSPA.

Tuned Design Parameters	Symbols	Values
Width of the patch	PW	3.3mm
Length of the patch	PL	2.47mm
Width of the ground plane	GW	8.5mm
Length of the ground plane	GL	8.5mm
Length of inset-feed	YO	0.9054mm
Length of inset-gap	Gp	0.23915mm
Substrate thickness	SH	0.244mm
Length of microstrip feeder line	LMFL	2.55mm
Width of microstrip feeder line	WMFL	0.4783mm

Table 2. Tuned parameters of 2x1 inset-feed rectangular MSPA array.

Design Parameters	Symbols	Values
Width of the patch	PW	3.2602mm
Length of the patch	PL	2.478mm
Width of the ground plane	GW	16mm
Length of the ground plane	GL	9mm
Substrate thickness	SH	0.244mm
Gap of inset-feed	Gp	0.23917mm
Length of inset feed	YO	0.745mm
Distance between the patch	D	5.4mm
Length of microstrip feeder line	LMFL	2.0219mm
Width of microstrip feeder line	WMFL	0.4784mm
Length of 1:2 microstrip power divider	LFMPD	0.23915mm
Width of 1:2 microstrip power divider	WFMPD	11mm

Table 3. Tuned parameters of 4x1 inset-feed rectangular MSPA array.

Design Parameters	Symbols	Values
Width of the patch	PW	3.2602mm
Length of the patch	PL	2.478mm
Width of the ground plane	GW	33.1mm
Length of the ground plane	GL	9.92mm
Length of inset-feed	YO	0.744mm
Gap of inset-feed	Gp	0.2392mm
Substrate thickness	SH	0.244mm
Length of microstrip patch feeder	LMFL	2.0209mm
Width of microstrip patch feeder	WMFL	0.4783mm
Length of 1:2 microstrip power divider	LFMPD	0.23915mm
Width of 1:2 microstrip power divider	WFMPD	11mm
Length of 1:4 microstrip power divider	LSMPD	0.23915mm
Width of 1:4 microstrip power divider	WSMPD	22mm

Table 4. Tuned parameters of 2x2 inset-feed rectangular MSPA array.

Design Parameters	Symbols	Values
Width of the patch	PW	3.3mm
Length of the patch	PL	2.4781mm
Width of the ground plane	GW	13mm
Length of the ground plane	GL	11.6mm
Substrate thickness	SH	0.244mm
Length of inset-feed	YO	1mm
Gap of inset-feed	GP	0.23916mm
Length of microstrip feeder line	LMFL	1.9694mm
Width of microstrip feeder line	WMFL	0.478301mm
Length of 1:2 microstrip power divider	LFMPD	0.239151mm
Width of 1:2 microstrip power divider	WFMPD	10.8mm
Length of last microstrip feeder line	LLMFL	0.23915mm
Width of last microstrip feeder line	WLMFL	5.9mm
First quarter transform width	FQTW	0.2mm
First-quarter transform Length	FQTL	0.47825mm
Second quarter transform length	SQTL	0.338mm
Second quarter transform width	SQTW	0.4783mm
Third-quarter transform width	TQTW	0.23913mm
Third-quarter transform length	TQTL	1.276mm

Table 5. Tuned parameters of 4x4 inset-feed rectangular MSPA array.

Design Parameters	Symbols	Values
Width of the patch	PW	3.261mm
Length of the patch	PL	2.47819mm
Width of the ground plane	GW	31mm
Length of the ground plane	GL	33.1mm
Substrate thickness	SH	0.244mm
Length of inset-feed	YO	0.9054mm
Gap of inset-feed	GP	0.23916mm
Length of microstrip feeder line	LMFL	2.55mm
Width of microstrip feeder line	WMFL	0.4783mm
Length of 1:2 microstrip power divider	LFMPD	0.23915mm
Width of 1:2 microstrip power divider	WFMPD	10.8mm
Length of last microstrip feeder line	LLMFL	0.23915mm
Width of last microstrip feeder line	WLMFL	15.38mm
First quarter transform width	FQTW	0.3mm
First-quarter transform Length	FQTL	0.47828mm
Second quarter transform length	SQTL	0.339mm
Second quarter transform width	SQTW	0.47831mm
Third-quarter transform width	TQTW	0.23916mm
Third-quarter transform length	TQTL	1.276mm

Table 6. Tuned parameters of 8x8 inset-feed rectangular MSPA array.

Design Parameters	Symbols	Values
Width of the patch	PW	3.2602mm
Length of the patch	PL	2.4781mm
Width of the ground plane	GW	66mm
Length of the ground plane	GL	60.5mm
Substrate thickness	SH	0.244mm
Gap of inset-feed	GP	0.23916mm
Length of inset-feed	YO	0.95mm
Length of microstrip feeder line	LMFL	2.227mm
Width of microstrip patch feeder	WMFL	0.4783mm
Length of 1:2 microstrip power divider	LFPD	0.23915mm
Width of 1:2 microstrip power divider	WFPD	10.8mm
Length of last microstrip feeder line	LLMFL	0.23915mm
Width of last microstrip feeder line	WLMFL	32.9726mm
First quarter transform width	FQTW	0.3mm
First-quarter transform Length	FQTL	0.47831mm
Second quarter transform width	SQTW	0.4783mm
Second quarter transform length	SQTL	0.338mm
Third-quarter transform width	TQTW	0.23915mm
Third-quarter transform length	TQTL	1.2769mm

Appendix-Two

Physical Structure of the Antenna for the Tuned parameters

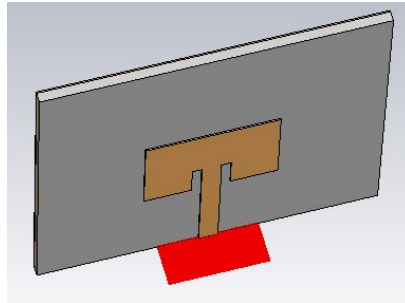


Figure 1. Single Inset-Feed Rectangular MSPA.

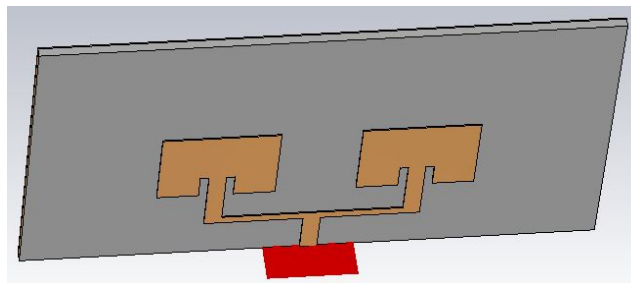


Figure 2. 2x1 inset-feed rectangular MSPA array.

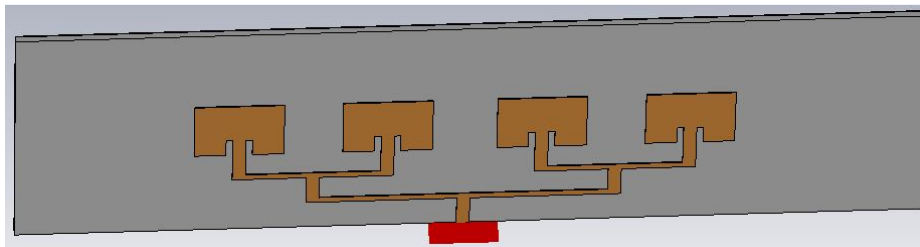


Figure 3. 4x1 Inset-Feed Rectangular MSPA Array.

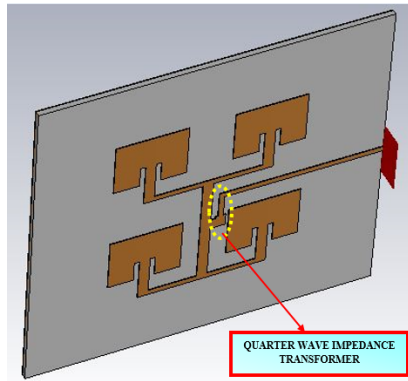


Figure 4. 2x2 Inset-Feed Rectangular MSPA Array.

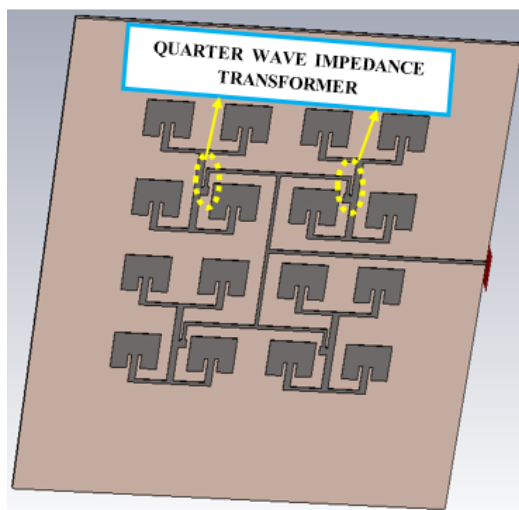


Figure 5. 4x4 Inset-Feed Rectangular MSPA Array.

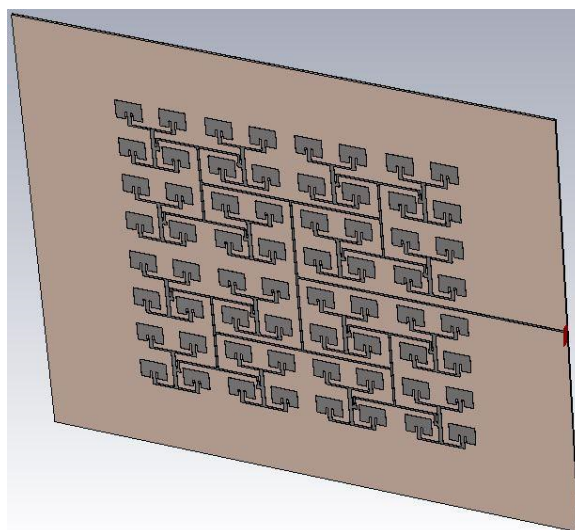


Figure 6. 8x8 Inset-Feed Rectangular MSPA Array.